The Regulation of Skeletal Muscle Growth via the Myostatin Signalling Pathway

Mohammad Al Khalaf

A Thesis

in

The Department

of

Chemistry and Biochemistry

Presented in Partial Fulfillment of the Requirements

for the Degree of Master of Science (Chemistry and Biochemistry) at

Concordia University

Montreal, Quebec, Canada

March 2010

Your file Votre référence
ISBN: 978-0-494-67310-2
Our file Notre référence
ISBN: 978-0-494-67310-2

Abstract

The Regulation of Skeletal Muscle Growth via the Myostatin Signalling Pathway

Mohammad Al Khalaf

Myostatin (Mstn) is a negative regulator of skeletal muscle fibre size and satellite cell proliferation whose role in mature fibre compensatory growth has not been fully characterized. Myostatin knockout (Mstn-/-) mice display consistently larger skeletal muscle masses, as well as an overall increase in size and number of myofibres within the muscle, compared to the wild-type mice. Previous research has shown that Mstn plays a major role in the attenuation of both the hypertrophic and hyperplasic pathways of myofibre growth. Immunohistochemical staining of overloaded plantaris muscles was performed to analyze phenotypic and morphological changes in wild-type and Mstn-/- muscles. Preliminary results of these analyses indicated a tendency for muscles from Mstn-/- mice to express an increased number of myofibres, whereas muscles from Mstn+/+ mice tended to display hypertrophied pre-existing mature myofibres as a response to the overload stimulus. Additionally, using semi-quantitative PCR and western blotting, changes were monitored, in mRNA transcripts and protein expression levels, for some of the major factors involved in muscle growth signalling. Our preliminary results also showed altered expression of genes and proteins that ultimately translate to increased satellite cell proliferation and maturation in Mstn-/- muscles. Taken together, myostatin's effect on muscle is most apparent in attenuating the hyperplasic growth response in stimulated muscle, and not the hypertrophic signalling pathway. This is the first *in vivo* study to specifically look at the function of myostatin in muscles that are induced to grow by means of functional overloading.

Acknowledgements

One cannot go through a long and hard journey like the one I have without the help of countless persons that helped me in ways that I cannot repay. It would be a futile attempt to try to thank everyone that deserves thanks and much more than that. Everyone, from my loving parents and sister, to my friends and work colleagues, all deserve more than simple acknowledgements. I owe them more than I can repay, and I hope that I can, in my humble way, contribute to their lives a fraction of what they have contributed to mine.

If forced to name a few individuals that were intimately involved in assisting me finish this thesis, I would start by thanking my supervisor, my committee members and whole department of Chemistry and Biochemistry, my friends and lab colleagues, especially, Ewa Kulig, Mathieu St. Louis, Patrick Sin-Chan, Michal Solecki and all the others that participated in the lab over the time I had in there.

This work was supported by funding from NSERC, CIHR and CRC to Dr. R. N. Michel.

As a final note, I would like to dedicate this body of work to my grandfather, for being one of the utmost important people in my life. May he rest in peace.

TABLE OF CONTENTS

List of Abbreviations

ActIIBR: Activin II B receptor

Akt: Protein Kinase B

Atgn: Atrogin-1

BDNF: Brain-Derived Neurotrophic Factor

BrdU: 5-bromo-2-deoxyuridine

CamBP: Calmodulin Binding Protein

CnA: Calcineurin A

CsA: Cyclosporine A

DAB: 3-3'-Diaminutesobenzidine

EDL: Extensor Digitorum Longus Muscle

FLRG: Follistatin Like Related Gene

Fstn: Follistatin

Gas: Gastrocnemius Muscle

GDF: Growth and Differentiation Factor

IGF1: Insulin-like Growth Factor 1

Mgn: Myogenin

Mstn: Myostatin

MyHC: Myosin Heavy Chain

NFAT: Nuclear Factor of Activated T-cells

OV: Overload

Pax7: Paired-box Factor 7

Pla: Plantaris Muscle

Sol: Soleus Muscle

TA: Tibialis Anterior Muscle

TnIs: Troponin I slow

LIST OF FIGURES

CHAPTER 1:LITERATURE REVIEW

CHAPTER 4: RESULTS

1: Literature Review

1.1: Muscle Structure

The human body is made up of approximately 40% muscle by weight (Gallagher et al., 1997). Muscle tissue is grouped into three major categories; cardiac muscle, smooth muscle and skeletal muscle. Cardiac muscle makes up the walls of the heart and is involuntarily regulated. Smooth muscle is located in the walls of hollow internal structures such as blood vessels, the stomach, intestines, and urinary bladder, and again it is mostly involuntarily regulated in the body. Skeletal muscle is primarily responsible for generating the voluntary movements the body is capable of performing. It is made up mostly of myofibres, as well as connective tissue that make up the tendons (Kääriäinen et al., 2000). Myofibres are multinucleated, resulting from multiple myoblasts fusing together during the maturation process to form the long myofibres that make up muscle tissue. The basic functional unit of myofibres is called the sarcomere, a short repeating unit made up primarily of myosin and actin proteins that can fold onto each other to contract the sarcomere (see Figure 1.1). This allows for overall myofibre shortening in length, executing the basic function of a muscle that allows for movement.

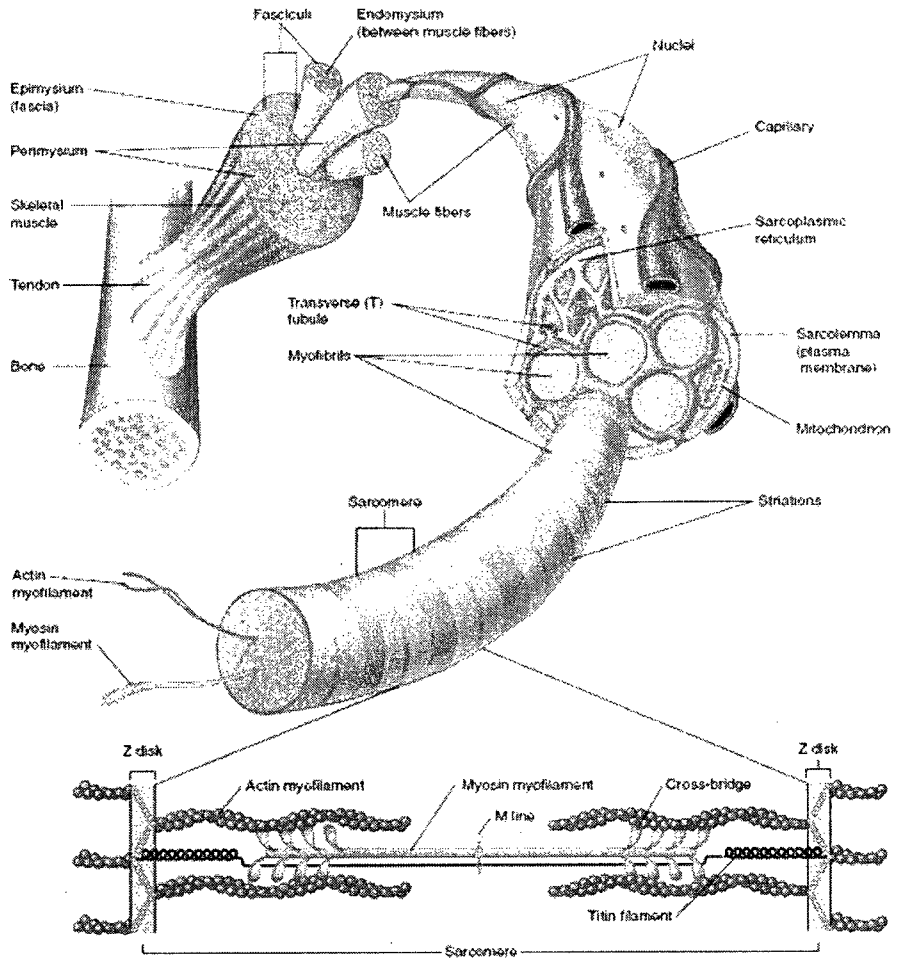

Figure 1.1: Skeletal Muscle structure diagram. Modified from: Essentials of Anatomy and Physiology, Elaine Marieb, 8th Edition

Myofibres are classified by the types of myosin heavy chain isoforms they express within their sarcomeres. There are different classifications for these proteins. The simplest form categorizes the myosin heavy chain proteins as slow twitch or fast twitch, slow twitch being the isoforms that employ an oxidative metabolic pathway for generating adenosine triphosphate (ATP) for energy, while the fast twitch proteins employ a glycolytic metabolic pathway for generating ATP for its use (Handschin et al., 2007). The oxidative pathway is initiated during aerobic respiration, meaning oxygen is utilized, with glucose, to produce ATP, as well as carbon dioxide and water as by-

products. This pathway is carried out in the mitochondria within cells, and this explains why slow twitch fibres are rich in mitochondria and are therefore characterized by the red-colored myoglobin content that is sometimes used to describe the tissue. The glycolytic pathway is initiated during anaerobic respiration, meaning glucose is metabolized to pyruvate, and the energy released from that reaction is used to produce ATP for energy. This reaction could occur without the involvement of oxygen in the cytoplasm, and under anaerobic conditions will produce lactic acid to replenish depleted nicotinamide adenine dinucleotide (NAD^+). While this form of metabolism is faster in producing ATP for the myofibre to use, it produces only a fraction of the amount of ATP that the body produces using aerobic respiration. Therefore, the fast twitch fibres are also known as fatigue-prone cells, showing great contractile force, but for only short periods of time (Girgenrath et al, 2005).

Myosin heavy chain (MyHC) proteins, which make up the myosin heads on the overall myosin protein, have at least four major types of isoforms that are expressed in the sarcomere mature myofibre. Those isoforms are named: I (the slowest type of MyHC), IIA, IIX and IIB, (the fastest type of MyHC), (Dunn et al., 1999). Myofibres that are characterised as "slow-twitch" express MyHC I isoform, while the fastest "fast-twitch" fibres express MyHC IIB. However it is observed constantly that fibres can co-express some of the isoforms (Michel et al., 2007), such that a myofibre expressing both MyHC I and IIA, or MyHC IIX and IIB, in an attempt to fine-tune the myofibre, and ultimately the overall muscle, to be in a position to have optimal energy consumption. There are various pathways that regulate the expression of the different myosin heavy chain isoforms as well as overall muscle mature size and growth rate.

Skeletal muscle applies two different mechanisms for repair or growth, named hypertrophy and hyperplasia (Joulia-Ekaza et al., 2006). Hypertrophy is the mechanism in which existing muscle fibres grow bigger in diameter and hence total volume causing the overall muscle to increase in mass. The increase is measured as cross-sectional area, where the area of the muscle fibre is increased as a result of higher protein production leading to larger size and increased number of myofibrillars (see Figure 1.1). Much of the early research reports that myostatin null animal models display a marked muscle hypertrophy. Hyperplasia is the mechanism in which new muscle fibres are formed, increasing the overall size of the muscle tissue by adding newly formed myofibres (Seale et al., 2000). Hyperplasia occurs by activating muscle progenitor cells known as muscle satellite cells. These cells are stem-like in nature, they are held in a quiescent form in adult muscle tissue, and when activated, they proliferate, differentiate and fuse to form new myofibres (Le Grand et al., 2007). Recently a new protein called myostatin was discovered to have a key role in how muscles grow. It has been shown to have an inhibitory effect on muscle hypertrophy and hyperplasia, and thus it has become vital to furthering our understanding of this protein so that muscle related diseases and syndromes can be better diagnosed and treated in the future.

1.2: Myostatin Gene and Protein

Growth/Differentiation Factor-8 (GDF-8) is a protein first discovered and identified in 1997 by the team of Dr. Se-Jin (McPherron et al., 1997). Using degenerate polymerase chain reaction they identified the sequence of GDF-8 and its similarity to other members of the Transforming Growth Factor-β (TGF- β) superfamily of proteins. The role of GDF-8 was qualitatively determined by generating mice models with a

disruption of the gene encoding this protein. The results showed that overall body mass was increased by 30% and that skeletal muscles were the sole contributor to this increase, showing an increase in muscle mass of 2-3 fold, irrespective of age or gender (McPherron et al., 1997). These authors showed GDF-8 to be expressed in early embryogenesis stages and mostly in adult skeletal muscle, with some detectable amounts in adipose tissue. Dr. Se-Jin Lee coined this new protein by the name of myostatin since it was clear that its function seemed to be primarily as a negative regulator of muscle growth (McPherron et al., 1997).

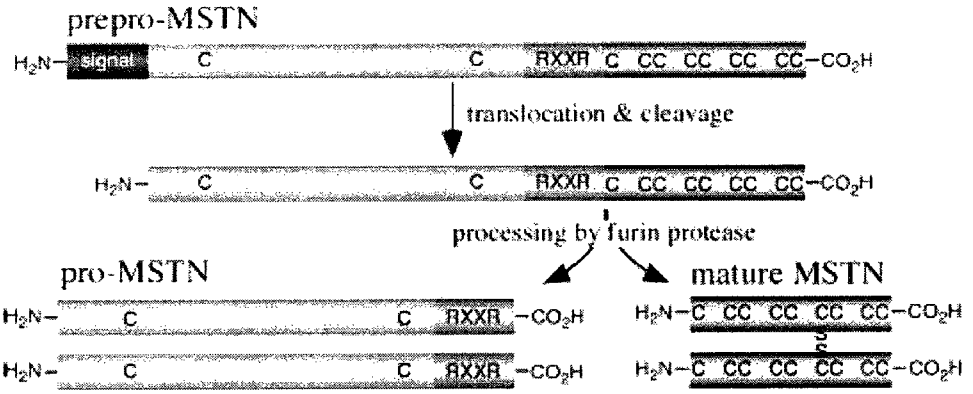

Figure 1.2: Myostatin protein processing into its active conformation. Modified from: Rogers et al., 2008

Myostatin mRNA is translated into a 53 kDa protein containing 376 amino acids (McPherron et al., 1997; Kocamis et al., 2002). It is secreted from the cell to affect adjacent cells. Therefore, it is identified as a paracrine hormone (Favier et al., 2008). It is proteolytically cleaved at a site close to its C-terminus, seen in Figure 1.2, producing a short active form of the peptide and a long inhibitory pro- peptide domain, with the shorter peptide homodimerizing to generate its final active state (McPherron et al., 1997; Kocamis et al., 2002; Armand et al., 2003). Figure 1.3 illustrates the active homodimer

and the inhibitory site of the pro-peptide domain of the protein. Myostatin is conserved across many species, showing high degree of homology between human, murine, rat, porcine, chicken, and turkey sequences (McPherron et al., 1997, Kocamis et al., 2002). Myostatin null mice show myofibre cross sectional area (CSA) increases of approximately 50% for the gastrocnemius muscle of 10 week old mice as an example (Lee, 2007). Total body fat also steadily decreases over time as Mstn $^{-/-}$ mice age, even though metabolic rate is reduced and food intake unchanged (Joulia-Ekaza et al., 2006), as tested by monitoring blood serum levels of leptin, a biological marker for total body fat accumulation. This could imply other roles for myostatin in the body, not only in skeletal muscles. Some of the research in the field that is looking at myostatin's role in adipose tissue, for example Dr. Mehan's group (Allen et al., 2008), show that there are several questions pertaining to myostatin-signalling in adipose tissue. Using obese mice as a model, they looked at levels of myostatin, activin receptor IIB and Follistatin-like gene 3 (FSTL3), three major components of the myostatin pathway, in visceral and subcutaneous fat tissue. Their results showed that compared to wild-type levels, myostatin and activin receptor IIB levels increase in VSF and SQF while FSTL3 levels decrease in obese mice, suggesting a role for myostatin in inhibiting the overall basal metabolic rate of the body, which is a cause of obesity (Allen et al., 2008).

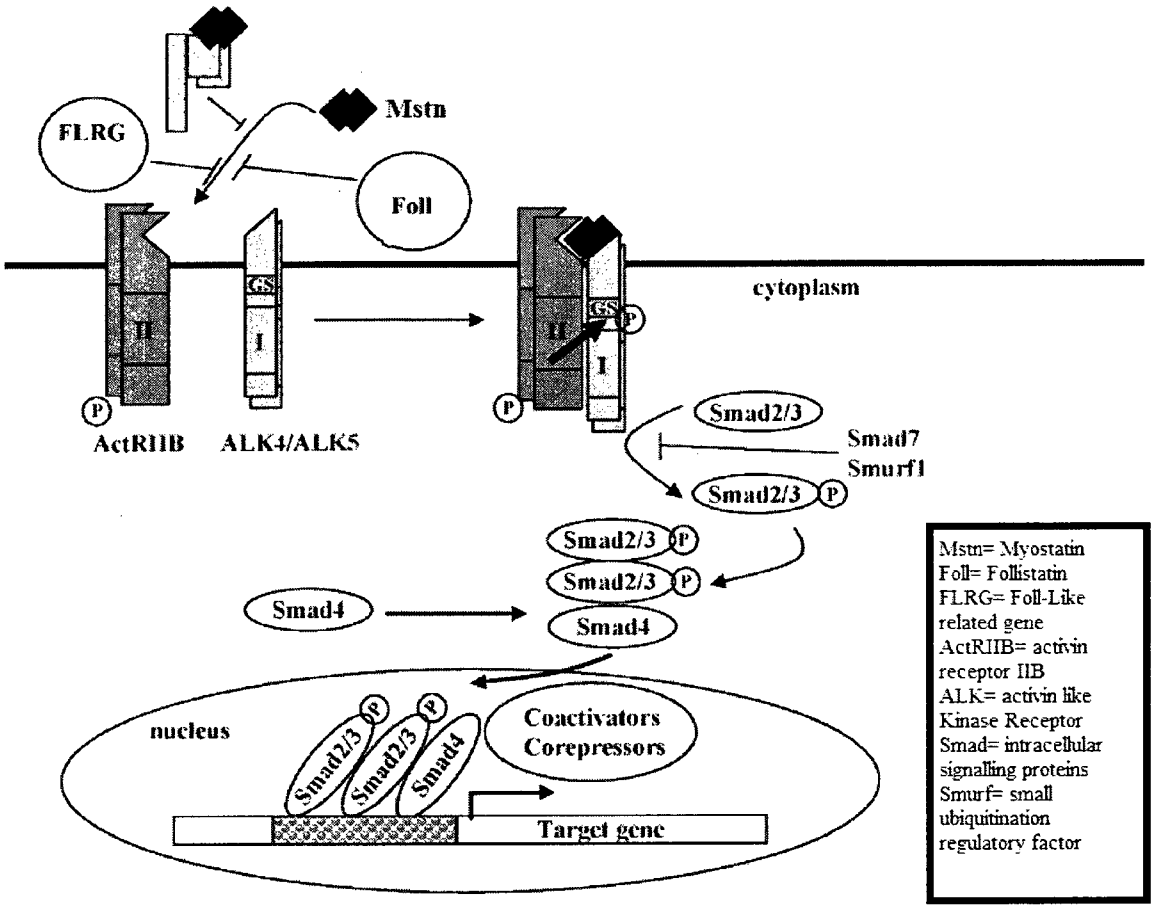

Figure 1.3: Summary of known signalling pathway initiated by myostatin. Modified from Joulia-Ekaza et al., 2006

The myostatin homodimer binds to a serine-threonine receptor kinase known as activin receptor IIB (ActRIIB) that initiates intracellular signalling involving Smad proteins (Baumann et al, 2003). The name of this class of proteins comes from the fact that they are homologs of a protein found in *C. elegans* named SMA and a protein found in Drosophila named *mothers against decapentaplegic protein* MAD, therefore the acronym SMAD was coined. The receptor is found on the cell membrane of myofibres, and is named after another GDF protein called activin, a protein first discovered to have a role in the development of the pituitary follicle-stimulating hormone in the reproductive axis. It has also been shown more recently to be involved in neuron development (review:

Tsuchida et al., 2008). After that pathway was elucidated, myostatin binding to the receptor was reported, which explains the non-related name of the receptor to myostatin. Binding of the myostatin homodimer to ActRIIB causes it to associate with activin receptor-like kinase 4 (ALK4) receptor, which then gets trans-phosphorylated from ActRIIB, allowing it to phosphorylate Smad2 and Smad3 (Joulia-Ekaza et al., 2006). Smad proteins are described as intracellular mediators. They become phosphorylated by the receptor kinases and start a cascade of secondary and tertiary messages that activate/deactivate specific nuclear transcription factors that affect gene expression in muscles (Joulia-Ekaza et al., 2006). Myostatin activates Smad2 and Smad3 which dimerize and can sometimes interact with co-Smad4 which potentiates the signalling (down-stream of 2/3). Smad7 and small ubiquitination regulatory factor 1 (Smurf1) are inhibitory smads to this pathway and myostatin is shown to induce expression of Smad7 causing a self-inhibitory feedback loop to be possible (Joulia-Ekaza et al., 2006).

For myostatin to be in its mature active homodimer, it must be proteolytically cleaved by furin, seen in Figure 1.2, a pro-protein convertase (Anderson et al., 2008). There is not much known about the specifics of this pathway, but Dr. Whitman's group (Anderson et al., 2008) published research showing some key events that occur in the pathway leading to myostatin maturation. Using immuno-precipitation techniques, they showed that when myostatin is first translated into the inactive full-length pro-peptide, 53kDa in size (which they call pro-myostatin), it would bind to a protein called latent-transforming growth factor β binding protein 3 (LTBP3) in the endoplasmic reticulum. It would shuttle the pro-myostatin to the Golgi and then out into the extracellular matrix. There, LTBP3 would dissociate from the pro-myostatin peptide, which would then bind

to another pro-myostatin peptide forming a homodimer, and furin would cleave the N-terminal pro-peptides, (40kDa), from myostatin's C-terminal active site (26kDa) within the homodimer (Anderson et al., 2008).

Myostatin's role in regulating muscle growth is being deciphered from many angles, and progress is clear and promising. An important aspect to consider is that myostatin has been shown to play a role in diseases such as AIDS, cachexia, scleraxis, and fast-twitch myofibre atrophy disease (Kocamis et al., 2002, Baumann et al., 2003, Mendias et al., 2008, Wojcik et al., 2008). In all of these diseases myostatin's serum levels are increased leading to muscle wasting in humans. A study by Dr. Faulkner's group (Mendias et al., 2008) also showed that myostatin-null mice showed muscles with weaker, more brittle tendons than wild-types. However, no other group has reported the same finding. As well, there is compounding evidence that shows knocking out myostatin in the mouse model for Duchenne Muscular Dystrophy displays a rescuing effect countering this muscle wasting disease (for review see: Haidet et al., 2008; Bradley et al., 2008).

1.3: Myostatin Gene Regulators

Studies have been performed to analyze the molecules that regulate myostatin's expression in muscle cells. It is known that myostatin is a negative regulator of muscle growth, however what is the purpose of producing a protein with such a role? To understand its purpose, one must examine the activators of this protein and identify the origin of their signalling. Dr. Sharma's group studied the promoter region of the myostatin gene in murine and cattle models. By designing various constructs of the

myostatin promoter region and linking them to a reporter (luciferase) and then injecting these into the quadriceps of mice, they were able to see how removing part of the promoter would affect the expression of myostatin protein *in vivo* (Salerno et al., 2004). This would help to identify certain regions of the promoter and to characterise the molecule involved with that specific promoter region. Using this method, these authors have identified regions for binding myogenic determination factor (MyoD) and Myocyte Enhancing Factor (MEF2) to the promoter (Salerno et al., 2004). These two transcription factors are both involved in muscle growth. They are upregulated when muscle fibres are in the process of developing, therefore it follows that they also signal the upregulators of myostatin as well since uncontrolled growth is detrimental to the body, wasting energy and resources to build muscles that are unnecessarily large. Myostatin may have a role as a molecular braking system to this acceleration of growth.

Other studies have also shown that the myostatin promoter has a binding region for glucocorticoids, called the glucocorticoid response element region (Joulia-Ekaza et al., 2006; Gilson et al., 2007). This feature explains the negative effects of injecting glucocorticoids since glucocorticoids promote proteolytic pathway initiation in muscles. The aforementioned group investigated whether myostatin gene deletion would lead to less atrophy caused by glucocorticoid administration. The deletion prevented dexamethasone-induced atrophy, characterised by measuring both muscle weight and CSA of myofibres of Mstn -/- mice. The loss of functional myostatin also led to the inhibition of Muscle –specific Ring Finger 1 (MuRF1), Atrogin-1, Forkhead box protein 3a (Foxo3a), and Cathepsin upregulation upon dexamethasone treatment (Joulia-Ekaza et al., 2007). Cathepsin is a lysosomal enzyme known to be involved in degradative

pathways (Joulia-Ekaza et al., 2007). MuRF1 and atrogin-1 are ubiquitin ligases that target proteins for proteolysis (Joulia-Ekaza et al., 2007), while Foxo3a is a transcription factor that regulates the expression of the genes encoding these two proteins (Joulia-Ekaza et al., 2007). The conclusion from this paper is that myostatin is needed to induce catabolic activity/proteolytic pathways in skeletal muscles.

1.4: Myostatin Antagonist: Follistatin

Most, if not all, proteins *in vivo* have antagonists that counteract or inhibit their actions. In the myostatin signalling pathway follistatin plays this role, acting directly to inhibit the myostatin pathway, by binding to myostatin and activin receptor IIB (Lee, 2007). Follistatin is a protein, first identified as a secreted hormone from the gonads that inhibits the actions of follicle stimulating hormone (FSH) during reproduction and developmental processes in the body (for review see Lin et al., 2003). More recent research has unrevealed a wider role for follistatin as an inhibitor to the TGF-β superfamily of proteins. Se-Jin Lee reported that in mouse models that have myostatin knocked out and follistatin over-expressed, the overall mass/size of skeletal muscle is quadrupled compared to wild-type mice (Lee, 2007). Follistatin null mice show a 2-3 reduction in overall skeletal muscle mass. Dr. Chanoine's group was interested in showing the reciprocal interactions between follistatin and myostatin (Armand et al., 2003). In their study, they used denervation and injections of cardiotoxin, (a poisonous compound found in cobra venom), to the soleus to test the levels of the mRNAs coding for myostatin and follistatin over a number of days post-intervention. They showed that while myostatin levels initially decrease presumably since the myofibres are atrophying, there would not be much need to transcribe more myostatin, follistatin levels increased,

presumably to quickly attempt to regenerate and grow new myofibres to counteract the loss. Other than follistatin, there are a number of peptides that inhibit myostatin in a similar fashion (see Figure 1.4). Follistatin-like related gene (FLRG) and the pro-peptide of myostatin (the large portion that gets cleaved to make the active homodimer) are both known to interact with the myostatin active homodimer to inhibit its ability to signal through the activin receptor IIB and Smads (Hill et al., 2002). This was discovered when Dr. Qiu's group performed mass spectrometric analysis of isolated myostatin protein in serum by binding it to JA16 coupled beads, JA16 being the monoclonal myostatin antibody, and running the serum containing native myostatin through affinity chromatography (Hill et al., 2002). They were able to isolate and characterise the different peptides that were associated with myostatin, and found that most of the serum myostatin was coupled to either FLRG or the pro-peptide of myostatin (reviewed by: Bradley et al., 2008).

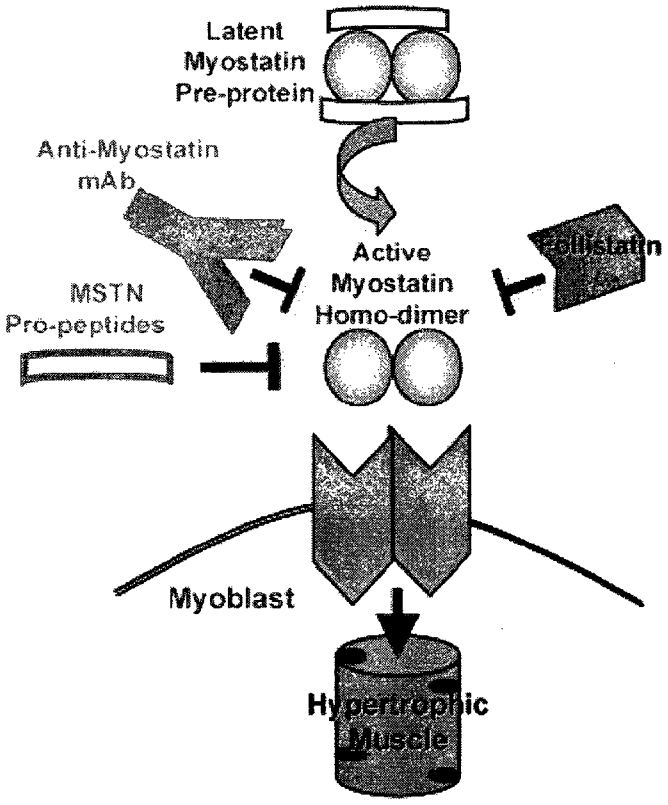

Figure 1.4: Summary diagram showing the multiple peptides that can bind and inhibit myostatin from interacting with its receptor. Modified from Bradley et al.,2008

Krasney's group (Schneyer et al., 2009) investigated the follistatin protein to further understand how it binds to myostatin and the Activin IIB receptor. The paper identifies the binding domain of follistatin that is specific for myostatin being different from the binding domain of follistatin specific to activin receptor. Follistatin and FLRG bind and neutralize activin irreversibly, and bind and neutralize myostatin with three to five fold less affinity. Using *in vitro* cells (26 follistatin mutants), they report that follistatin domain 1 (FSD1) is the domain necessary for myostatin binding and FSD2 is necessary for activin receptor IIB binding.

Thiessen's group has published another study addressing the role of follistatin in muscle growth. In this study, the group showed that overexpression of follistatin increases the cross-sectional area (CSA) of muscle fibres, as well as total DNA content (Gilson et al., 2009) which they use as a measure of satellite cell proliferation, since more cells would lead to more DNA content as they measured it. The study showed that the overexpression of follistatin even in myostatin null transgenic mice induced an even greater increase in muscle mass and CSA of fibres (Gilson et al., 2009). Thus, his study further characterises follistatin as an antagonist to myostatin's role in muscle growth.

1.5: Hypertrophy: The Akt pathway

The Akt pathway in muscle growth has been extensively researched and is regarded as the major pathway involved in muscle hypertrophy (Amirouche et al., 2009). The link between the Akt pathway and the myostatin pathway has been studied by a number of groups in efforts to discover if there is an inhibitory role by myostatin on this hypertrophy-inducing pathway. Dr. Rosenzweig's group has published recently a study showing Akt levels are higher in myostatin knockout muscles compared to those of wild-type (Morissette et al., 2009). Additionally, they have shown that phosphorylated Akt (active) is higher in those knockout muscles as well. These authors conclude that myostatin does in fact have a role in inhibiting the Akt pathway based on their research and, therefore, myostatin works to block hypertrophy by acting on its main signalling protein, Akt.

Another group that has examined the link between myostatin and the Akt pathway is headed by Damien Freyssent. In their recently published paper, they demonstrate that

overexpressing myostatin in tibialis anterior (TA) muscles causes atrophy to occur in those muscles (Amirouche et al., 2009). Electrotransfering myostatin loaded plasmids into the TA muscles and then extracting muscles after 7 days allowed them to look into the effects of overproducing the protein. They found that both Akt and one of its downstream target S6 protein was both downregulated in the myostatin overexpressing muscles. That coupled with the overall muscle weight decrease that shows the after electrotransfering was seen as evidence of the link between myostatin and the Akt pathway.

The logical question that follows is how does myostatin negatively regulate muscle fibre growth? It was shown that hypertrophy occurs when myostatin is altered. The next step was to see whether myostatin controls muscle fibre number, since muscle can grow in mass by making more fibres, a state known as hyperplasia (McCroskery et al., 2003). To answer this question, one must consider satellite cells. These are quiescent stem-like cells found in muscles, which can, when activated, grow and differentiate into adult myofibres (Seale et al., 2000). These are used by the body to recover from muscle injury and increase muscle size triggered by exercise (Seale et al., 2000). McCroskery's group showed first that myostatin is in fact expressed in satellite cells (Wagner et al., 2002). They also showed that Mstn-/- cultured cells extracted from the tibialis anterior muscle had more satellite cells present per 100 myonuclei, and faster myoblast proliferation than wild-type cells. Finally, the addition of exogenous myostatin inhibited satellite cell activation and myoblast proliferation *in vitro*. These data suggest that myostatin is involved in the hyperplasic response within muscles; when absent, myostatin causes muscle to increase myofibre number.

1.6: Hyperplasia: Satellite Cells

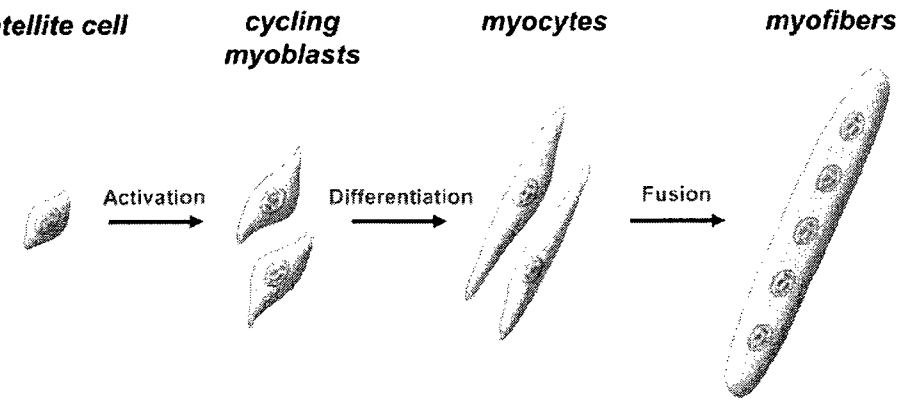

Figure 1.5: Satellite cells go through a number of phases before reaching mature myofibre status. Modified from Le Grand et al., 2007.

The transformation of a satellite cell to an adult myofibre, it would have to go through multiple stages, (Figure 1.5), controlled by certain proteins that are temporally expressed to drive this maturation process (Le Grand et al., 2007). Satellite cells exist as quiescent mono-nucleated small entities found on the periphery of mature myofibres (Seale et al., 2000). Once activated, satellite cells are committed to proliferate and the majority of the newly formed satellite cells differentiate into myoblasts and finally fuse to form myofibres (Kuang et al., 2007). Not all of the proliferating satellite cells mature to myofibres however, as some are arrested after proliferation and kept dormant in a process called self-renewal, therefore ensuring that there are enough satellite cells for future needs (Olguin et al., 2004). Paired-box transcriptional factor 7 (Pax7) is a conserved marker for quiescent satellite cells studied extensively by Dr. Rudnicki's group using immunofluorescence microscopy in myofibre cell cultures (Kuang et al., 2007). It plays

an important role in the development and function of these satellite cells. Pax7 null mice show premature lethality and a complete lack of satellite cell population (Seale et al., 2000),as deduced using electron microscopy to visualise cells from wild-type mice and Pax7-/- mice (Chen et al., 2003). Pax7 expression is seen in satellite cells as they progress from quiescent to activated and proliferating cells, but once the cells reach the myoblast maturation stage, the expression of Pax7 is turned off and the cell is considered mature (for review see Shi et al., 2006). The nature of Pax7 expression makes it an optimal target marker for satellite cell identification, both at the level of gene expression and final protein product. Many researchers use Pax7 expression analysis as a basis for assessing satellite cell activation and maturation (Kuang et al., 2007, Seale et al., 2000, Le Grand et al., 2007). While Pax7 is expressed early in the life of a satellite cell, once activated, Pax7 is downregulated and myogenin expression is upregulated in those cells, making it a prime target to test for mature myofibre increase (Day et al., 2009). A study by Olwin and collegues states that Pax7 acts in a manner that prevents the to maturation of satellite cells, and it is only after Pax7 expression is turned off, that the process of differentiation and maturation of satellite cells into myotubes occur (Olguin et al., 2004). This conclusion was reached after immunofluorescence analysis of proliferating and maturing myoblasts showed Pax7 is not expressed in the more mature myoblasts as compared to the proliferating and quiescent satellite cells.

Once activated, satellite cells express other signalling molecules called myogenic regulatory factors (MRFs), which are transcription factors that regulate myogenesis, promoting the transition from quiescent to mature myofibre (Yafe et al., 2008). When activated and committed to differentiate beyond the quiescent phase, satellite cells begin

to express myogenic factor 5 (Myf5) and myogenic determination factor (MyoD) (for review see Seale et al., 2000). These factors induce proliferation of satellite cells. Following this proliferation phase, these cells begin to express myogenin and muscle regulatory factor 4 (MRF4), which are factors that drive the cell differentiation and maturation to adult myofibres (for review see Le Grand et al., 2007). All MRFs regulate gene expression by binding to E-box motifs, highly conserved stretches of DNA sequence (CANNTG) found in the promoter region upstream of muscle specific genes, and turning on expression of specific gene targets that are involved in myofibre formation (Yafe et al., 2008). It is prudent to note that looking at all the research regarding satellite cells put together, it becomes clear that not all satellite cells are exactly the same. There is heterogeneity among satellite cell populations, with some being more readily committed to myogenic proliferation while others are in a noncommitted form. This phenomenon is discussed in more detail in Rudnicki's review paper (Kuang et al., 2007). Suffice it to say that it is not surprising then that while the overall pathway for satellite cell activation to maturation is described rather well by examining the MRFs, there are clearly other factors that come into play as well, and not much is known about the exact signalling of these pathways.

The role of myostatin in satellite cell-related muscle fibre growth is a controversial one. Some research indicates that myostatin is responsible for arresting satellite cells in quiescent stage, therefore preventing them from proliferating and leading to increased muscle fibre numbers (Amthor et al., 2006), this work was done by Dr. Patel's group, and it shows that addition of myostatin protein to muscle cell culture causes a downregulation of MyoD, Myogenin, and Myf5 but not Pax7 (the quiescence

marker). This supports the notion that myostatin null mice would have greater satellite cell proliferation and consequently, a greater number of mature fibres, the process of hyperplasia. The same group, however, published another study stating that myostatin does not act on satellite cells, and that hypertrophy of existing fibres is the main outcome of blocking myostatin action (Amthor et al., 2009). They concluded this after counting the overall number of myofibres in the EDL muscle in wild-type and myostatin null mice and simultaneously analyzing the CSA of those fibres. They found that the CSA in the myostatin null mice does, in fact, differ while the overall number of fibres is not significantly different between wild-type or knockout mice. Other research shows that myostatin up-regulates/activates the cell cycle arrest protein p21, thereby limiting the proliferation of satellite cells (Manceau et al., 2008). This conclusion was reached when the group performed myostatin overexpression and myostatin inhibition experiments on chick and mouse embryos. Using immunofluorescence, the aforementioned author reported that in the increased myostatin pool of cells, less proliferation of satellite cells was observed and more p21 was apparent. In the myostatin deficient pool of cells the opposite was true, more proliferating satellite cells and less p21 expression was observed. Dr. Kambadur's group published a study focusing on myostatin's role in inhibiting Pax7, and found that adding myostatin to cultured developing myoblasts decreased their expression of Pax7 by 80% (McFarlane et al., 2008). In the same study they show that myostatin-null cultured cells express more Pax7+ quiescent cells than the wild-type cells do further showing the early involvement of myostatin in regulating the self-renewal abilities of satellite cells. While myostatin is definitely characterized as a protein that

inhibits the overall growth of muscle fibres, the debate continues to be whether it is primarily through increased hyperplasia or hypertrophy that myostatin null muscles grow.

Dr. McCullough's group investigated the role of myostatin in satellite cell activation (Dasarathy et al., 2004). They studied myostatin and insulin-like growth factor-1 (IGF-1) expression (a known player in the muscle growth pathway, stimulating AKT-PI3K pathway), and how that would affect the expression of cyclin-dependent kinase inhibitor (CDKI p21), myf5, MyoD, and Myogenin (Dasarathy et al., 2004). These are all stimulators of satellite cell differentiation; CDKI p21 is controlled in opposite fashions by myostatin and IGF-1. The results showed that muscle wasting due to induced liver cirrhosis of rats had myostatin, ActRIIB, and CDKI p21 all increased one to three fold, while MyoD, myf5, and myogenin all decreased two to three fold, also IGF-1, and IGF-1 receptor decreased (Dasarathy et al., 2004). These data show that myostatin does, in fact, inhibit satellite cell proliferation and differentiation, thereby retarding the ability to make new myofibres. This supports the idea that hyperplasia does occur in the myostatin null model. Other research has shown that myostatin arrests myoblast transition from G1 to S phase and from G2 to M phase in the cell cycle (for review, see Kocamis et al., 2002). Some research shows that myostatin inhibits Pax-7. Using in vitro assays on C2C12 cells, Dr. Kambadur and collegues showed that myostatin null clones showed higher expression of Pax-7, while increasing myostatin in culture decreased Pax-7 detection using western blots, as well as immunohistochemical fluorescence detection (McFarlane et al., 2008). This provides further insight into how myostatin directly affects satellite cells in muscles by promoting the quiescence of satellite cell activation and proliferation and, therefore, overall muscle ability to grow or regenerate.

Another study from Dr. Kambadur's group shows that fast fibre types (Myosin heavy Chain IIX and IIB) express MyoD in much greater amounts than slow fibre type (MyHC I and IIA). This could explain why Myf5 and MyoD appear to have overlapping functions in inducing satellite cell proliferation (Hennebry et al., 2009) since MyoD would act more specifically on the fast fibres only. In this paper, myostatin is reported to negatively regulate MyoD, showing that its absence allows for higher expression of MyoD in bicep, as well as tibialis anterior muscles. Their results show that myostatin is a direct inhibitor of satellite cell proliferation, and in myostatin null mice the ability for these quiescent cells to proliferate and mature is enhanced through higher expression of MyoD and its ability to turn on expression of genes related to cell activation and proliferation. In this same paper, Kambadur's group also shows that in the absence of myostatin, another transcription factor, myocyte enhancer factor 2 (Mef2) is downregulated, as is Calcineurin. The latter observation was reported by Dr. Michel and his collegues earlier (Dunn et al., 1999). Both of these proteins are known to be inducers of the slow fibre type generation, and their downregulation explains why in myostatin null mice, there is a decrease in slow fibre numbers. Dr. David Goldhammer's group also studied satellite cell proliferative action as it relates specifically to MyoD, and their study shows that MyoD is expressed in committed proliferating satellite cells, and its expression was maintained through to mature myofibres, reaffirming the fact that MyoD and Myf5 have an overlapping function that is distinct from Pax7 (Kanisicak et al., 2009).

1.7: Myostatin and Calcineurin

While the IGF-Akt pathway is the most well known signalling pathway leading to skeletal muscle hypertrophy, there are other pathways that contribute to this physiological

result. In the last decade several studies have been published linking muscle hypertrophy to calcium ion fluctuations and more specifically the actions of calcium on the calcineurin (Cn) pathway (Dunn et al., 1999). In their study, using inhibitors of calcineurin, Dr. Michel's group showed a link between calcineurin and the expected fibre-type switching to slow fibres associated with plantaris overload. They also show that when treating the muscle with the calcineurin inhibitor cyclosporine A (CsA), there was a marked inhibition of myofibre hypertrophy, which further links Cn to muscle growth pathways. Dr. Engvall's group treated C2C12 cells with metalloprotease inhibitors, known as HIMPs, and examined the effect on muscle cell growth and maturation (Heut et al., 2001). Using TAPI and BB-3103, two known HIMPs, they showed maturation from myoblasts to multi-nucleated myotubes and hypertrophy measured as cell diameter increases (Heut et al., 2001). They introduced proteins known to be involved in the calcineurin pathway for muscle cell growth, specifically IGF-I, cyclosporine A, and calcineurin. While there was no change to cell culture sizes with the addition of HIMPs, introduction of these metalloprotease inhibitors did cause an increase in the full-length myostatin (the pro-peptide) and, therefore, an attenuation of the proteolytically cleaved active homo-dimer of myostatin. Taken together their data suggests that HIMPs act on myostatin and not the calcineurin pathway to allow for cell hypertrophy.

Dr. Wackerhage's group isolated whole cell proteins from extensor digitorum longus and soleus muscles from rats. Using antibodies specific to signalling pathways known to be involved in muscle cell growth, they compared the concentrations of these proteins to show the difference between fast and slow muscle fibre signalling pathways (Atherton et al., 2004). Their results showed that EDL has 1.43 times the amount of

calcineurin, 1.95 times more myostatin, 1.44 times more Akt and 6.86 times more p70S6K compared to soleus. The EDL showed lower amount of extracellular signal regulated kinase (ERK) compared to soleus muscle (ERK1 0.38, ERK2 0.61, ERK6 0.15) as well as lower amounts of NF-κB (0.32) and GSK3β (0.69). Overall this paper showed that fast (glycolytic) muscle fibres have different concentrations of important signalling proteins as compared to slow (oxidative) muscle fibres.

Dr. Yasuhara's group treated mice with cyclosporine A (CsA) injections into the TA, over a progressive time-course of 1, 2, 4, 6, 9 and 14 days. Using RT-PCR, western blots and immunohistochemistry, they monitored the changes in several proteins involved in the growth and atrophy pathways in muscle cells (Sakuma et al., 2005). Their data showed that CsA injections showed a significant upregulation of myostatin, as well as Smad3 and TGF-β2. This is of great interest to us since it suggests that there might be *in vivo* proteins that can have a role similar to CsA, inhibition of the hypertrophy inducing calcineurin pathway and upregulation to the negative regulation/atrophy inducing myostatin pathway.

Several of the studies done on myostatin were performed by James Reecy's group. Using microarray assays and proteomic profiling, they identified hundreds of genes and dozens of proteins that express differently in myostatin null muscles as compared to wild-type muscles (Steelman et al., 2006, Ilham et al., 2009). In these studies they show that generally there is a definite switch in myostatin null muscle away from oxidative pathways (employed by slow fibre types) to the glycolytic pathways (employed by fast fibre types). This is further illustrated by Dr. B Spiegelman's group, where they show using fluorescence microscopy a 30% increase in myosin heavy chain

IIB fibres (fast fibres) and in IIX in myostatin knockout mice as compared to wild-type mice (Handschin et al., 2007).

Another study from Yasuhara's group showed that CsA injection blocked mechanical overload of the soleus muscle, achieved by surgical ablation of the ipsilateral gastrocnemius muscle (Sakuma et al., 2008). In this paper they show Mef2c and myogenin are down-regulated both at the mRNA and protein levels following 4 and 10 days of mechanical overloading performed on CsA injected muscle. This result is noteworthy because McCullough's group (Dasarthy et al., 2004) had shown that the myostatin gene has binding sites for myogenin as well as MyoD, Myf5. This is a further indirect link between the calcineurin and myostatin pathways, raising questions concerning whether there are any *in vivo* molecular signals that can have the same dual role that CsA appears to have on these pathways.

1.8: Myostatin and Muscle Atrophy

With compounding evidence showing the effects of myostatin on muscle growth, researchers set out to understand the role of myostatin in muscle atrophy. What might be the role of myostatin in muscle wasting? Is it directly linked to upregulation of proteolytic pathways in muscle, or not. If muscles are growing, would myostatin be downregulated because of its link to proteolysis within muscles? These questions led have researchers to investigate if there was a link between myostatin and muscle atrophy. Atrophy is described as a decrease in muscle mass due to protein degradation (proteolysis) is stemming from the disuse of muscle or from a diseased state. Muscle fibres being excitable cells would not be able to survive if not stimulated. Therefore,

using models that inhibit or hinder muscle stimulation, such as sciatic nerve denervation, or hind-limb suspension, as well as drug administration (glucocorticoids and neurotoxins) can be helpful models to test atrophying muscle in *in vivo* and *in vitro* experiments.

The molecular signalling pathway that is most relevant to muscle atrophy is known to go through the Forkhead family of transcription factors, also known as Forkhead boxes, or Foxo's. These are transcription factors that bind to and arrest the transcription of genes involved in the proteolytic catabolism of muscle cells (for review see: Zhang et al., 2007). Specifically, Foxo1a and Foxo3a are shown to be involved in muscle fibre atrophy by arresting the transcription of ubiquitin ligase genes MuRF and MAFbx (also known as atrogin-1). When phosphorylated, FoXo is translocated out of the nucleus promoting the transcription of these ubiquitin ligases is allowed to occur. The ubiquitin ligases can then begin ear-marking muscle fibre proteins with multiple ubiquitins which then signal and direct proteins to be degraded by the massive proteosome complexes that breakdown proteins into amino acids that can be recycled for other uses (for review see Nader et al., 2005).

To link myostatin to atrophy, Dr. Fei Ding's lab examined a time-course expression profiles of myostatin after denervation, a model known to cause muscle atrophy due to disuse of the excitable muscle fibres (Shao et al., 2007). As deduced from RT-PCR and protein expression experiments, a marked increase for mRNA and myostatin protein was observed, peaking between days 3 and 7 (for mRNA) and days 7 and 14 (for protein), suggesting the strong correlation between myostatin presence and muscle atrophy due to denervation.

Dr. Thissen's group tested the effect of injecting the glucocorticoid drug dexamethasone into the tibialis anterior, gastrocnemius, and soleus muscles of myostatin knockout mice versus wild-type mice, and their results showed that dexamethasone did not cause atrophy in muscles where myostatin is not present, further suggesting that myostatin is involved in the atrophy pathway (Gilson et al., 2007). They also showed that there was a greater increase of FoXo3a, MuRF1, atrogin-1, and Cathepsin L in wild-type mice versus myostatin knockout mice. This suggests that myostatin does have a role in the FoXo signalling pathway for protein degradation. Dr. Freyssenet has reviewed the potential link between myostatin and the Foxo pathway (Favier et al., 2008). The following figure summarizes the proposed pathway of control from myostatin to FoXo.

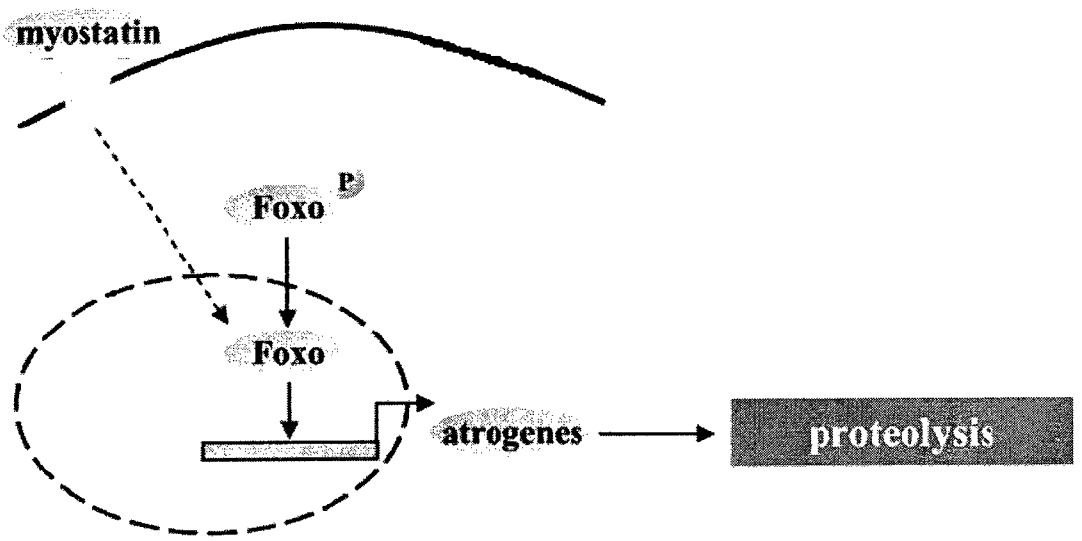

Figure 1.6: Hypothesized interaction between myostatin and Foxo leading to protein degradation. Modified from Favier et al., 2008

Dr. Unterman's group tested the relation between FoXo and myostatin *in vitro* by mutating the myostatin promoter region in C2C12 cells, which is hypothesized to be the binding site of FoXo, and noticed a significant decrease in myostatin promoter activity using luciferase and GFP as assay markers for protein activation (Allen et al., 2007). This suggests that myostatin is a downstream effector protein of the Foxo signalling pathway for muscle atrophy, as shown in Figure 1.6. The study also examined the protein levels of myostatin, Foxo1, and activin receptor IIB in fast versus slow muscles. Consistent with previous findings, all these proteins were found elevated in fast muscles as compared to slow muscles, suggesting different pathways for atrophy between the different types of muscle fibres.

2: Introduction

2.1: Overview

Studies mentioned earlier (Amthor et al., 2009, Gilson et al., 2009) lend their support to the idea that myostatin controls muscle growth by inhibiting or attenuating the hypertrophy pathways in muscles. Other groups, such as the Kambadur and Sharma (McCroskery 2003 & 2005, Salerno 2004, McFarlane 2005 & 2008, Hennebrt 2009) and Cabello groups (Joulia-Ekaza 2006 & 2007) published studies that support the idea that myostatin is involved in inhibiting hyperplasia by attenuating the proliferative capacity of muscle satellite cells. There are also studies that propose a dual role for myostatin in regulating both hypertrophy and hyperplasia. Dr. Se-Jin Lee, the first to characterize myostatin as a protein involved in muscle signalling, and the designer of the myostatin knockout mouse model, states that both hypertrophy and hyperplasia are inhibited by the actions of myostatin (Lee 2001 & 2007).

Evidence from all of the research mentioned above can be summarized to suggest that under normal maturation conditions, alterations to myostatin levels *in vivo* as well as *in vitro* cause an increase in myofibres size and number. However little is known when the growth rates are altered to test how myostatin's inhibition is affecting the pathways involved. Specifically, it is not understood whether inhibiting myostatin and inducing growth stimuli will lead myofibres in vivo to react by up-regulating pathways involved in hypertrophy or hyperplasia, and how different are these pathways from wild-type myofibres with their myostatin levels un-interfered with prior to the growth stimulus induction. To state more clearly: Does genetic manipulation resulting in the genesis of myofibres lacking myostatin cause a significantly altered method of reacting to growth stimuli as compared to wild-type myofibres, or do myostatin null fibres react in the same

manner as wild-type fibres when facing a similar growth stimulus. Our research group set out to elucidate the true effect of myostatin in vivo and the subsequent reaction of these myofibres to a substantial growth stimulus in the form of functional plantaris overloading.

2.2: Objective and Hypothesis

To further understand the role of myostatin in regulating muscle growth, a study was initiated in our research lab that concentrated on comparing myostatin null mice to wild-type mice and how the plantaris muscle is affected by the lack of myostatin or in its presence. Using the same knockout mouse model that was generated by Dr. Se-Jin Lee, we set out to study muscle growth over short, intermediate, and long periods of time, concentrating on deciphering the pathway of growth that muscle cells would take in the presences or absence of myostatin. The objective was to try to better characterize the method of growth that myostatin null muscle cells undertake to achieve their enhanced phenotype of larger sized muscles as compared to wild-type muscle cells. Specifically, we wanted to observe whether the preferred path of muscle growth was hypertrophic in nature, meaning increased size of pre-existing cells, or hyperplasic in nature, meaning increased proliferation of cells adding new fibres to the muscle. We hypothesized that the hypertrophic and hyperplasic growth pathways will be more potentiated in myostatin null mice as compared to their wild-type counterparts. Meaning, we proposed that myostatin was a type of "molecular braking system" that would slow down both types of muscle growth, and removing this protein will result in the ability to use both types of growth pathways more often. As it was said earlier in the introduction, there seems to be some controversy regarding what pathway myostatin is involved in downregulating in wild-

type muscle, and we attempted to produce a set of experiments that would lead to deciphering this question.

2.3: Experimental Design

In order to study muscle growth in mice, there can be several experimental designs that have been utilized previously. Some include voluntary or involuntary exercising, like rolling exercise balls or cage wheels, also shallow pool swimming is utilized by some groups. However, while these designs do show measurable results, in our group we sought an experimental method that would cause maximal effect on the muscle studied, in this case the plantaris muscle. Therefore, we employed the surgical operation known as plantaris functional overloading (Dunn et al., 1999). Used for decades, the compensatory overloading of the plantaris muscle is achieved through the surgical removal of the synergistic muscles, the soleus and gastrocnemius that are found surrounding the plantaris muscle in the calf of the hind limbs. By removing these two muscles, and then carefully suturing the limb and allowing the mouse to regain consciousness, the whole weight of the mouse then falls on this one muscle whenever the mouse utilizes its hind limb to move or stand (Dunn et al., 1999). This permanent added weight on the plantaris acts as a permanent method of increasing the workload on the muscle, allowing for rapid growth until the muscle plateaus (usually reaching double the original size) at a point when it reaches the proper size to compensate for the lack of soleus and gastrocnemius (Dunn et al., 1999).

Overloading was allowed for certain predetermined periods of time, a short overload period of three days, an intermediate overload period of two weeks and a long

overload period of six weeks. These time points would serve to help us understand the changes that occur from a relative beginning of the overload period, to a relative ending of the overload period, when the plantaris has presumable reached its full compensatory ability for the lacking gastrocnemius and soleus. When the period of overload is reached, the plantaris is extracted from the anesthetised mouse and weighted, then it is stored in -86°C freezers either in Eppendorf vials or with cutting compound (O.C.T) surrounding it to preserve it for histological cryosectioning at a later point. Histological and biochemical experiments are then performed using these stored tissues so that we can more specifically analyze the differences in muscle growth patterns between the myostatin null mice to the wild-type mice. Details of the experiments performed are found in the Materials and Methods section.

3: Materials and Methods

3.1: Transgenic Mice Models and Breeding

The main strain of wild-type mouse used for this study was C57/BL6 purchased from Charles-River laboratories, and the myostatin null ($Mstn^{-/-}$) mice from C57/BL6 background strain with a disruptive neomycin insert in their myostatin gene (McPherron et al, 1997). Heterozygotes ($Mstn^{+/-}$) were donated by Dr. Se-Jin Lee (Johns Hopkins, MD). Breeding of male and female heterozygotes resulted in 25% progeny that lacked functional myostatin and subsequent Mstn-/- mice were generated from mating those homozygote offspring. Other transgenic animals used in this project were: CnA* mice generated from C57/BL6 background strain over-expressing a constitutively active form of the Calcineurin A subunit due to absence of an auto inhibitory domain (Dunn *et al*, 2000); CaMBP mice from CD1 (white) wild-type mouse background strain over-expressing a calmodulin binding protein (Dunn *et al*, 2000); PV-HA mice on from CD1 background strain over-expressing parvalbumin, a calcium buffering protein that sequesters internal calcium (Corin *et al*, 1994); NFATc2-/- mice from Balb/c (white) wild-type mouse background strain null for the Nuclear Factor of Activated T cells c2 isoform donated by Dr. Grace Pavlath (Hodge *et al*, 1996).

Whenever a strain was to be studied, the sex and age were matched up with a wild-type strain of the same background as the generated transgenic strain. This was done to minimize the number of variables that differ from mouse to mouse.

3.2: Plantaris Functional Overloading Procedure

All mice studied in this project were around the age of 9 weeks, considered full grown adult at that time period. The overload surgery was performed on pairs of wild-

type and myostatin knockout mice in the same manner as previous published work (Dunn et al., 1997, 1999). Briefly, the mice were anaesthetized with a cocktail of 1.6:1 Ketamine: Rompun the amount being 1µl/100mg of body weight and allowed to resume living for the duration of the overload period previously agreed upon. Muscles were extracted on the day the overload period was complete, with the mice similarly anaesthetized with the same dose of Ketamine: Rompun. After the plantaris was extracted, the mice were euthanized using rapid cervical dislocation and the muscles were weighed and stored in OCT compound frozen in chilled isopentene followed by rapid submersion in liquid nitrogen. All muscles were stored at -86˚C until experimental testing was done on those muscles.

3.3: Semi Quantitative RT-PCR

RNA (2µg) was reverse transcribed to produce cDNA of each sample to test gene expression (Dunn et al., 1997). Negative RT tubes were prepared for each sample and consisted of the same components of the positive RT reaction tubes with ultra-pure water substituting for the addition of reverse transcriptase; this was used as an internal control for the RT-PCR process. Briefly, each reaction tube consisted of 2µg of RNA, 2.5µl of 10pmol/µl random primers (GE healthcare) working solution and ultra-pure water to make equal volumes for each sample. The samples were heated for 10 minutes at 70°C and cooled on ice for 15 minutes to optimize primer binding. Reaction components consisting of 4µl of 10X reaction buffer, 2µl of 10mM dNTP mix (Invitrogen, CA), 1µl of RNAse inhibitor (Ambion, CA) and 1µl of MMLV-RT (Ambion, CA) were added to each reaction tube. Reaction tubes were incubated at 20°C for 15 minutes, 37°C for 60 minutes and finally 65°C for 10 minutes to obtain cDNA. The cDNA obtained after RT

was used for semi quantitative PCR analysis for the various targets via use of specific primer sets. Cycling conditions consisting of an initial denaturation step at 94°C and depending on the target, between 30 to 40 cycles of 1 minute at 94°C, 1 minute at the $T_{Annealing}$, 1 minute at 72°C followed by a termination step at 72°C for 10 minutes. Each PCR reaction tube contained 5µl of KCl PCR buffer (Fermantas), 2.5µl of $MgCl_2$(Fermantas), 2µl of 2.5mM dNTPs, 5µl of each 1µM forward and reverse primer, 0.5µl of Taq polymerase (Fermantas) and 2.5µl of cDNA made up to a total volume of 50ul with ultra-pure water.

Primer	T_{anneal} (°C)	Product size (bp)	Sequence
28S	55°C	142	F 5'-TTGTTGCCATGGTAATCCTGCTCAGTACG-'3
			R 5'-TCTGACTTAGAGGCGTTCAGTCATAATCCC-'3
Atrogin-1	60°C	138	F 5'-GCTTGTGCGATGTTACCCAAGAA-'3
			R 5'-GAAAGTGAGACGGAGCAGCTCT-'3
CnA	53°C	215	F 5'-CGATTCTCCGACAGGAAAAA-'3
			R 5'-AAGGCCCACAAATACAGCAC-'3
BDNF	60°C	486	F 5'-CTGGCTGACACTTTT-'3
			R 5'-AGTAAGGGCCCGAACATACGATTGG-'3
Follistatin	53°C	420	F 5'-CCTACTGTGTGACCTGTAATC-'3
			R 5'-CTCCTCTTCCTCCGTTTCTTC-'3
Myostatin	60°C	495	F 5'-GACGATTATCACGCTACCACGGAAAC-'3
			R 5'-CATCGCAGTCAAGCCCAAAGTCTCTC-'3
Pax-7	58°C	223	F 5'-GTAAGCAGGCAGGAGCTAAC-'3
			R 5'-GGTTCATGAAGCTGTCAGAG-'3
Myogenin	58°C	392	F 5'-AGTGAATGCAACTCCCACAGC-'3

			R 5'- TCAGAAGAGGATGCTCTCTGC-'3

3.4: Ribonucleic Acid (RNA) Extraction

Total RNA was extracted from plantaris muscle using a phenol-chloroform extraction whereby two phases were formed, organic and aqueous layers, with RNA remaining in the aqueous layer, and after centrifugation, the resulting pellet is resuspended in ultra-pure water. Briefly, tissue samples were weighed and homogenized with a hand-held Tissue Tearor (Biospec Products Inc, OK) for 30 seconds in 1ml/100mg of tissue of a solution comprising 4M Guanidium thiocyanate (Sigma-Aldrich, MO), 25mM Sodium Citrate (Sigma-Aldrich, MO), 0.5% w/v N-laurylsarcosine (Sigma-Aldrich, MO) and 0.1M β-Mercaptoethanol (Sigma-Aldrich, MO).Then 1:10 v/v of 2M Sodium Acetate (Sigma-Aldrich, MO) was added after homogenization to neutralize the negative charge of the RNA. This is followed by the addition of 1:1 v/v of phenol and 1:5 v/v of chloroform, followed by vortexing and incubation on ice for 15 minutes. Centrifugation of homogenates resulted in phase separation; the aqueous upper phase was transferred to a fresh microfuge tube and 2:1 v/v of 99% v/v ethanol added. The contents were vortexed, centrifuged and then the resulting pellet was re-suspended in 70% v/v ethanol to remove excess salt. A final centrifugation was done to pellet the RNA. Lastly, the pellet was air-dried for approximately and hour and then re-suspended in ultra-pure water. RNA/DNA ratio and RNA concentration is determined using a spectrophotometer (Eppendorff Biophotometer, Gernamy).

3.5: Cryosectioning and Immunohistological Experiments

For all immunostaining procedures, the whole muscle was placed on cardboard and the distal, mid-belly and proximal ends marked on the cardboard after extraction from mice. The muscle was then evenly coated with Optimal Cooling Temperature (OCT) mounting medium (Sakura Finetek USA Inc, CA) and placed in a pool of isopentane pre-cooled in liquid nitrogen. The cardboard with mounted frozen muscle was than stored in the larger liquid nitrogen dewer awaiting transfer to a -86°C ultra-freezer for long term storage. All cyrosectioning was done using a Leica cryostat (CM 3050 S model, Leica Microsystems, Heidelberger, Germany) cooled to -23°C and set to a thickness of 10μm. Serial sections were mounted on all slides, and control muscles as well as treated muscle tissue sections were always mounted on the same slide to accurately compare different conditions and eliminate any irregularities between slide treatments. The method was adapted from previous Michel procedures (Dunn et al., 1997).

Briefly, midbelly cryosections of plantaris hind-limb muscles were circled with a hydrophobic PAP pen and blocked in 200μl of blocking solution consisting of 5% w/v Goat Serum (Sigma-Aldrich, MO) in 0.5% w/v Bovine Serum Albumin (BSA) (Sigma-Aldrich, MO) for 30 minutes. They were then stained for the various MyHC isoforms using 250μl of primary antibody developed against MyHC types I (A4.840), IIa (SC-71), IIx (6H1), IIb (BF-F3), Embryonic I (F1.652), Embryonic II (47A) and Neonatal isoforms (N2.261) (Developmental Studies Hybridoma Bank, University of Iowa, Iowa) in 0.5% w/v BSA overnight at 4°C. Three washes in 250μl of 1X Phosphate Buffered Saline (PBS) were done for 10 minutes each before addition of the 250μl of secondary antibody prepared in 0.5% BSA, consisting of either IgG-Horse Radish Peroxidase

(HRP) or IgM-HRP (Sigma-Aldrich, MO) as required by the primary antibody make-up. After incubation in secondary antibody for 2 hours, three washes were done using 250µl of 1X PBS for 10 minutes each. Detection was accomplished using a horse-radish peroxidase substrate, 3-3'-Diaminutesobenzidine [DAB] (Pierce Biotechnology Inc, IL) in hydrogen peroxide (H_2O_2) (ACP, QC) in a coplin jar; air-drying of the slides, and mounting in glycerin jelly was done as a final step.

3.6: Protein Extraction and Western Blotting

Plantaris muscle samples were homogenized on ice using a hand-held Tissue Tearor (Biospec Products Inc, OK) in 6µl/mg of 1X RIPA buffer consisting of 100µl of each of 10X PBS and 5% w/v Sodium Deoxycholate, 10ul of each of Igepal (Sigma-Aldrich, MO), 10% w/v SDS, 1M Sodium Fluoride (Sigma-Aldrich, MO), 1mg/ml Aprotinin (Sigma-Aldrich, MO), 1mg/ml Leupeptin (Sigma-Aldrich, MO), 100mM Phenylmethanesulphonylfluoride (PMSF) (Sigma-Aldrich, MO), and 5µl of 0.2M Sodium Orthovanadate (Sigma-Aldrich, MO) filled to 1ml using autoclaved water. Homogenates were left to incubate on ice for 45 minutes in the RIPA buffer. Centrifugation at 15000 x *g* for 20 minutes followed in a centrifuge pre-cooled to 4°C. The supernatant was then transferred to a clean 1.6ml closed cap vial, and a second round of centrifugation was performed. The final supernatant is transferred to a clean 1.6ml vial for storage at -86°C ultra-freezer.

Proteins in the amount of 50µg were loaded in 8 - 12% w/v SDS acrylamide gels prepared as per the SDS-PAGE Bio-RAD Protocol (Bio-Rad Laboratories Inc, CA) and electrophoresed at 120V through the stacking gel and 120V through the separating gel.

The separating gel consisted of 2.5ml of Tris buffer at pH 8.8, 100µl of 10% w/v SDS, 30% acrylamide solution and autoclaved water amounts that depended on the percentage of gels. The stacking gel consisted of 1.25ml of Tris buffer at pH 6.8, 50µl of 10% w/v SDS, 3.0 ml of autoclaved water and 0.65ml of 30% acrylamide solution. Blotting of the proteins onto a PVDF membrane (Amersham Biosciences, UK) was done by initially soaking the membrane in 100% methanol for 10 seconds, followed by a wash in distilled water for three minutes and incubation in transfer buffer. The filter paper and sponges were also incubated in transfer buffer. Transfers were done for 1 hour at 100V. Membranes are first stained with Ponceau S solution to verify the transfer was successful. The Ponceau S (Sigma-Aldrich, MO) is then washed off using 0.1% Tween-Tris Buffered Saline buffer (T-TBS), and the membrane is then ready for specific protein probing. Membranes were initially blocked for one hour in the proper blocking solution, and then membranes were incubated with primary antibody overnight on a shaker at 4°C. Membranes were then washed 3x 10 minutes with T-TBS, before incubation with a secondary antibody. Membranes were again washed 3x 10 minutes with T-TBS prior to incubation with developing solution. Protein blots were quantified using alpha-Innotech imaging software and analyzed as the integral of band width and intensity

3.7: Statistics

Statistical analysis of data comprised of 1-way ANOVAs were performed for the PCR experiments for the overload time course samples. Student T-tests were performed for all other experiments involving overload and calcineurin pathway PCR analysis. Confidence level of 95% was used to indicate significance for all statistical analyses.

4: Results

4.1: Identification and Characterization of the Myostatin Knockout Model

Myostatin knockout mice have distinct genotypic and phenotypic differences from the wild-type mice used in the study. To verify that the mice used were in fact null for myostatin, several tests were used. Figure 4.1 illustrates some of the characteristics utilized to verify whether the generated mice were in fact null for myostatin. Figure 4.1.A depicts the map of where the neomycin cassette, the homologous construct introduced, is placed within the myostatin gene thus disrupting the nucleotide sequence causing myostatin to be either untranslated to its polypeptide sequence or for myostatin protein to be degraded at once after translation because of the improper folding caused by the introduction of the cassette. To verify that the mice that we generated did have the inserted neomycin cassette, genotyping primers designed to span the sequence encompassing the cassette were used to perform PCR to analyze whether the mouse had the cassette or not, with the bands showing only the larger size PCR product indicating that the mouse had the inserted cassette disrupting myostatin, as seen in Figure 4.1.B. The second step in the verification process was testing for the presence of myostatin mRNA transcripts. Semi-quantitative PCR using primers designed to amplify a section of the C-terminal end of the myostatin sequence produced either a band of 495 base pairs in the wild-type mouse, or an absence of this band in myostatin knockout mice, seen in Figure 4.1.C. This was used to confirm that the myostatin knockout mice were in fact missing the mRNA for the active protein. To further support the absence of mRNA from the Mstn-/- samples, an additional PCR experiment was performed, with increasing number of cycles for the Mstn-/- samples. As seen in Figure 4.1.D, there were never any observed bands in the knockout samples.

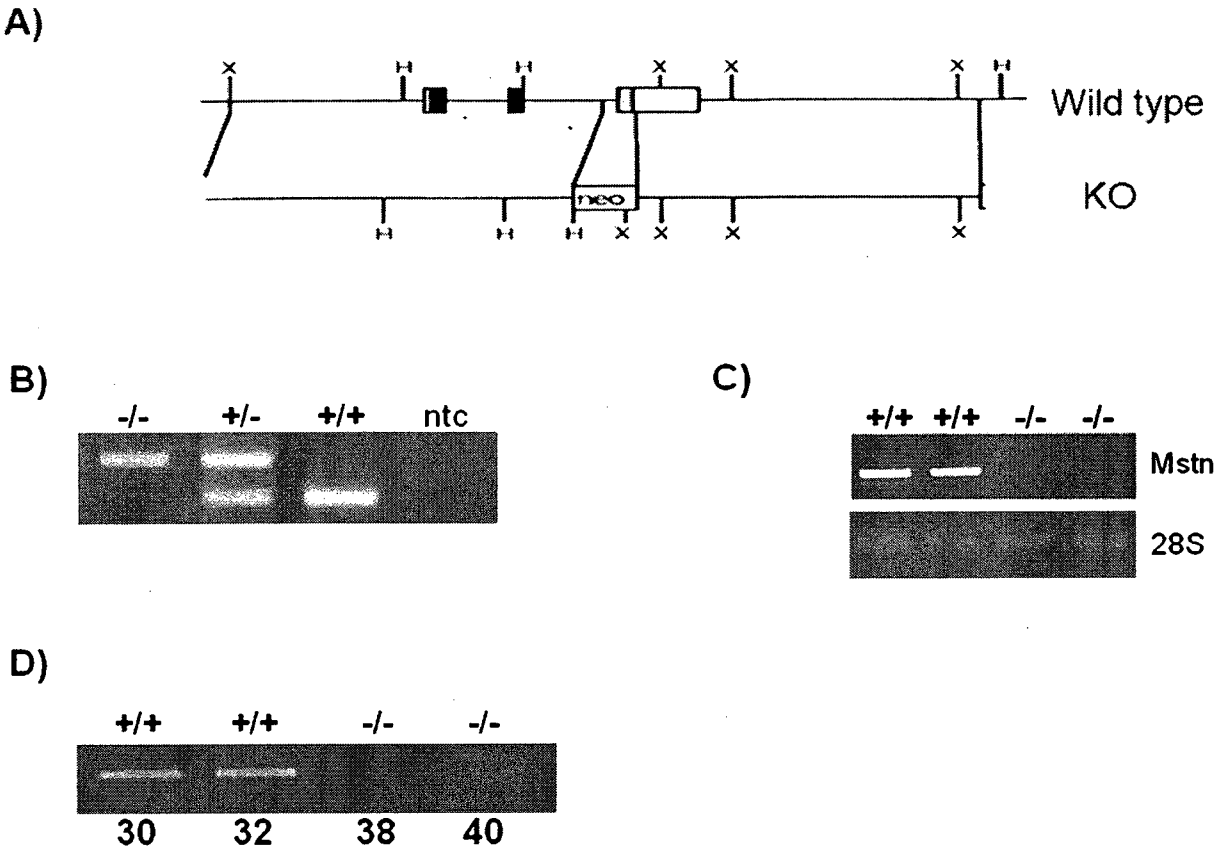

Figure 4.1: Identification of Myostatin Knockout Model A) The myostatin knockout gene has a neomycin cassette inserted to disrupt its transcription (McPherron et al, 1997); B) Representative image for genotyping from mouse tail clippings using primers that recognize DNA portions specific for the Mstn+/+ and Mstn-/- homozygotes or both portions representing heterozygote mice; C) Representative image of PCR product from Mstn mRNA on EtBr stained agarose gel, 28S used as a loading control; D) Mstn PCR product on EtBr stained agarose gels with increased cycle number for the Mstn-/- samples to verify lack of PCR product

Figure 4.2 displays phenotypic changes observed in Mstn-/- mice to validate the effectiveness of the knockout condition. One of the phenotypic data sets is absolute wet weight of the muscles extracted, shown in Figure 4.2.A, which is a primary characterization technique since myostatin knockout mice have muscles that are on average larger than wild-type mice. To illustrate that more clearly, as in Figure 4.2.B, we

used a measurement called relative muscle mass, which includes a correction for the body weight of the mouse, as it relates to muscle weights. By doing so, we could see more clearly that myostatin knockout tissues were larger, with ranges from 20% increases for the soleus muscles, up to 60% increases for muscles like the gastrocnemius and tibialis anterior. In Figure 4.2.C we see an H&E tissue stain for the plantaris muscles from Mstn+/+ and Mstn-/- mice. It illustrates that myostatin knockout mice had muscles that are larger in diameter than the wild-type counterparts. Considering that our functional overload technique is used on plantaris muscles, further analysis for characterization was performed on that specific tissue. Figure 4.2.D-F shows our quantified data for some of the categories that were studied more closely in our overload experimental samples sets. We measured the overall midbelly area from both wild-type and knockout mice, and the results showed that the knockout midbelly is approximately double the size of the wild-type (Fig 4.2.D). This doubling effect was attributed to two separate factors, namely the mean myofibre cross sectional area, seen in Figure 4.2.E, and mean number of myofibres, seen in Figure 4.2.F. Both overall size of the myofibres and their numbers were approximately 50% greater in Mstn-/- plantaris as compared to Mstn +/+ tissue. In Figure 4.2.G we used a different way of analyzing myofibre size to illustrate how the Mstn-/- muscle did exhibit larger fibres than wild-type. All these techniques were used in the study to verify and correctly characterize that the mice used for the study were in fact wild-types or myostatin knockouts.

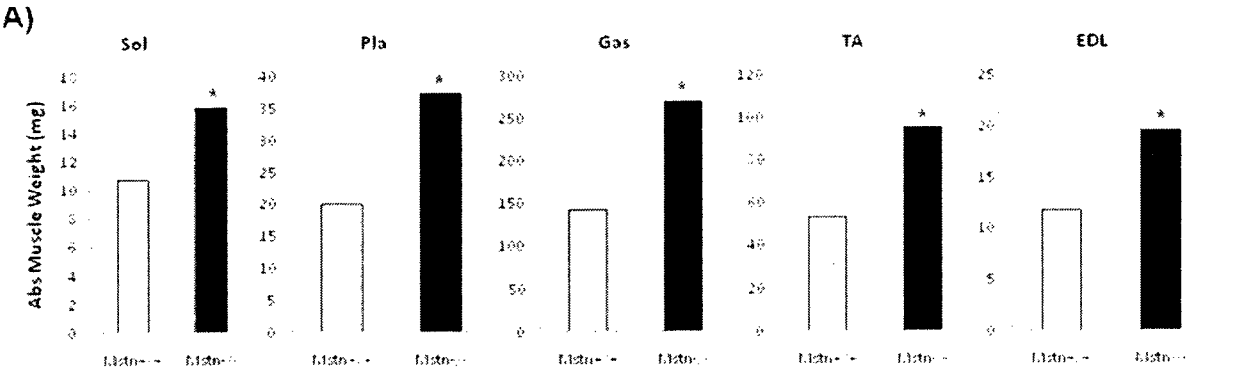
A)
Sol
Pla
Gas
TA
EDL
Abs Muscle Weight (mg)
Mstn+/+
Mstn-/-

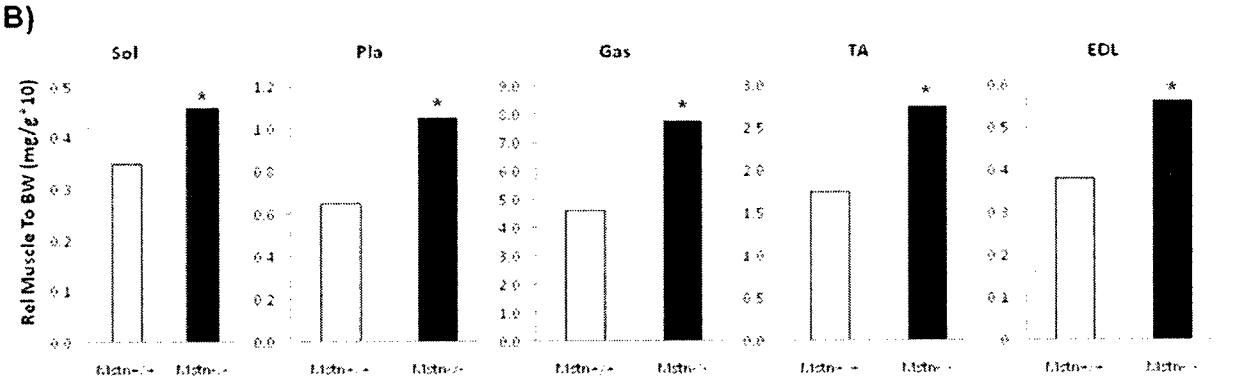
B)
Sol
Pla
Gas
TA
EDL
Rel Muscle To BW (mg/g*10)
Mstn+/+
Mstn-/-

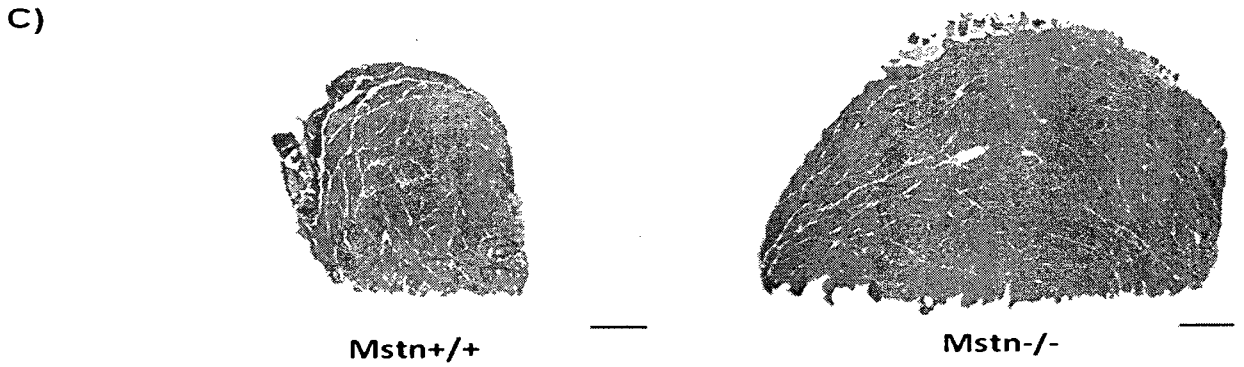
C)
Mstn+/+
Mstn-/-

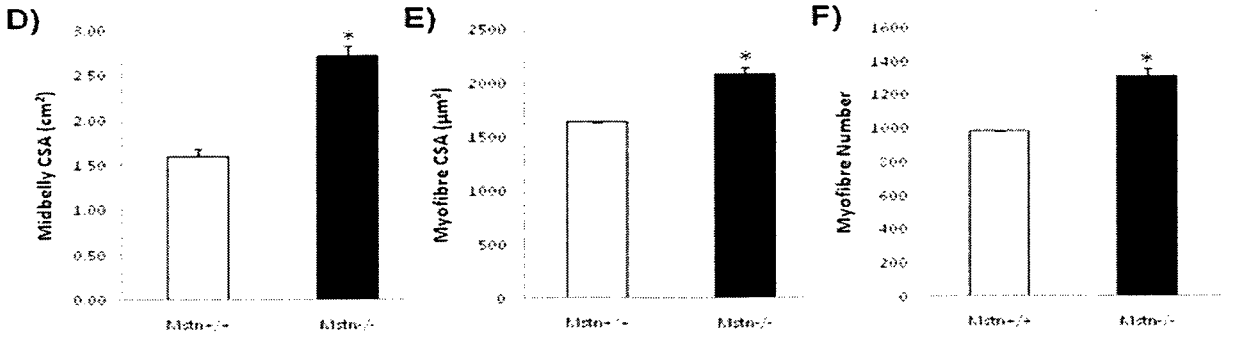
D)
Midbelly CSA (cm²)
E)
Myofibre CSA (µm²)
F)
Myofibre Number
Mstn+/+
Mstn-/-

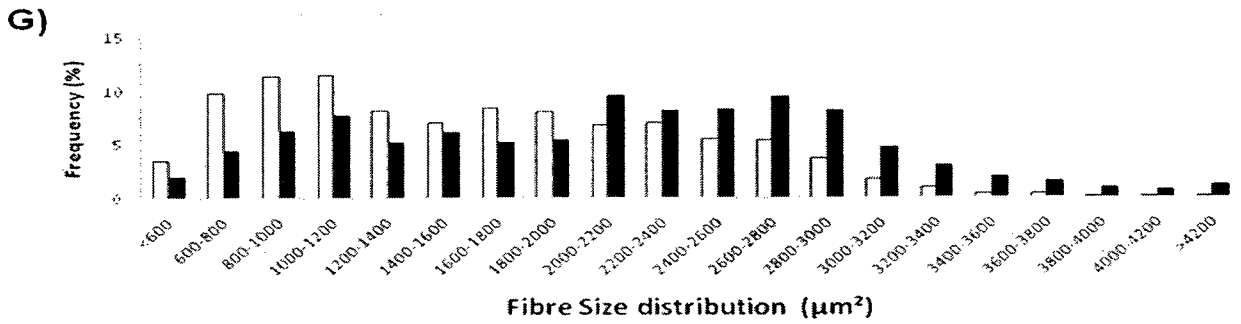

Figure 4.2: Phenotype Characterization of Muscles from Mstn-/- Mice A) Absolute mass of muscle extracted from mouse calf; B) Relative Muscle mass to Body weight graph; C) Haematoxylin and Eosin stain for Plantaris midbelly cross-sections from Mstn+/+ or Mstn-/- mice, Bar scale= 100µm; D) Mean Plantaris Midbelly cross-sectional area; E) Mean Myofibre cross-sectional area; F) Mean myofibre number comparing Mstn+/+ to Mstn-/- plantarii. G) Myofibre Size distribution comparing Mstn+/+ to Mstn-/- plantaris muscle; * indicates $p<0.05$ relative to wild-type group

4.2: Plantaris Muscle Response to Functional Overload

One of the preliminary tests performed after harvesting all of the overloaded plantaris muscles from the various time course points used for the study was testing the mRNA expression of myostatin in the wild-type tissues only (since the knockouts do not express the mRNA, as seen in Figure 4.1.C), to verify that our overload procedure did in fact properly work. In Figure 4.3 we show that myostatin is significantly reduced to approximately one fifth of the original quantity in all overload time course periods, which was consistent with what was previously published regarding the overload protocol (Dunn et al., 1999). This allowed us to continue our experimental analysis of all muscles with the knowledge that the overload procedure was successful from the onset.

Figure 4 is a summary of the overall quantitative measurements analyzed from the overloaded plantarii used in the study. Figure 4.4.A shows the relative weight of overloaded plantarii harvested for the study. The graph shows that while the non-overloaded sample was noted to be significantly different comparing wild-type to knockout muscle, the significance was lost within all the other overload time points, which hinted towards having differential muscle growth paces between wild-type and knockout tissue. Figure 4.4.B represents images taken for some of the muscles extracted for the study, the purpose being to have an estimate of the overall midbelly area of these muscles from wild-type and myostatin knockout mice over the time course of the study. Figure 4.4.C shows the mean cross sectional area from all myofibres analyzed in the study, with the standard error bars indicated. This was a method used to quantify hypertrophy due to the overloading. The hypothesis was with overloading, the average cross sectional area of myofibres would increase in both wild-type and knockout, with the knockout maybe showing greater hypertrophic potential than the wild-type. This was not reflected in the results, which showed a tendency in the overall wild-type fibres to undergo hypertrophy more than the knockout counterparts. This is interesting because it suggests an underlying difference in response between wild-type and myostatin knockout muscle, which was further investigated further. In figure 4.4.D we showed the overall midbelly area from all the muscles for the study. This measurement was expected to be similar in trend (upregulation) in both the wild-type and myostatin knockout mice. Interestingly, after six weeks of overload, our plantarii from wild-type mice showed an overall midbelly area very close in average to the myostatin knockout tissue. The last graph, Figure 4.4.E, shows the mean fibre number in midbelly, calculated by dividing the

overall average midbelly area by the average size of the myofibres. The goal was to try to verify if the knockout muscle had more myofibres on average as compared to the wild-type counterparts, a tendency that was confirmed in the non-overload muscle, but in the overloaded muscle samples we had analyzed this trend was not fully apparent. However it is not hard to predict that if more sampling is done that the trend showing more fibres in the myostatin knockout muscle is indeed true, since it would account for the overall increase in midbelly area and lack of compensatory hypertrophy matching that of the wild-type tissue.

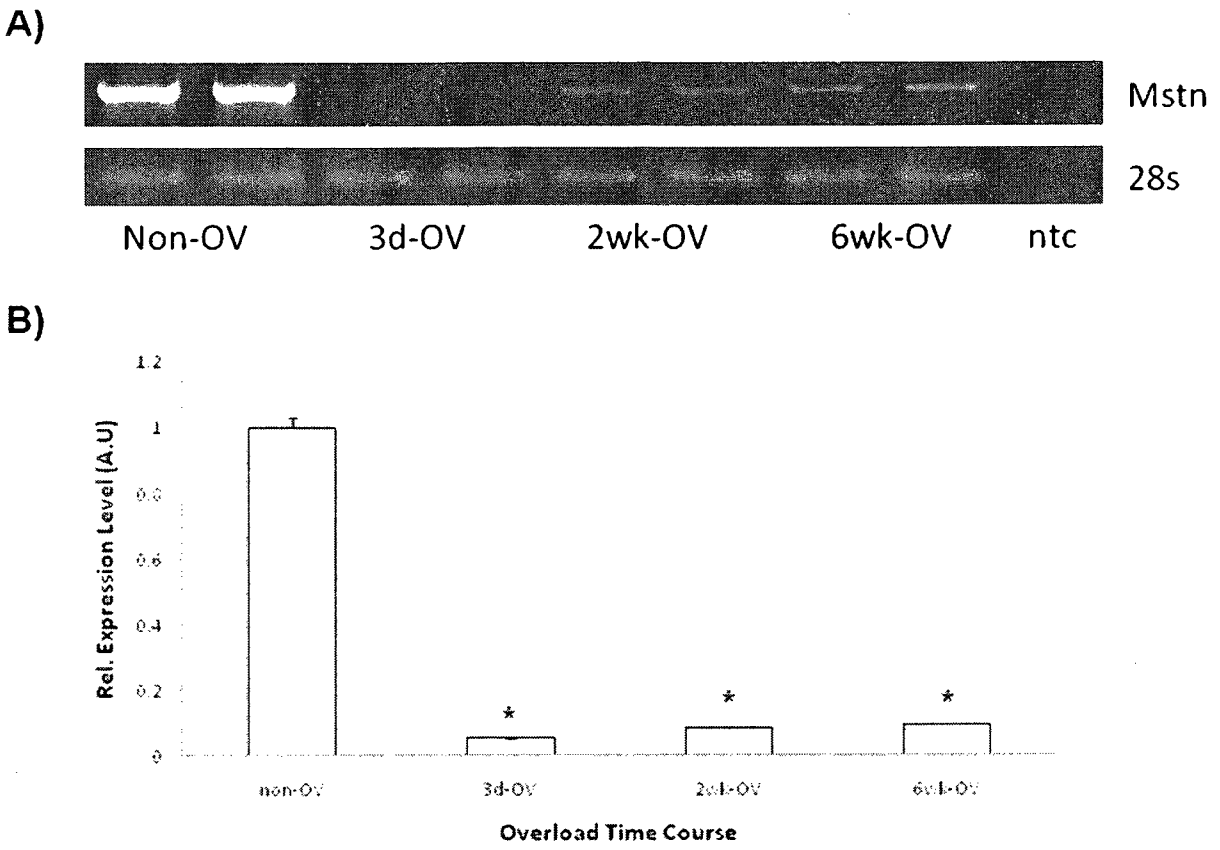

Figure 4.3: Myostatin mRNA Expression in Mstn+/+ plantaris of mice exposed to Functional Overload. A) Representative image of Mstn mRNA on an EtBr stained agarose gel across the various overload periods, 28S used as a loading control; B) Bar graph quantification of mRNA expression relative to 28S. * indicates significance within $p<0.05$ from the non-OV level; ntc= control sample with no cDNA loaded; N=2 per group, preliminary data (experimentally conducted in duplicate).

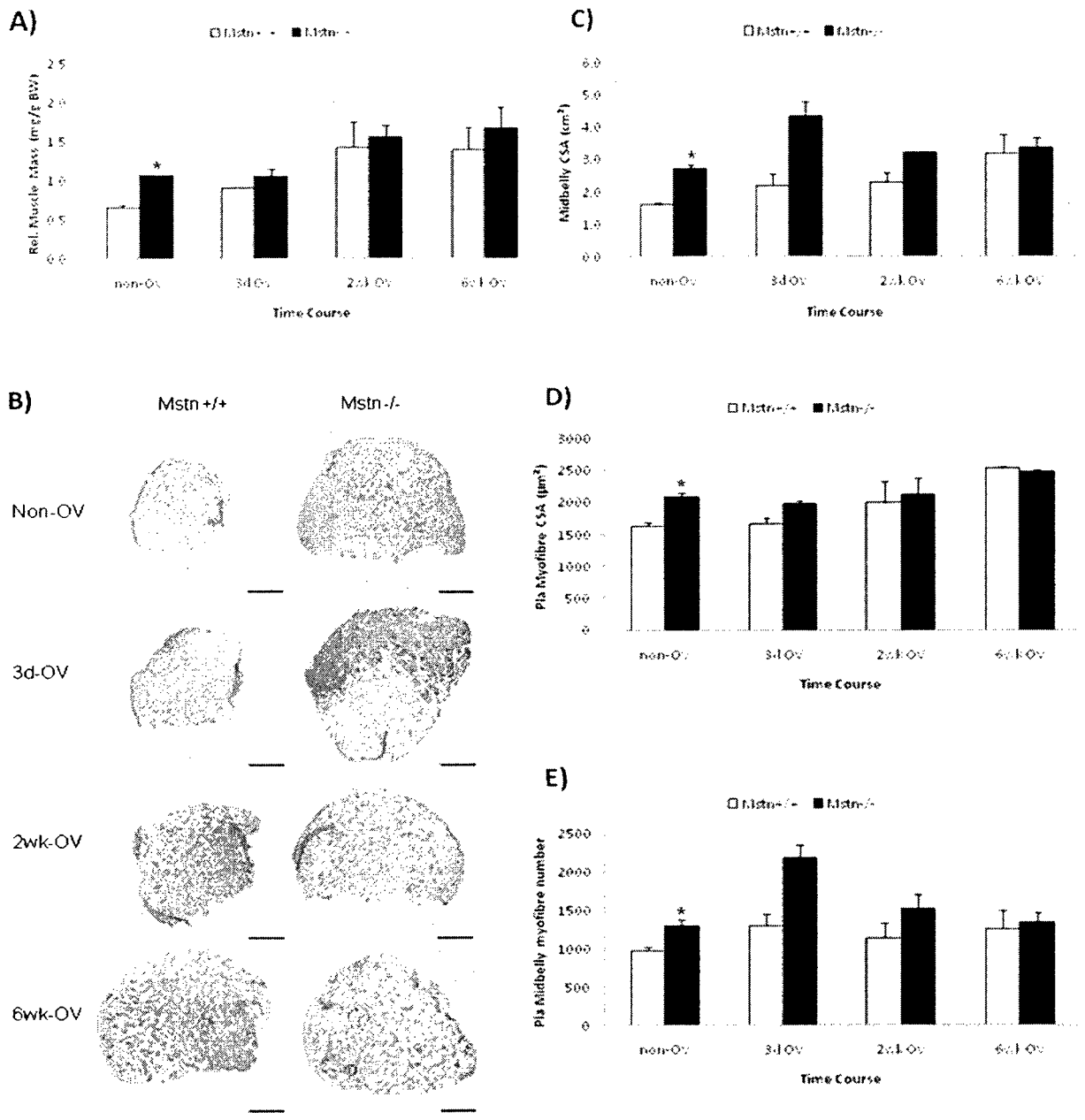

Figure 4.4: Quantitative measurements for Plantaris in Response to Functional Overload. A) Plantaris to Body weight ratio comparing Mstn+/+ Mstn-/- across different overload periods; B) Representative images from sections of plantaris midbellies analyzed, Bar scale= 100μm; C) Mean myofibre cross sectional area comparing Mstn+/+ Mstn-/- across different overload periods; D) Mean Midbelly Area comparing Mstn+/+ Mstn-/- across different overload periods; E) Mean myofibre number in midbellies comparing Mstn+/+ Mstn-/- across different overload periods. * indicates $p<0.05$ relating to the wild-type measurements; N=3 for the Non-OV samples, N=2 for OV time course samples

4.3: Myofibre Size and Fibre-Type Proportions Response to Functional Overload

Figure 4.5 lends more evidence to what was previously seen as a difference in hypertrophy response between the wild-type and myostatin knockout plantarii tested. We measured the increase of myofibre cross sectional area of the different MyHC isoform expressing fibres. In the non-overloaded tissue, seen in Figure 4.5.A, all myofibre types showed a tendency to be smaller than the knockout myofibres, by an average measure of approximately 5-10%, not enough to be significant with our limited number of samples tested, but enough to register a tendency that could be significant if more samples are tested. After only three days of overload, a marginal change was registered in terms of overall myofibre size, (Figure 4.5.B), which is understandable given the knowledge that it takes weeks for muscle proteins to be synthesized. The results showed that over longer periods of overload, the hypertrophy of all myofibre types was more evident in wild-type plantarii tested as opposed to the knockout muscles, as seen in Figures 4.5.C and 4.5.D. After 6 weeks of overload, the tendency was shifted towards showing bigger CSA averages for the wild-type muscles as compared to the knockout counterparts.

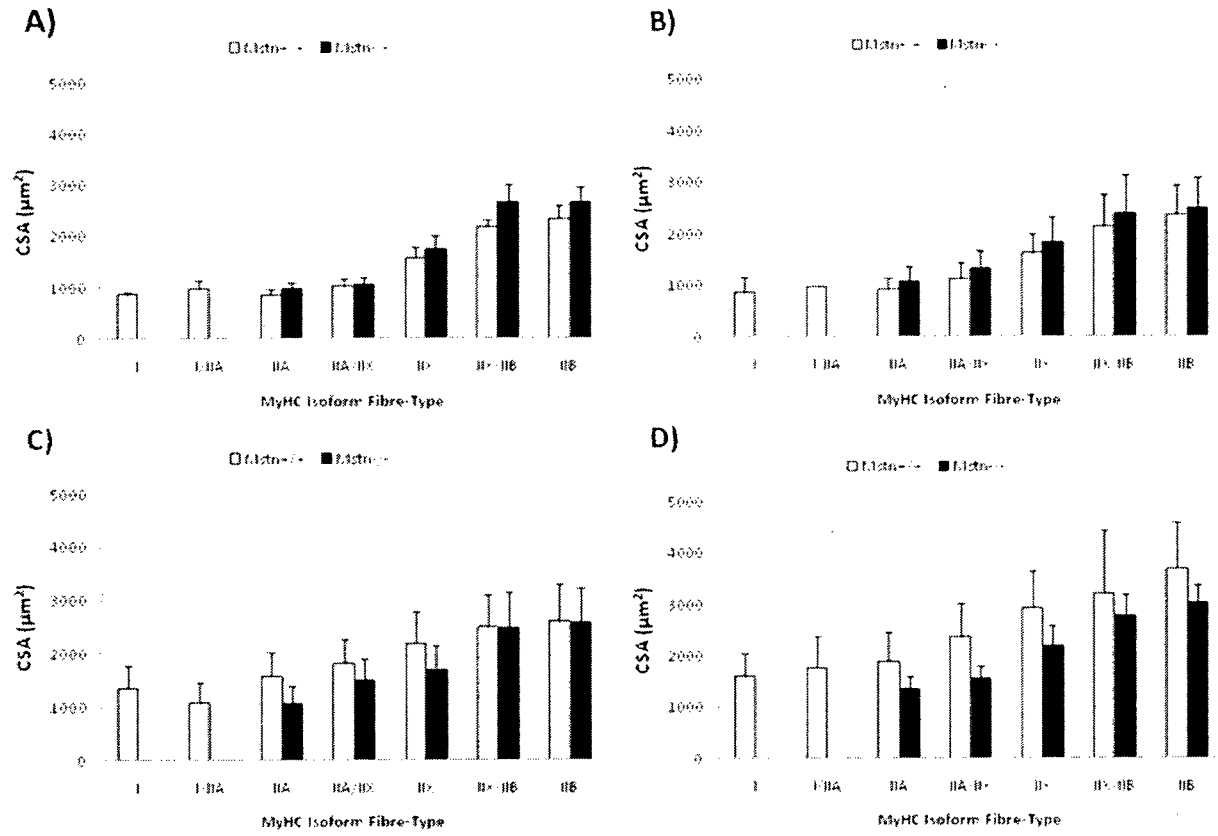

Figure 4.5: Muscle Fibre Size Response to Functional Overload. Myofibre Cross sectional area sizing according to Myosin Heavy Chain Isoform type expressed, A) Non-OV CSA; B) 3day-OV CSA; C) 2wk-OV CSA; D) 6wk-OV CS; N=3 for the Non-OV samples, N=2 for the OV time course samples

Figure 4.6.A through 6.D illustrate that MyHC isoform specific myofibre composition within the muscle changes upon overloading, and the differences were more evident in the wild-type than the knockout muscle. Again due to the small sample size analyzed, the tendencies did not reach statistical significance, but showed a trend that is interesting. The trend was that the wild-type muscle seems to be more capable of fibre-type switching towards the more energy-efficient, oxidative myosin isoforms, than the myostatin knockout fibres. The most evident difference was seen in the complete lack of

the slowest fibre-types (MyHC I, and MyHC I/IIA) in the knockouts, while in the wild-types these fibres steadily increased in proportion as the overload period was extended.

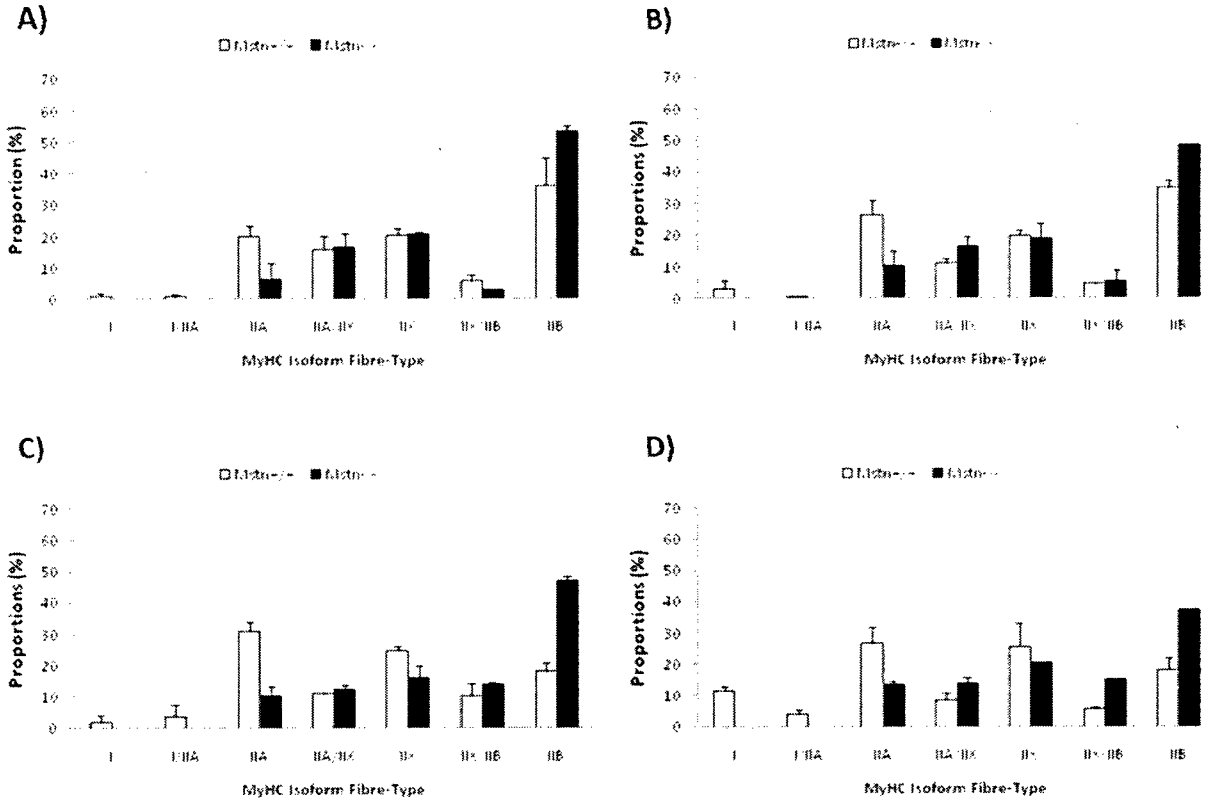

Figure 4.6: MyHC Fibre-Type Proportions Response to Functional Overload. Myofibre Expression Proportions according to Myosin Heavy Chain Isoform type expressed, A) Non-OV CSA; B) 3day-OV CSA; C) 2wk-OV CSA; D) 6wk-OV CS; N=3 for the Non-OV samples, N=2 for the OV time course samples

4.4: mRNA Transcript Expression of Target Genes in Response to Overload

In an effort to explain the observed differences in response between wild-type muscle and myostatin knockout muscle, we tested overloaded tissue for some well known factors induced in muscle growth. Using the RT-PCR technique, (Figure 4.7.A), we measured the mRNA transcript levels of these different targets to try to pinpoint what are

the targets that respond differently in wild-type muscle as compared to knockout muscle. Figures 4.7.B-E represents histograms showing the relative expression levels of the different targets tested in this project. Atrogin-1 did not show any difference between Mstn+/+ and Mstn-/- animals in reacting to overloading stimulus, with both sample groups showing a similar decrease as overloading is extended. The same response was seen with the expression Calcineurin A i.e., no difference between Mstn+/+ and Mstn-/- mice, but a similar decrease in both over extended overloading periods. Brain-derived neurotrophic factor (BDNF) expression initially was measured to be different between Mstn+/+ and Mstn-/-, with an increase of BDNF showing in the knockout muscle relative to its wild-type counterpart. However, with overloading, both Mstn+/+ and Mstn-/- mice showed similar decreases in expression, negating the original discrepancy seen in the non-overloaded samples. Myogenin and Follistatin were the only targets tested that showed differential expression patterns in wild-type and knockout muscle. Myogenin mRNA levels gradually increased during overload, with a tendency for the increase to be more prominent in the knockout muscle as opposed to the wild-type muscle. Follistatin expression dramatically increased in the wild-type group after 3 days of overload and stayed higher than the control group throughout the other overload time points, while the knockout registered only a slight increase that was similar across all time points, much unlike the follistatin expression profile. These findings lent evidence to the assumption that wild-type muscle employs a different signalling pathway for growth than the myostatin knockout muscle.

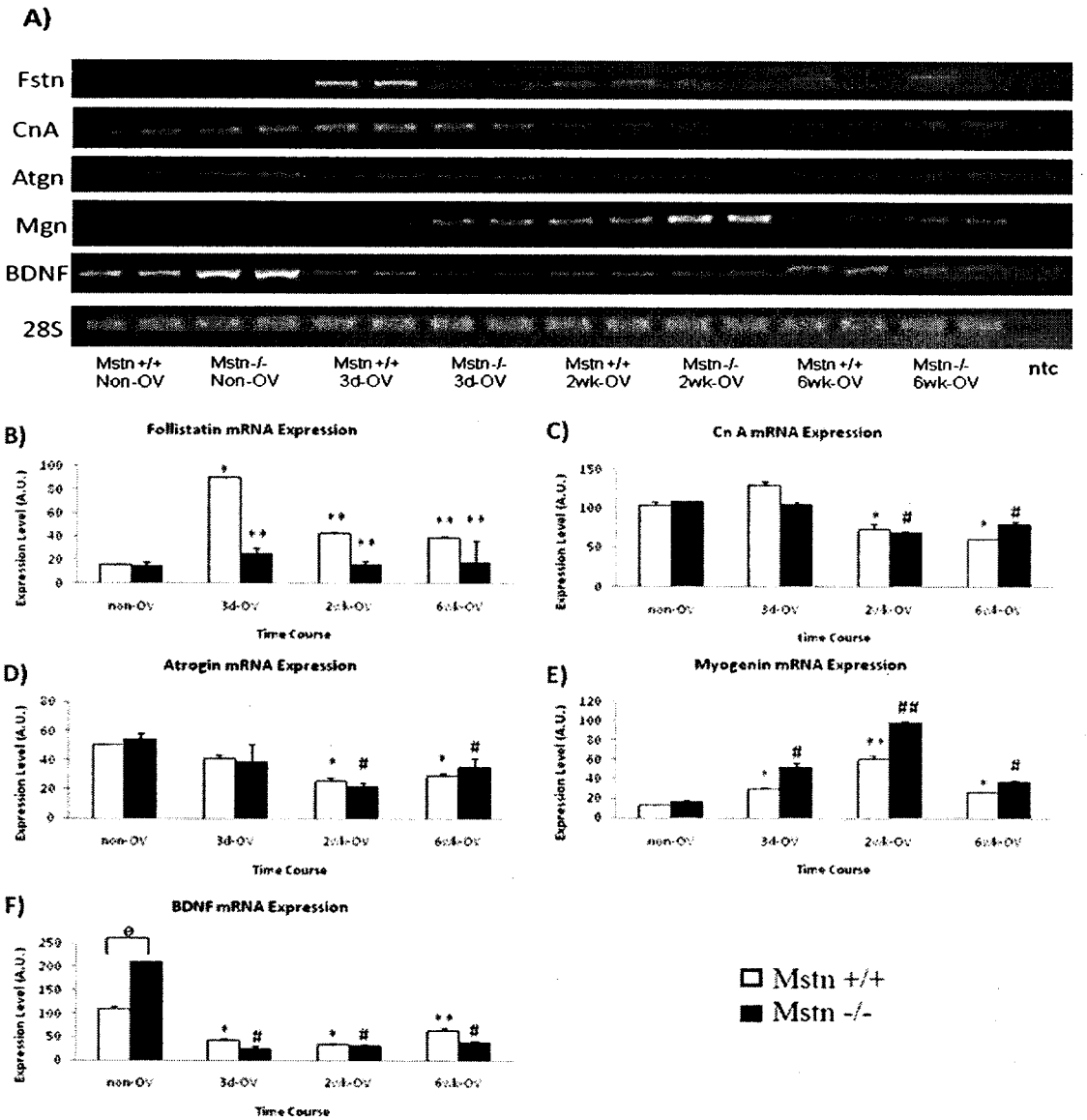

Figure 4.7: mRNA Expression of Target Genes in Response to Functional Overload. A) Representative images of mRNA on EtBr stained agarose gels across the various overload periods for: Follistatin (Fstn), Calcineurin A (CnA), Atrogin-1 (Atgn), Myogenin (Mgn), Brain-derived neurotrophic Factor (BDNF), 28S used as a loading control; B-F) B) Bar graph quantification of mRNA expression. * $p<0.05$ from the Non-OV Mstn+/+ expression levels, ** $p<0.05$ from the 3day-OV Mstn+/+ expression levels, # $p<0.05$ from the Non-OV Mstn-/- expression levels; ## $p<0.05$ from the 3day-OV Mstn-/- expression levels; Θ $p<0.05$ between the paired bars. N=2 per group, preliminary data run once in duplicate

4.5: Protein Expression Response to Functional Overloading

The western blot in Figure 4.8, for protein extracted from the same plantarii that were originally cut and stained for MyHC isoform IHC (n=2 for each time point), and probed for Pax7 protein. The resulting histogram indicated a similar pattern to what follistatin exhibited in mRNA transcript analysis; that being a marked increase in wild-type three day overloaded muscle, then a gradual reduction over the following two time points. The only difference between Mstn+/+ and Mstn-/-, muscle was seen in the three day overloaded muscle, which indicated a fast response to functional overloading early in the process, a response that is evidently different in knockout from wild-type muscle.

Early testing with anti-myogenin antibody on wild-type and myostatin knockout muscle showed, a significant difference in expression of myogenin between the two groups (n=2), namely a three-fold increase in myogenin protein expression in the myostatin knockout plantaris as compared to the wild-type counterparts (in Figure 4.9). The difference was more pronounced at the protein level than the observed expression at the mRNA level that was measured earlier (Figure 7.E).

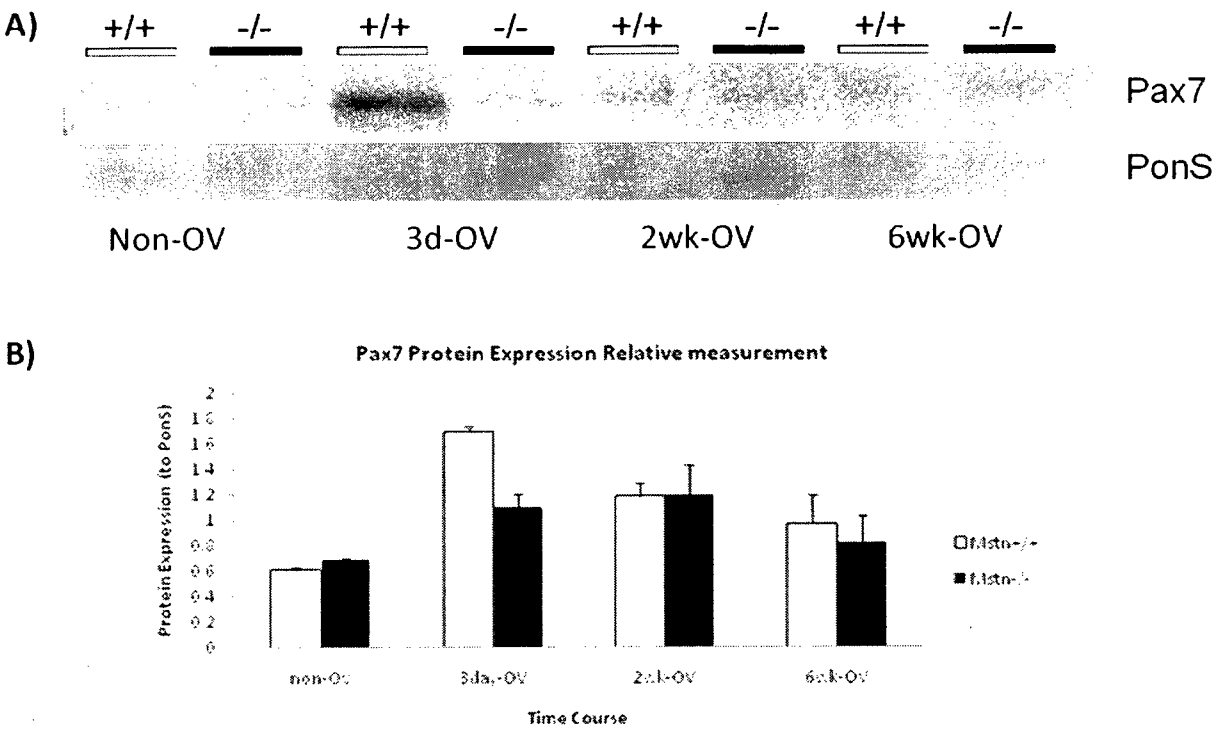

Figure 4.8: Plantaris Pax7 Protein Expression in response to Functional Overload. A) Representative protein western blot representing Pax7 expression across the various overload periods, Ponceu S staining was used as a loading control; B) Bar graph quantification of protein expression; N=2 per group, preliminary data run once per sample

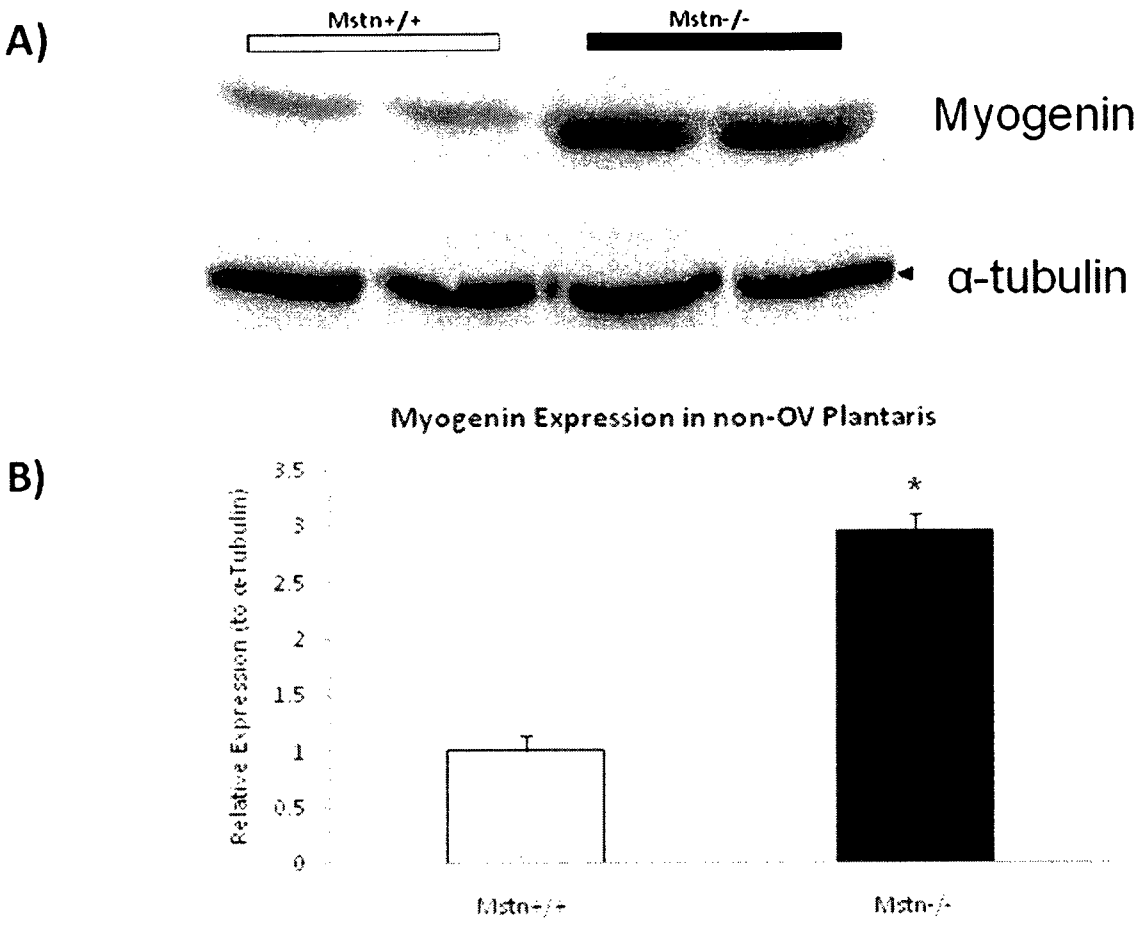

Figure 4.9: Myogenin is differentially expressed in Non-Ov Mstn+/+ or Mstn-/- Plantaris. A) Western blot membrane representing Mstn+/+ or Mstn-/- samples probed with anti-myogenin antibody, α-tubulin was used as loading control; B) Bar graph quantification of protein expression. *indicates significance within $p<0.05$ from the Mstn+/+ expression levels. N=2 per group, preliminary data performed once

4.6: Myostatin Levels in Transgenic Mice variants of Calcineurin Expression

By testing the mRNA transcript levels of myostatin in different transgenic mice models that were engineered to overexpress or lack proteins known to be players in the calcineurin pathway, we tried to shed light on any possible link between the hypertrophy linked calcineurin pathway and the regulatory role of muscle growth dictated by

myostatin. Results in Figure 4.10 showed that mice overexpressing CamBP (n=3) showed a decrease in the myostatin mRNA transcript, while no significant change was observed for the PV-HA transgenic mice (n=3), both compared to CD-1 wild-type mice (n=3), the mouse strain used for generating these transgenic lines. Also tested were the NFATc2 knockout mice (n=3), NFAT being a downstream signalling propagator of calcineurin, and the results showed a marked increase in the myostatin mRNA transcript as compared to the wild-type Balb/c wild-type strain (n=3) that was used to generate this NAFTc2-/- mouse strain. This is interesting because it gives us evidence that inhibiting a direct signal propagator of the calcineurin protein does show a strong upregulatory response in myostatin levels.

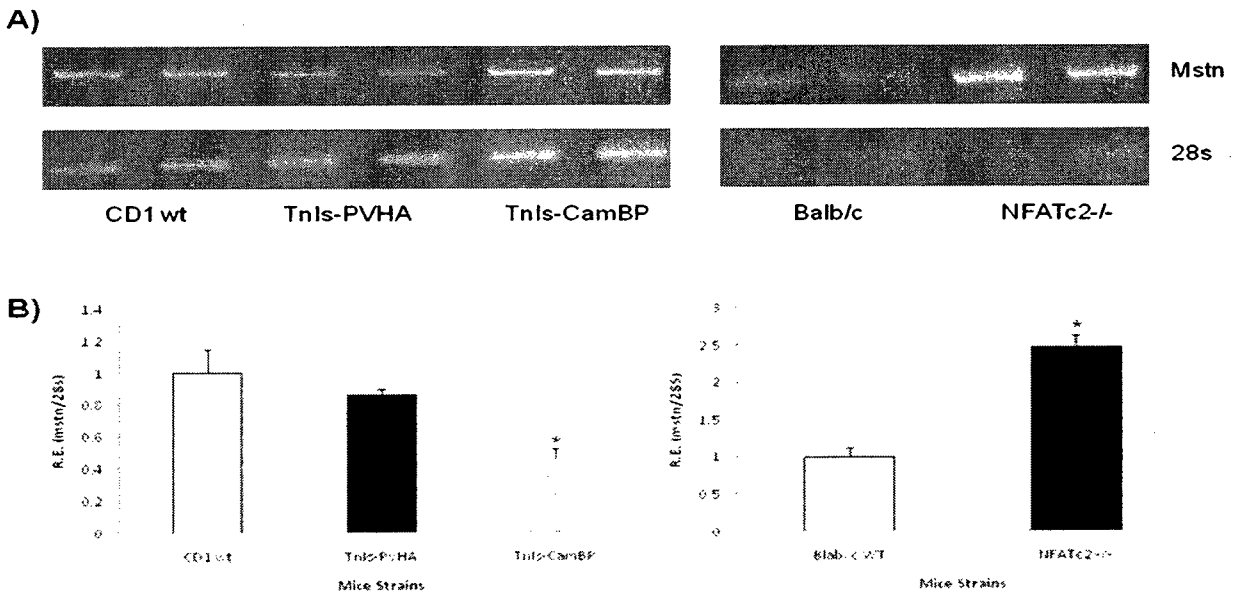

Figure 4.10: Myostatin mRNA expression in muscles of TG mouse variants of Calcineurin Expression. A) Representative image of Mstn mRNA run on EtBr stained agarose gel across the various Transgenic mice models, 28S was used as a loading control; B) Bar graph quantification of mRNA expression. *indicates significance within $p<0.05$ from the wild-type expression levels; N=3 per group, preliminary data run once in duplicate

5: Discussion

We set out to study the effects of myostatin in muscles that are, due to increased load and neural activation, in the process of growing using a process known as plantaris functional overloading. It is achieved by the surgical ablation of the synergist muscles of the plantaris, namely the gastrocnemius and soleus leaving the plantaris with the sole task of performing ankle plantar flexion. By analyzing wild-type and myostatin null genetically engineered mice, we set out to understand the role that myostatin plays in overload-induced muscle growth, specifically how myostatin affects the hypertrophic and hyperplasic signalling pathways implemented by muscles during the growth process. We hypothesized that the hypertrophic and hyperplasic growth pathways will be more potentiated in myostatin null mice as compared to their wild-type counterparts. Our results suggest that myostatin is involved in inhibiting the hyperplasic growth signalling pathway in a higher capacity than the hypertrophic pathway leading to a differential response to functional overload between myostatin null mice and wild-type mice.

We performed several initial identification and characterization experiments to assess the knockout mouse model that was generously provided to us by Dr. Se-Jin Lee's John Hopkins' lab. As shown in Figures 1 and 2, our resulting data analysis was similar to what other groups have shown when using the same myostatin knockout model and the original wild-type strain C57BL. Our data were consistent with what Dr. Se-Jin Lee (Lee, 2007) and Dr. Patel (Matsakas et al., 2009) have published earlier, with Dr. Lee reporting approximately 50% increase in absolute muscle mass of the gastrocnemius muscle for the myostatin knockout mice. As well, in that study, Dr. Lee reports that Mstn-/- plantaris/gastrocnemius muscles show a relative increase in fibre number of approx 50% and an increase of approx 40% in the cross-sectional area of fibres in these muscles.

These data sets were collected from mice aged 10 weeks which is younger than our testing age, which could explain why our results are slightly different than their reported data. Dr. Patel reports an increase in muscle weight in the EDL and gastrocnemius muscles after injecting wild-type mice with the inhibitory propeptide of myostatin loaded vectors to overexpress that protein to counter the effects of myostatin in these muscles. This method, however, only produced a 20% increase in overall muscle weight, with its inherent inability to completely neutralize myostatin's presence in muscles. These studies allow us to compare our results regarding muscle overload to that of what others have studied even when their methods for experimentally altering the muscles are different from our technique.

Our results showed that myostatin does play an inhibiting a role in regulating muscle growth, and more specifically it seems to be controlling the satellite cell participation in muscle growth as opposed to regulating the existing mature myofibres present prior to the induction of exercise stimulus by means of functional overload. What this means is that wild-type muscles, with their native expression of myostatin, respond to functional overload by activating hypertrophy-related pathways, while myostatin null muscles respond by activating less the hypertrophy and more the hyperplasia related pathways for muscle growth. As seen in Figure 4, both wild-type and myostatin knockout muscle midbellies appeared to grow to the same extent. However the overall composition of the muscles differed, with a tendency for wild-type muscle to show bigger mature myofibres, while the knockout model showed a tendency for increased number of myofibres in the midbelly.

By analyzing the mean cross sectional area of the different myofibre types, as seen in Figure 5, the results showed a tendency for wild-type myofibres to respond by increasing their CSA to a greater extent than what Mstn-/- myofibres were able to accomplish. The results from this study show that the overall increase for the wild-type myofibre CSA is approximately 65% while previous results from Dr. Michel's (Dunn et al., 1999) group report a doubling effect from functional overloading of plantaris muscle. Considering that our study was performed on a limited number of mice, the results might be underestimating the gap from hypertrophy in the wild-type muscle compared to the knockout muscle. It is prudent to note that Mstn-/- myofibres at rest are known to be overall larger than Mstn+/+ myofibres (Lee, 2007), as seen in Figure 2.D, but over the time course studied, their size is eclipsed by the wild-type myofibres. This increase alone would suggest that wild-type muscles would grow to be larger than myostatin knockout tissue over the course of the overload period. However this was not observed, and is explained by the greater hyperplasic response seen in knockout tissue as compared to wild-type tissue. This increase is seen in Figure 4.E, where the mean number of myofibres in the midbelly of plantaris muscle was calculated based on dividing the midbelly overall area by the mean cross sectional are of the myofibres present in the midbelly. While the tendency shows a slightly greater number of myofibres in the midbelly of knockouts, it did not reach statistical significance with the limited number of samples. However, it is conceivable that with a larger pool of samples, the numbers would reach significance, being larger in the knockout muscle compared to the wild-type counterparts. As reported earlier, myostatin knockout mice have a greater number of myofibres, approximately 50% more relative to wild-type muscle (Lee, 2007) before any

experimental procedures are performed. Also it has been shown earlier by Dr. Kambadur's group, by performing IF analysis on myoblasts and colocalizing myostatin to the nuclei of these developing cells, that myostatin does inhibit satellite cell activation (McCroskery et al., 2003) and comparing these to Mstn-/- samples that show a lack of myostatin presence in these cells and an overall increase number of these myoblasts. Taken together, published research establishes that in the absence of a myostatin inhibitory role in muscles, satellite cell rate of proliferation is increased. Here we showed that when Mstn-/- plantaris muscles are stimulated to grow, they had a tendency to up-regulate the rate of satellite cell proliferation, inducing a hyperplasic growth response, that is unmatched by the wild-type muscle stimulated in a similar fashion.

Another important parameter that we analyzed is the fibre-type proportion changes that would occur over a prolonged overload period. Previous work done with similar techniques reported that with overload, there would be a significant amount of fibre-type remodelling that change towards expression of more oxidative (slow) MyHC isoforms (Dunn et al., 1997, Dunn et al., 2001, Olsen et al., 2000, Pehme et al., 2004). In Figure 6, the graphs show that the Mstn+/+ tissue did exhibit the normal shift of fibre-type proportions towards the slow phenotype, while the Mstn-/- proportions did not show the tendency to shift their fibre-type composition to any significant extent. This fact, coupled with the knowledge that Mstn-/- muscles have a higher activation state for glycolytic pathways (Steelman et al., 2006, Ilham et al., 2009), lends to the idea that myostatin may control the expression of oxidative MyHC isoforms. In cases where it is not present, the muscle tends to express only the energy inefficient, glycolytic fibre-types (Handschin et al., 2007).

This is one of the significant findings of this project, namely the inability of Mstn-/- muscle to express or remodel existing myofibres to more energy efficient MyHC isoforms. This allowed us to explore in more detail what the function of myostatin is, beyond the already understood role of regulating the size of muscles. Here we showed that without myostatin's expression, muscle is at risk of becoming more energetically inefficient by producing myofibres that are biochemically more taxing on the energy expenditure of the body with their increased need for ATP when induced to grow. Also knowing that MyHC isoforms that utilize glycolytic pathways for producing their energy are also easily fatigued, and unable to perform their forceful contraction for a prolonged period of time, this leads to muscles that lack great physical endurance.

In order to understand the signalling pathways that are altered differently in the Mstn-/- model compared to the wild-type controls, we pursued looking at the expression of mRNA from target genes that are known to be associated with muscle growth, and in one case muscle atrophy. Specifically, we looked at follistatin (Lee, 2007), calcineurin A (Dunn et al., 1999, 2001), atrogin-1 (Zhang et al., 2007), myogenin (Yafe et al., 2008), and brain-derived neurotrophic factor (Mousavi et al., 2006). These preliminary sets of experiments were done using polymerase chain reaction techniques to assess the levels in which certain genes were transcribed. Comparing Mstn+/+ and Mstn-/- plantaris mRNA across all of the time points analyzed provided an understanding of the expression profiles of these chosen targets. Figure 7.A represents the images acquired after performing polymerase chain reaction experiments, with all graphs representing the level of PCR product relative to the expression of controls.

Our preliminary results showed that out of the five tested gene targets, both calcineurin and atrogin-1 reacted in similar fashion in both Mstn+/+ and Mstn-/- across all the overload time points, as seen in Figures 7.C-D. In both instances the mRNA transcript levels decreased after 2 weeks, and maintained that lowered expression level up to the 6 week overload period. Atrogin-1 is an agent of protein degradation, an ubiquitin ligase that marks proteins for proteolysis (Zhang et al., 2007) making it a prime target for downregulation during muscle growth phase. Its expression was decreased after prolonged overload which can easily be explained by the fact that the overload process increases anabolic processes and decreases catabolic/proteolytic pathways. The graph indicates that the decrease of calcineurin and atrogin-1 is similar in both wild-type and myostatin knockout muscle which indicates that myostatin is not acting on these two proteins directly in our growth stimulus procedure. The fact that atrogin-1 mRNA acted similarly between wild-type and myostatin knockout tissue has been reported before, at least for control groups, by Dr. Thissen's group (Gilson et al., 2007), specifically, they reported no significant difference in mRNA levels between the two groups. Calcineurin expression mirrored the trend seen with atrogin-1, namely the expression is decreased significantly after 2 weeks and maintained at the same decreased level up to the 6 week overload period.

With the knowledge that calcineurin is part of the signalling pathway that increases the expression of slow MyHC isoform fibre-types, with published results showing a 2-fold increase in MyHC I in the plantaris after 4 weeks of overload (Olsen et al., 2000, Dunn et al., 2001), it is difficult to explain why the mRNA transcript of this gene has decreased over the prolonged overload period. One explanation might be that

the protein expression levels might not mirror the mRNA transcript levels, which is not uncommon in these kinds of studies. Another explanation might be that other signalling pathways that induce myofibre remodelling are more affected by the overload procedure than the calcineurin pathway, studies by Dr. Glass's group (Bodine et al., 2001) and Dr. Powers's group (Sugiura et al., 2005), point to the Akt pathway as a major role player in remodelling within muscle in response to functional overload stimuli. We did show that slower MyHC-expressing myofibres are produced with prolonged overload, as in Figure 6.C-D where the proportion of MyHC I and I/IIA are seen in greater frequency after 2-6 weeks as compared to the control tissue. It is worthwhile to note that since Mstn-/- muscle is shifted towards expressing more glycolytic myosin heavy chain isoforms, it is then understandable that the calcineurin expression is decreased in those muscles, since it does not seem that these knockout muscles are capable of producing many oxidative (slow) myofibres from the initial stages, a finding supported by Dr. Cessar-Malek's group (Ilham et al., 2009). This group use microarray bioinformatic analysis of samples taken from Mstn-/- and wild-type counterparts, and concluded that the myostatin knockout mouse model shows a significant downregulation of gene expression related to oxidative myofibres and an upregulation for the glycolytic pathways in those samples. In our study we analyzed the expression of MyHC isoforms by immunohistochemical staining and our results showed a lack of fast-to-slow fibre-type switching in the Mstn-/- plantarii tested which is in line with what is expected of the knockout model.

Since both atrogin-1 and calcineurin have responded in a similar fashion when comparing Mstn+/+ and Mstn-/- overloaded muscles, we decided to probe for more targets that would show a difference in expression profiles. This would shed light on the

apparent variation in reacting to functional overload that led the wild-type tissue to express more of a hypertrophic growth response while the myostatin null tissue expresses more of a hyperplasic response. Figure 7.B shows the graph resulting from preliminary measurements of follistatin mRNA transcript levels across the various overload periods tested. In this graph the results showed a marked difference between wild-type and myostatin knockout tissue. After only three days of overload, the follistatin expression in the wild-type has increased by approximately 4-fold as compared to the non-overloaded controls, while the Mstn-/- levels do not change. This difference is however temporary, since at all subsequent time points, the levels returned to approximately non-OV expression patterns in both types of tissue. The difference seen after three days of overload in the wild-type tissue allowed us to speculate that follistatin, the competitive inhibitor of myostatin, was preferentially upregulated in wild-type tissue to accomplish multiple roles. One role being to neutralize the myostatin present in the muscles of wild-type tissue (allowing the wild-type tissue to grow). Another role suggests that follistatin is involved in activating hypertrophy-promoting signalling pathways, as reported by Dr. Kaspar in his study of follistatin injection into wild-type mice (Haidet et al., 2008). In this study, they use a method of injecting the follistatin gene in mice and analyzing muscle weight as well as myofibre number. Their result indicate that increased follistatin within muscles leads to increased weight of those muscles accompanied by decreased myofibre number, a clear indicator for hypertrophy over hyperplasia. In our case, the lack of upregulation of follistatin in Mstn-/- tissue does explain the inability for the myofibres of myostatin null mice to match the hypertrophic increase seen in the wild-type tissue.

Follistatin is an agent of hypertrophic growth response of muscle (Haidet et al., 2008), and knowing that it is, in fact, differentially regulated between wild-type and myostatin knockout tissue, we proceeded to test for a gene implicated in hyperplasic growth response in skeletal muscle in order to verify that the myostatin knockout tissue does employ this pathway more heavily than in the wild-type tissue. One of the genes involved in the hyperplasia pathway is myogenin, a muscle regulatory factor that is known to be involved with satellite cell activity, specifically its increased expression during the proliferation stage of satellite cells and locking the myoblasts into path of maturation (Kuang et al,, 2007, Le Grand et al., 2007). Figure 7.E presents the graph of the preliminary expression profile of myogenin protein, and in this graph we did in fact register a statistically significant difference between wild-type and myostatin knockout tissue. Myogenin seems to be preferentially upregulated in the Mstn-/- tissue more so than the wild-type, with the peak of its expression coming around the 2 week mark in our study. This allowed us to conclude that satellite cell proliferation and maturation is more evident in myostatin null tissue as compared to wild-type tissue, allowing us to verify that myostatin is in fact an inhibitor to satellite cell activation and proliferation. Myostatin's involvement in satellite cell inhibition was mentioned earlier in and is supported by the work of Dr. Kambadur (McCroskery et al., 2003). As further illustration that myogenin is a key regulator in the hyperplasic growth response in muscle, Dr. Bodine's (Cohen et al., 2007), and Dr. Goldman's (Macpherson et al., 2006) groups have shown that myogenin has a role in stabilizing neuromuscular junction formation. They have identified that myogenin promotes the clustering of acetylcholine receptors where the neuron forms a synapse with the myofibre. This is linked to hyperplasia in the sense that newly formed

myofibres would require formation of neuromuscular junctions and, therefore, it would be logical that myogenin can serve the dual role of signalling as a maturation agent for satellite cells to form new myofibres and as a neuromuscular junction formation agent.

One final gene target that was of interest to us is brain-derived neurotrophic factor (BDNF). It is a stabilizer of synaptic connections between myofibres and their motor neurons (Mousavi et al., 2007). It is also expressed within satellite cells in the same manner as Pax7 (Mousavi et al., 2007). This means it is implicated in maintaining the present state of communication between motor neurons and the mature myofibre state (Mousavi et al., 2007). With functional overload, the pre-existing state of motor neuron connections and myofibres would not be sufficient to the muscle because of the extensive remodelling due to hypertrophy and hyperplasia. Therefore it is logical for BDNF expression to be reduced, allowing a new state of neural branching and remodelling of neuromuscular junctions to occur within the growing muscle. We tested the mRNA transcript levels of BDNF, Figure 7.F, and our results showed that BDNF was upregulated in the knockout muscle in a statistically significant manner. However after overload, the levels in both wild-type and knockout mice are reduced significantly across all overload time points. Put together, the mRNA transcript analysis lends support to the hypothesis that myostatin is responsible for regulating pathways involved in activation of satellite cells, and thus Mstn-/- tissue employs the hyperplasic growth pathway, rather than the hypertrophy pathway, as a response to functional overload more readily than wild-type tissue that has native myostatin levels inhibiting the activation of these pathways.

We pursued the analysis of Pax7 at the protein level in order to investigate whether it is differentially regulated between wild-type and myostatin knockout tissue. The reasoning behind this is that Pax7 is a well known quiescence marker of satellite cells (Kuang et al., 2007, Seale et al., 2000, Le Grand et al., 2007), and its expression level is used as a measuring parameter on whether satellite cells are being activated or maintained quiescent. Our resulting preliminary western blot analysis, as seen in Figure 8, did not achieve statistical significance in any of the groups tested. However, a tendency for Pax7 protein to be upregulated in the wild-type group after only 3 days of functional overload was noted. This tendency might become significant if more samples are tested. We thus speculate that Pax7 plays a role in inhibiting wild-type muscles from activating the quiescent satellite cells, as would be supported by the findings of Dr. Olwin's group (Olguin et al, 2004) as well as Dr. Kambadur's group (McFarlane et al., 2008). Both studies performed immunofluorescence staining of satellite cells, specifically Pax7 protein, and concluded that when satellite cells are activated, Pax7 protein ceases to be expressed in these cells. Taken together, the research states Pax7 is an inhibitor to satellite cell activation and proliferation. Therefore, an initial increase in its protein level would suggest the wild-type tissue is attempting to prevent the signalling propagation that would lead to increased myofibre formation, and hence direct muscle growth towards increasing the size of already available mature myofibres, causing myofibre hypertrophy.

Preliminary analysis was also performed on myogenin at the protein level, as it was determined to be a key determinant showing the differential signalling pathways that are employed by the muscle in response to overload when comparing Mstn+/+ and Mstn-/- tissues. Figure 9 illustrates how in non-overload state, the myostatin knockout

expressed myogenin at a 3-fold greater level than in wild-type plantaris muscle. This replicated the trend seen at the mRNA transcript level seen in Figure 7.E, and therefore, provides further evidence that myogenin is, in fact, differentially regulated between Mstn+/+ and Mstn-/- tissue. Future experiments would have to analyze the myogenin expression profile of both types of tissue across all the time points used in the overload study, similar in fashion to what was done for Pax7 in Figure 8, in order to fully support the findings at the mRNA transcript levels that indicated an increased upregulation of myogenin in all overload time points as compared to their wild-type paired groups. This will solidify the findings of the earlier results and it would implicate myogenin as a key regulator of myofibre hyperplasia due to increased satellite cell proliferation and maturation, leading to the observed increase in myofibre number noted.

Our analysis of all the results leads us to suggest that myostatin has an inhibitory effect on the hyperplasic muscle growth response more profound than its effect on the hypertrophic growth response. As mentioned earlier, the calcineurin pathway is an established map for muscle hypertrophy response to functional overload (Dunn et al., 1999, 2001), we set out to analyze the mRNA transcript levels of myostatin in several transgenic mice models engineered to affect the calcineurin signalling pathway. It was interesting to try to investigate whether transgenic mouse models engineered to have an effect on the signal propagation involved in the calcineurin pathway would result in an effect on the expression of myostatin, at least in the mRNA transcript level. One of the threads of interest was based on previous research done by Dr. Pavlath's group, where they show that the calcineurin-NFAT pathway was implicated in satellite cell activation (Friday et al., 2001). In their published study, they use myotubes cultured cells and

precursor cells (used as models for satellite cells *in vivo*) as samples that they treat with activation or inhibitory agents on calcineurin, and they analyzed the mRNA levels of Myf5, one of the myogenic regulator factors involved in satellite cell maturation and differentiation (Friday et al., 2001). Their work indicates that inhibiting calcineurin effectively inhibits the expression of Myf5 and thus they conclude that there is a link between the calcineurin-NFAT pathway and satellite cell activation (Friday et al., 2001). Therefore, we saw it as prudent to assess the levels of myostatin mRNA expressed in some of the transgenic models available to us, namely the TnIs-PVHA mouse model, the TnIs-CamBP mouse model and the NFATc2-/- mouse model, as well as the proper wild-type mouse backgrounds to each model. The TnIs-PVHA model was designed previously (Chin et al., 2003) to allow for slow myofibres to implement calcium oscillatory patterns that mimic fast fibre states without leading to complete myofibre remodelling from slow to fast. The TnIs-CamBP model was previously designed (Wang et al., 1995) to overexpress the calmodulin binding protein (CamBP) protein, essentially lowering the availability of Ca-Cam complex concentrations and hence the activation of calcineurin. The CamBP gene was coupled to the TnIs promoter region allowing for increased expression of CamBP within slow myofibres. The NFATc2-/- model was designed by knocking out the functional NFATc2 protein by the introduction of a neomycin cassette within the gene to cause the generation of a non-functioning transcript (Hodge et al., 1996). This is similar to the myostatin knockout model generation process done by Se-Jin Lee (McPherron et al., 1997). Figure 10.A shows the resulting agarose gels of the PCR performed on the various muscles to properly test myostatin mRNA expression. For TnIs-PVHA and TnIs-CamBP mice, the soleus muscle was selected for testing because

the designed transgenic model allows for overexpression of CamBP and PVHA in slow fibres and not fast fibres, and soleus is composed of mostly slow, oxidative myofibres at about 58% in proportion (Girgenrath et al., 2004). The PVHA genetic model is designed to have an irregular calcium oscillatory rhythm within the myofibre, affecting the calcium concentrations found in the cytoplasm of these fibres. This in effect lowers the availability of calcium ions that would normally be able to bind to calmodulin forming the Ca-Cam complex.

Decreasing the Ca-Cam concentration effectively lowers the activation of calcineurin since the Ca-Cam complex is found upstream of calcium (Olsen et al., 2000). Our results did not show a significant alteration of myostatin mRNA in this specific model. This might indicate that the decrease of activated levels of calcineurin do not necessarily have a direct effect on myostatin transcription levels. As for the TnIs-CamBP model, which over expresses calmodulin-binding protein, our results show a decrease in the myostatin mRNA transcript level that is approximately one half of the wild-type levels. However, since CamBP, in effect, is expressed in the body to decrease the activity of Ca-Cam complex, one would have assumed that it would ultimately have the same effect on myostatin as in the TnIs-PVHA model, which is not the case. This could be explained by noting that the TnIs-PVHA mice, which were studied by Dr. Michel's group (Chin et al., 2003) did not show a tendency to remodel their soleus myofibres from slow to fast, and therefore maintaining the same myofibre expression profile similar to CD1 wild-type mice can account for the non-significant change of myostatin mRNA expression. Finally we tested NFATc2-/- tissue for the expression of myostatin. NFAT isoforms are known to be downstream effectors of calcineurin, and their role in gene

activation is extensively researched. Dr. Michel's group is actively studying the exact role that knocking out NFAT isoforms plays in skeletal and cardiomyocyte hypertrophy. Dr. De Windt's group's published a study showing in NFATc2-/- mice, cardiac hypertrophy was fully attenuated (Bourajjaj et al., 2008). In our study, we analyzed the expression of myostatin as a result of knocking out the c2 isoform of NFAT. Our results show that by removing the final link between the calcineurin pathway and its target genes, the levels of myostatin mRNA transcripts are increased to 3-fold. This is a significant alteration that lends support to the idea that calcineurin and myostatin pathways are cross-linked and work in opposite fashions, therefore lending control mechanisms that would keep both hypertrophic and anti-hypertrophic pathways in check.

In conclusion, our study showed that myostatin's effect on growing muscle is most apparent in attenuating the hyperplasic growth response in stimulated muscle, and not the hypertrophic signalling pathway. By analyzing both physiological and molecular parameters in functionally overloading plantaris muscles from wild -type and myostatin knockout mice, we determined that the knockout muscles showed a tendency to increase myofibre number as a response to growth stimuli, while wild-type muscle showed a tendency to enlarge the pre-existing mature myofibres. This is the first *in vivo* study to specifically look at the effect of myostatin in muscles that are induced to grow by means of functional overloading.

6: Future Work

In order to verify the tendencies seen in this project, we have to increase the number of mice tested for each treatment group so that the measurements can be statistically shown to be significant. Also, it is of importance to analyze the mRNA expression levels using a technique that is more accurate than semi-quantitative PCR. Therefore, it is planned to use real time PCR experiments to acquire a more accurate assessment of the expression levels of our target genes of interest, as well as other targets that also participate in hypertrophy and hyperplasia pathways. Hence targets such as activin, activin IIB receptor, and smad2/smad3 are seen as future targets to assess in relation to the hypertrophy pathway. As for the hyperplasia-related pathway, targets such as MyoD, MRF4 and Myf5 are all interesting to analyze so that we can track the different phases of satellite cell activation, to maturation.

Further experiments such as immuno-fluorescence detection of satellite cells in the functionally overloaded plantaris tissues are also important to visually verify the activation of satellite cells. Therefore, simultaneous staining of Mstn+/+ and Mstn-/- tissue for satellite cell markers such as BrdU or m-cadherin are important, coupled with staining for myogenin to assess the number of activated satellite cells.

Finally, in an attempt to investigate in more detail the association between myostatin and the calcineurin pathway, it would be prudent to generate cross breeds of myostatin knockout mice with transgentically modified mice overexpressing calcineurin, as well as other cross breeds between myostatin knockouts and targets involved in the calcineurin pathway.

References

Allen, D. L., Cleary A. S., Speaker K. J., Lindsay S. F., Uyenishi J., Reed J. M., Madden M. C., and Mehan R. S., **2008**. Myostatin, activin receptor IIb, and follistatin-like-3 gene expression are altered in adipose tissue and skeletal muscle of obese mice. *Am J Physiol Endocrinol Metab.* Vol.294 p.E918–E927

Allen, D. L., and Unterman T. G., **2007**. Regulation of myostatin expression and myoblast differentiation by FoxO and SMAD transcription factors. *Am J Physiol Cell Physiol.* Vol.292 p.188–199

Amirouche, A. D., Banzet S., Koulmann N., Bonnefoy R., Mouret C., Bigard X., Peinnequin A., and Freyssenet D., **2009**, Down-Regulation of Akt/Mammalian Target of Rapamycin Signaling Pathway in Response to Myostatin Overexpression in Skeletal Muscle. *Endocrinology.* Vol.150 (1) p.286–294

Amthor, H., Otto A., Vulin A., Rochat A., Dumonceaux J., Garcia L., Mouisel E., Hourde C., Macharia R., Friedrichs M., Relaix F., Zammit P. S., Matsakas A., Patel K., and Partridge T., **2009.** Muscle hypertrophy driven by myostatin blockade does not require stem/precursor-cell activity, *PNAS.* Vol. 106 (18) p.7479-84

Amthor, H., Otto A., Macharia R., McKinnell I., and Patel K., **2006**. Myostatin Imposes Reversible Quiescence on Embryonic Muscle Precursors, *Developmental Dynamics.* Vol. 235 p.672–680

Anderson, S. B., Goldberg A. L., and Whitman M., **2008**. Identification of a Novel Pool of Extracellular Pro-myostatin in Skeletal Muscle. *Journal Of Biological Chemistry.* Vol. 283 p.7027–7035

Armand, A. S., Gaspera B. D., Launay T., Charbonnier F., Gallien C. L., and Chanoine C., **2003**. Expression and Neural Control of Follistatin Versus Myostatin Genes During Regeneration of Mouse Soleus. *Developmental Dynamics.* Vol.227 p.256-265.

Atherton, P. J., Higginson J. M., Singh J. and Wackerhage H., **2004**. Concentrations of signal transduction proteins mediating exercise and insulin responses in rat extensor digitorum longus and soleus muscles. *Molecular and Cellular Biochemistry.*Vol. 261 p.111-116

Baumann, A.P., Ibebunjo C., Grasser W.A., Paralkar V.M., **2003**. Myostatin expression in age and denervation induced skeletal muscle atrophy. *J Musculoskel Neuron Interact.* Vol.3 (1) p.8-16

Bellinge, R. H. S., Liberles D., Iaschi S., O'Brien P. A. and Tay G. K., **2005**. Myostatin and its implications on animal breeding: a review. *Animal Genetics.* Vol.36 p.1-6

Bodine, S. C., Stitt T. N., Gonzalez M., Kline W. O., Stover G. L., Bauerlein R., Zlotchenko E., Scrimgeour A., Lawrence J. C., Glass D. J. and Yancopoulos G. D., **2001**. Akt/mTOR pathway is a crucial regulator of skeletal muscle hypertrophy and can prevent muscle atrophy in vivo, *Nature Cell Biology*. Vol 3 p.1014-1019

Bourajjaj, M., Armand A. S., Da Costa Martins P. A., Weijts B., Van der Nagel R., Heeneman S., H. Wehrens X., and De Windt L. J., **2008**. NFATc2 Is a Necessary Mediator of Calcineurin-dependent Hypertrophy and Heart Failure, *Journal of Biological Chemistry*. Vol 283, p. 22295–22303

Bradley, L. P., J. Yaworsky and F. S. Walsh; **2008**. Myostatin as a therapeutic target for musculoskeletal disease. *Cellular and Molecular Life Sciences*. Vol. 65 p.2119-2124

Carlson, C. J., Booth F. W., and Gordon S. E., **1999**. Skeletal muscle myostatin mRNA expression is fiber-type specific and increases during hindlimb unloading. *Am J Physiol Regulatory Integrative Comp Physiol.* Vol.277 p.601-606

Chen, J. C, and Goldhamer D. J, **2003.** Skeletal muscle stem cells, *Reproductive Biology and Endocrinology*. Vol.13 p.101-108

Chin, E. R., Grange, R. W., Viau, F., Simard, A. R., Humphries, C., Shelton, J., Bassel-Duby, R., Williams R. S., and Michel, R. N., **2003**. Alterations in slow-twitch muscle phenotype in transgenic mice overexpressing the Ca2+ buffering protein parvalbumin, *Journal of Physiology*. Vol 547 p.649-663

Cohen, T. J., Waddell, D. S., Barrientos, T., Lu, Z., Feng, G., Cox, G. A., Bodine, S. C., and Yao, T., **2007**. The Histone Deacetylase HDAC4 Connects Neural Activity to Muscle Transcriptional Reprogramming, *Journal of Biological Chemistry*. Vol 282, p. 33752–33759

Dasarathy, S., Milan D., Muc S. M., Kalhan S. C., and McCullough A. J., **2004**. Skeletal muscle atrophy is associated with an increased expression of myostatin and impaired satellite cell function in the portacaval anastamosis rat, *Am J Physiol Gastrointest Liver Physiol.* Vol.287 p.1124-1130

Day, K., Paterson B., and Yablonka-Reuveni Z., **2009**. A Distinct Profile of Myogenic Regulatory Factor Detection Within Pax7 Cells at S Phase Supports a Unique Role of Myf5 During Posthatch Chicken Myogenesis. *Developmental Dynamics*. Vol. 238 p1001–1009

Drummond, M. J., Glynn E., Lujan H., Dicarlo S., and Rasmussen Blake., **2008**. Gene and protein expression associated with protein synthesis and breakdown in paraplegic skeletal muscle. *Nerve Muscle*. Vol.37 p.505-513

Dunn, S., and Michel, R., **1997**. Coordinated expression of myosin heavy chain isoforms and metabolic enzymes within overloaded rat muscle fibers, *American Journal Physiology Cell Physiology*. Vol 42 p371-383

Dunn, S. E., Burns, J. L., and Michel, R. N., **1999**. Calcineurin Is Required for Skeletal Muscle Hypertrophy. *The Journal of Biological Chemistry*. Vol 74 p21908-21912

Dunn, S. E., Simard, A. R., Bassel-Duby, R., Williams, R. S., and Michel, R. N, **2001**. Nerve Activity-dependent Modulation of Calcineurin Signaling in Adult Fast and Slow Skeletal Muscle Fibers. *Journal of Biological Chemistry*, Vol 276 p. 45243–45254

Favier, F. B., Benoit H. and Freyssenet D., **2008**. Cellular and molecular events controlling skeletal muscle mass in response to altered use. *Pflugers Arch - Eur J Physiol*. Vol 456 p.587-600

Friday, B. B., and Pavlath, G. K. **2001**. A calcineurin- and NFAT-dependent pathway regulates Myf5 gene expression in skeletal muscle reserve cells. *Journal of Cell Science*, Vol 114 p.303-310

Gallagher, D., Visser, M., De Meersman R. E., Lveda D. S., Baumgartner R. N., Pierson R. N., Harris T., and Heymsfield, S. B., **1997**. Appendicular skeletal muscle mass: effects of age, gender, and ethnicity. *Journal Applied Physiology*. Vol 83, p.229-239

Gilson, H., Schakman O., Combaret L., Lause P., Grobet L., Attaix D., Ketelslegers J. M., and Thissen J. P., **2007**. Myostatin Gene Deletion Prevents Glucocorticoid-Induced Muscle Atrophy. *Endocrinology*. Vol.148 p.452-460

Gilson, H., Schakman O., Kalista S., Lause P., Tsuchida K., Thissen J.P., **2009**. Follistatin induces muscle hypertrophy through satellite cell proliferation and inhibition of both myostatin and activin. *Am J Physiol Endocrinol Metab*. Vol 297 p.157-164

Girgenrath, S., Song, K., and Whittemore, L., **2004**. Loss of myostatin expression alters fiber-type distribution and expression of myosin heavy chain isoforms in slow- and fast-type skeletal muscle, *Muscle Nerve*. Vol 31, p. 34-40

Haidet, A. M., Rizo L., Handy C., Umapathi P., Eagle A., Shilling C., Boue D., Martin P. T., Sahenk Z., Mendell J. R., and Kaspar B. K., **2008**. Long-term enhancement of skeletal muscle mass and strength by single gene administration of myostatin inhibitors. *Proceedings of the National Academy of Sciences*. Vol.105 p.4318-4322

Handschin, C., Chin S., Li P., Liu F., Maratos-Flier E., LeBrasseur N. K., Yan Z., and Spiegelman B. M., **2007**. Skeletal Muscle Fiber-type Switching, Exercise Intolerance, and Myopathy in PGC-1α Muscle specific Knock-out Animals. *Journal of Biological Chemistry*. Vol. 282 p. 30014–3002

Hennebry, A., Berry C., Siriett V., O'Callaghan P., Chau L., Watson T., Sharma M. and Kambadur R., **2009.** Myostatin regulates fibre type composition of skeletal muscle by regulating MEF2 and MyoD gene expression. *Am J Physiol Cell Physiol.* Vol 296 p.C525-34

Hill, J. J., Davies M. V., Pearson A. A., Wang J. H., Hewick R. M., Wolfman N. M., and Qiu Y., **2002**. The Myostatin Propeptide and the Follistatin-related Gene Are Inhibitory Binding Proteins of Myostatin in Normal Serum. *Journal Of Biological Chemistry*. Vol. 277 p. 40735–40741

Hodge, M. R., Ranger, A. M., De La Brousse, F. C., Hoey T., Grusby, M. J., and Glimche L.H., **1996**. Hyperproliferation and Dysregulation of IL-4 Expression in NF-ATp-Deficient Mice, *Immunity*. Vol 4 p397-405

Huet, C., Li, Z., Liu, H., Black, R. A., Gallian, M.F., and Engvall E., **2001**. Skeletal muscle cell hypertrophy induced by inhibitors of metalloproteases; myostatin as a potential mediator. *Am J Physiol Cell Physiol.* Vol.281 p.1624–1634

Ilham, C., Bruno, M., Picard, B., Reecy, J. M., Chevalier C., Hocquette J. F. and Cassar-Malek ,I., **2009**. Molecular profiles of Quadriceps muscle in *myostatin*-null mice reveal PI3K and apoptotic pathways as myostatin targets. *BMC Genomics*. Vol. 10 p.196

Joulia-Ekaza, D., and Cabello G., **2007**. The myostatin gene: physiology and pharmacological relevance. *Current Opinion in Pharmacology*. Vol.7 p.310–315

Joulia-Ekaza, D., Cabello G., **2006**. Myostatin regulation of muscle development: Molecular basis, natural mutations, physiopathological aspects. *Experimental Cell Research*. Vol.312 p.2401-2414

Kääriäinen, J. M., Järvinen, M. T., Rantanen J., and Kalimo, H., **2000**. Relation between myofibers and connective tissue during muscle injury repair, *Scand J Med Sci Sports*. Vol.10, p.332-337

Kanisicak, O., Mendez J. J., Yamamoto S., Yamamoto M., and Goldhamer D. J., **2009.** Progenitors of skeletal muscle satellite cells express the muscle determination gene, MyoD. *Developmental Biology*. Vol.332, p.131-141

Kocamis, H., and Killefer, J, **2002**. Myostatin expression and possible functions in animal muscle. *Domestic Animal Endocrinology*. Vol.23 p.447-454

Kuang, S., and Rudnicki M. A., **2007.** The emerging biology of satellite cells and their therapeutic potential. *Trends in Molecular Medicine* Vol.14 p.82-91

Kuang, S., Kazuki K., Le Grand F., and Rudnicki M. A., **2007.** Asymmetric Self-Renewal and Commitment of Satellite Stem Cells in Muscle. *Cell.* Vol.129 p.999–1010

Kuang, S., Gillespie M. A., and Rudnicki M. A., **2007.** Niche Regulation of Muscle Satellite Cell Self-Renewal and Differentiation. *Cell Stem Cell.* Vol.2 p.22-31

Le Grand, F., and Rudnicki M. A, **2007.** Skeletal muscle satellite cells and adult myogenesis. *Curr Opin Cell Biol.* Vol.19 p.628–633

Lee, S.J. and McPherron A. C., **2001.** Regulation of myostatin activity and muscle growth. *PNAS.* Vol. 98 p9306-9311

Lee, S.J., **2007.** Quadrupling Muscle Mass in Mice by Targeting TGF-ß Signalling Pathways, *PLoS ONE.* Vol.2 p.789

Lin, S.Y., Morrison, J. R., Phillips, D. J., and de Kretser, D. M, **2003.** Regulation of ovarian function by the TGF-β superfamily and follistatin. *Reproduction.* Vol. 126, p133-148

Macpherson, P., Cieslak, D., and Goldman, D., **2006.** Myogenin-dependent nAChR clustering in aneural myotubes, *Molecular Cellular Neuroscience*, Vol 31, p.649-660

Matsakas, A., Foster K., Otto A., Macharia R., Elashry M., Feist S., Graham I., Foster H., Yaworsky P., Walsh F., Dickson G., Patel K., **2009.** Molecular, cellular and physiological investigation of myostatin propeptide-mediated muscle growth in adult mice, *Neuromuscular Disorders*, Vol. 19 p.489-499

Manceau, M., Gros J., Savage K., **2008.** Myostatin promotes the terminal differentiation of embryonic muscle progenitors. *Genes Dev.* Vol.22 p.668-681

Marieb El. Essentials of Anatomy and Physiology, 8h Edition

McCroskery, S., Thomas M., Platt L., Hennebry A., Nishimura T., McLeay L., Sharma, M., and Kambadur R., **2005.** Improved muscle healing through enhanced regeneration and reduced fibrosis in myostatin-null mice. *Journal of Cell Science* Vol.118 p.3531-3541

McCroskery, S., Thomas M., Maxwell L., Sharma M., and Kambadur R., **2003.** Myostatin negatively regulates satellite cell activation and self-renewal. *Journal of Cell Biology.* Vol.162 p.1135-1147

McFarlane, C., Hennebry A., Thomas M., Plummer E., Ling N., Sharma M., Kambadur R., **2008**. Myostatin signals through Pax7 to regulate satellite cell self-renewal, *Experimental Cell Research.* Vol.314 p.317-329

McFarlane, C, Langley B., Thomas M., Hennebry A., Plummer E., Nicholas G., McMahon C., Sharma M., Kambadur R., **2005**. Proteolytic processing of myostatin is auto-regulated during myogenesis, *Developmental Biology* Vol. 283 p.58 – 69

McPherron, A.C., Lawler, A.M., Lee, S.J, **1997**. Regulation of skeletal muscle mass in mice by a new TGF-β superfamily member, *Nature.* Vol.387 p.83-90

Mendias, C. L., Marcin J. E., Calerdon D. R., and Faulkner J. A. **2006**. Contractile properties of EDL and soleus muscles of myostatin-deficient mice, *J Appl Physiol* Vol.101 p.898–905

Mendias, C. L., Bakhurin K. I., and Faulkner J. A., **2008**. Tendons of myostatin-deficient mice are small, brittle, and hypocellular. *Proceedings of the National Academy of Sciences.* Vol.105 p.388-393

Michel, R. N., Chin, E. R., Chakkalakal, J. V., Eibl, J. K., and Jasmin, B. J., **2007**. Ca/Calmodulin-based signalling in the regulation of the muscle fibre phenotype and its therapeutic potential via modulation of utrophin A and myostatin expression, *Applied Physiology Nutrition Metabolism.* Vol 32 p921-929

Morissette, M. R., Cook S. A., Buranasombati C., Rosenberg M. A., and Rosenzweig A., **2009**, Myostatin Inhibits IGF-I Induced Myotube Hypertrophy through Akt. *American Journal of Physiology Cell Physiology.* Vol.297 p.1124-132

Mousavi, K., and Jasmin, B. J., **2006**. BDNF Is Expressed in Skeletal Muscle Satellite Cells and Inhibits Myogenic Differentiation, *Journal of Neuroscience*, Vol. 26 p.5739-5749

Nadeau, Amelie, MD, and George Karpati, MD, **2008**. Are Big Muscles Necessarily Good Muscles?. *Annals of Neurology.* Vol.63 p.543-545

Nader, Gustavo A., **2005**. Molecular determinants of skeletal muscle mass: getting the "AKT" together. *The International Journal of Biochemistry & Cell Biology* Vol.37 p.1985–1996

Olguin, Hugo C., Bradley B. Olwin, **2004**. Pax-7 up-regulation inhibits myogenesis and cell cycle progression in satellite cells: a potential mechanism for self-renewal. *Developmental Biology* 275, 375– 388

Olson, E. N. and Williams, R. S., **2000**. Remodeling muscles with calcineurin, *BioEssays.* Vol 22 p.510-519

Pehme, A., Alev, K., Kaasik, P., Julkunen, A., Seene, T., **2004**. The effect of mechanical loading on the MyHC synthesis rate and composition in rat plantaris muscle, *Physiology and Biochemistry*. Vol.25, p.332-338

Rodgers, B. D., and Garikipati D. K., **2008**. Clinical, Agricultural, and Evolutionary Biology of Myostatin: A Comparative Review, *Endocrine Reviews*. Vol.29 p.513–534

Sugiura, T., Noritaka A., Mai N., Katsumasa G., Kunihiro S., Hisashi N., Toshitada Y., and Powers, S. K., **2005**. Changes in PKB/Akt and calcineurin signaling during recovery in atrophied soleus muscle induced by unloading, *Am J Physiol Regul Integr Comp Physiol*. Vol. 288 p.1273-1278

Sakuma, K., Mai A., Nakashima H., Nakao R., Hirata M., Inashima S., Yamaguchi A., Yasuhara M., **2008**. Cyclosporin A modulates cellular localization of MEF2C protein and blocks Wber hypertrophy in the overloaded soleus muscle of mice, *Acta Neuropathol*. Vol.115 p.663–674

Sakuma, K., Nakao R., Aoi W., Inashima S., Fujikawa T., Hirata M., Sano M., Yasuhara M., **2005**. Cyclosporin A treatment upregulates Id1 and Smad3 expression and delays skeletal muscle regeneration. *Acta Neuropathol* Vol.110 p.269–280

Salerno, M. S., Thomas M., Forbes D., Watson T., Kambadur R., and Sharma M., **2004**. Molecular analysis of fiber type-specific expression of murine myostatin promoter. *Am J Physiol Cell Physiol*. Vol.287 p.1031-1040

Schneyer, A. L., Sidis Y., Gulati A., Sun J. L., Keutmann H., and Krasney P. A; Differential Antagonism of Activin, Myostatin and GDF11 By Wild-type And Mutant Follistatin. *Endocrinology*. Vol.149 p.4589-4595

Seale, P., and Rudnicki M. A., **2000.** A New Look at the Origin, Function, and "Stem-Cell" Status of Muscle Satellite Cells, *Developmental Biology*. Vol.218 p.115–124

Seale, P., Sabourin L. A., Girgis-Gabardo A., Mansouri A., Gruss P., and Rudnicki M. A., **2000**. Pax7 Is Required for the Specification of Myogenic Satellite Cells. *Cell*. Vol 102, p777-786

Shao, C., Liu M., Wu X., and Ding F., **2007**. Time-dependent expression of myostatin RNA transcript and protein in gastrocnemius muscle of mice after sciatic nerve resection. *Microsurgery*. Vol.27 p.487-493

Shi, X., and Garry D. J., **2006.** Muscle stem cells in development, regeneration, and disease. *Genes and Development*. Vol.20 p.1692-1708

Steelman, C. A., Recknor J. C., Nettleton D., and Reecy J. M., **2006**. Transcriptional profiling of myostatin-knockout mice implicates Wnt signaling in postnatal skeletal muscle growth and hypertrophy. *FASEB Journal*, Vol. 20 p.580-582

Tsuchida, K., Masashi N., Akiyoshi U., Tatsuya M., and Xueling Cui., **2008**. Signal Transduction Pathway Through Activin Receptors as a Therapeutic Target of Musculoskeletal Diseases and Cancer. *Endocrine Journal*. Vol 55 p.11-21

Wagner, K. R., McPherron A. C., Winik N., and Lee S.J., **2002**. Loss of Myostatin Attenuates Severity of Muscular Dystrophy in *mdx* Mice. *Ann Neurol.* Vol.52 p.832–836

Wang, J., Campos, B. A., Jamieson, G. A., Kaetzel, M. A., and Dedman, J. R., **1995**. Functional Elimination of Calmodulin within the Nucleus by Targeted Expression of an Inhibitor Peptide, *Journal of Biological Chemistry*. Vol 270 p.30245–30248

Wójcik, S. A., Nogalska, W.K. Engel, Askanas V., **2008**. Myostatin and its precursor protein are increased in the skeletal muscle of patients with Type-II muscle fibre atrophy. *Folia Morphol.* Vol.67 p.1-7

Yafe, A., Shklover J., Weisman-Shomer P., Bengal E., and Fry M., **2008.** Differential binding of quadruplex structures of muscle-specific genes regulatory sequences by MyoD, MRF4 and myogenin. *Nucleic Acids Research*, Vol. 36 p.3916-3925

Zhang, Peng, Xiaoping Chen, Ming Fan, **2007**. Signalling mechanisms involved in disuse muscle atrophy. *Medical Hypotheses* Vol.69 p.310–321

Zhi-fang, Li, G. Diane Shelton, and Eva Engvall, **2005**. Elimination of Myostatin Does Not Combat Muscular Dystrophy in dy Mice but Increases Postnatal Lethality. *American Journal of Pathology.* Vol.166p. 491-497

APPENDICES

APPENDIX I

Non-Overloaded Control Mice Muscle Weights

Soleus

	L (mg)	R (mg)	Avg	Avg REL	BW	STD	SE
F67-5	11.0	10.8	10.9	0.333333	32.7		
G54-5	10.0	10.4	10.2	0.280992	36.3		
C57	11.3	10.9	11.1	0.431907	25.7		
AVG			**10.7**	**0.348744**		**0.472582**	**0.272853**
						0.076629	**0.044243**

J91-4	16.5	17.5	17.0	0.420792	40.4		
J92-1	17	16.8	16.9	0.478754	35.3		
J90-2	13.3	13.5	13.4	0.470175	28.5		
AVG			**15.8**	**0.456574**		**2.050203**	**1.18372**
						0.031283	**0.018062**

	ABS	REL
Mstn+/+	10.7	0.348744
SE	0.044243	0.044243
Mstn-/-	15.8	0.456574
SE	0.018062	0.018062

Plantaris

	L (mg)	R (mg)	Avg ABS	avg REL	BW	STD	SE
F67-5	21.5	22.5	21.5	0.672783	32.7		
G54-5	20.1	21.8	20.1	0.577135	36.3		
C57	18.3	18.1	18.3	0.708171	25.7		
AVG			**20.0**	**0.652696**		**1.604161**	**0.92619**
						0.067788	**0.039139**

J91-4	43.2	41.9	43.2	1.053218	40.4		
J92-1	38.5	34.7	38.5	1.036827	35.3		
J90-2	30.1	31.2	30.1	1.075439	28.5		
AVG			**37.3**	**1.055161**		**6.636515**	**3.831706**
						0.019379	**0.011189**

REL

Mstn+/+	20.0	0.652696
SE	0.039139	0.039139
Mstn-/-	37.3	1.055161
SE	0.011189	0.011189

Gastrocnemius

	L (mg)	R (mg)	Avg	Avg REL	BW	STD	SE
F67-5	153	152	152.5	4.663609	32.7		
G54-5	138.8	132.2	135.5	3.732782	36.3		
C57	142.5	134.5	138.5	5.389105	25.7		
AVG			**142.2**	**4.595165**		**9.073772**	**5.238898**
						0.83028	**0.479376**

J91-4	320	314.7	317.4	7.855198	40.4		
J92-1	269.6	275.2	272.4	7.716714	35.3		
J90-2	221.1	216.4	218.8	7.675439	28.5		
AVG			**269.5**	**7.749117**		**49.36393**	**28.50111**
						0.094159	**0.054364**

		REL
Mstn+/+	142.2	4.595165
SE	0.479376	0.479376
Mstn-/-	269.5	7.749117
SE	0.054364	0.054364

Tibialis Anterior

	L (mg)	R (mg)	avg ABS	Avg REL	BW	STD	SE
F67-5	54.4	55	54.7	1.672783	32.7		
G54-5	49.7	45.3	47.5	1.30854	36.3		
C57	60.1	55.2	57.7	2.243191	25.7		
AVG			**53.3**	**1.741504**		**5.221191**	**3.014544**
						0.4711	**0.271998**

J91-4	118	110.6	114.3	2.829208	40.4		
J92-1	95.4	93.1	94.3	2.669972	35.3		
J90-2	75.8	79.4	77.6	2.722807	28.5		

AVG			**95.4**	**2.740662**		**18.37623**	**10.60983**
						0.081106	**0.046828**

		REL
Mstn+/+	53.3	1.741504
SE	0.271998	0.271998
Mstn-/-	95.4	2.740662
SE	0.046828	0.046828

Extensor Digitorum Longus

	L (mg)	R (mg)	Avg	Avg REL	BW	STD	SE
F67-5	13.6	13.4	13.5	0.412844	32.7		
G54-5	11.3	10.4	10.9	0.298898	36.3		
C57	11.3	10.6	11.0	0.42607	25.7		
AVG			**11.8**	**0.379271**		**1.501943**	**0.867173**
						0.069918	**0.040368**

J91-4	22.8	23.5	23.2	0.57302	40.4		
J92-1	19.5	20.7	20.1	0.569405	35.3		
J90-2	14.9	16	15.5	0.542105	28.5		
AVG			**19.6**	**0.56151**		**3.877607**	**2.238803**
						0.016902	**0.009759**

		REL
Mstn+/+	11.8	0.379271
SE	0.040368	0.040368
Mstn-/-	19.6	0.56151
SE	0.009759	0.009759

APPENDIX II

Extracted Mice for Overload Project

A) Muscle Weight Data

Mouse	Pla Left (mg)	Pla Right (mg)	BW (g)	Pla L/R Avg	Rel Pla
F67-5wt non-OV	21.5	22.5	32.7	22.0	0.67278287
G54-5wt non-OV	20.1	21.8	36.3	21.0	0.57713499
c57wt non-OV	18.3	18.1	25.7	18.2	0.70817121
J91-4ko non-OV	43.2	41.9	40.4	42.6	1.05321782
J92-1ko non-OV	38.5	34.7	35.3	36.6	1.0368272
J90-2ko non-OV	30.1	31.2	28.5	30.7	1.0754386
F74-1wt 3day-OV	29.0	32.1	33.5	30.6	0.9119403
E65-1wt 3day-OV	19.4	21.9	23.1	20.7	0.89393939
Jack1wt 3day-OV	30.5	28.8	29.9	29.7	0.9916388
J104-1ko 3day-OV	46.4	20.1	35.3	33.3	0.94192635
J107-1ko 3day-OV	27.2	34.1	26.8	30.7	1.14365672
J110-2ko 3day-OV	39.9	39.3	36.8	39.6	1.07608696
c57stk 2wk-OV	53.5	58.0	32.0	55.8	1.7421875
F70-2wt 2wk-OV	26.0	27.1	24.3	26.6	1.09259259
J95-1ko 2wk-OV	60.3	38.8	29.2	49.6	1.69691781
J95-2ko 2wk-OV	48.0	55.8	37.0	51.9	1.4027027
E55-1wt 6wk-OV	49.4	49.7	29.6	49.6	1.67398649
B122-1wt 6wk-OV	32.2	42.2	33.5	37.2	1.11044776
J85-1ko 6wk-OV	38.0	53.0	32.5	45.5	1.4
J85-3ko 6wk-OV	64.7	63.8	33.2	64.3	1.93524096

Absolute Mass Table

	non-OV	3day-OV	2wk-OV	6wk-OV
Mstn+/+	20.38333	25.60000	41.15000	43.37500
STD	1.96235	7.00036	20.64752	8.73277
SE	1.13300	4.95075	14.60221	6.17593
Mstn-/-	36.60000	31.95000	50.72500	54.87500
STD	5.95000	1.83848	1.66170	13.25825
SE	3.43533	1.30020	1.17518	9.37642

Relative Mass Table

	non-OV	3day-OV	2wk-OV	6wk-OV
Mstn+/+	0.65270	0.90294	1.41739	1.39222
STD	0.06779	0.01273	0.45933	0.39848
SE	0.03914	0.00735	0.26520	0.23007
Mstn-/-	1.05516	0.90294	1.54981	1.66762
STD	0.01938	0.14264	0.20804	0.37847
SE	0.01119	0.08236	0.12012	0.21852

B) Physiological Measurement Summaries

ctl Pla	Whole Midbelly	Avg cell size (μm²)	# (midbelly/cell avg)
C57stk	1649659	1743	946
F67-5	1700053	1586.12266	1072
G54-5	1448761	1558.450339	930
AVG	**1599491**	**1629**	**983**
STD	132945	100	78
J90-2	2545629	2203.630481	1155
J91-4	2932506	2061.665061	1422
J92-1	2667716	1984.718709	1344
AVG	**2715284**	**2083**	**1307**
STD	197776	111	137

3day-OV	Whole Midbelly	Avg cell size (μm²)	# (midbelly/cell avg)
F74-1	2553059	1755	1455
E65-1 (F)	1822437	1580	1153
AVG	**2187748**	**1668**	**1304**
STD	516628	124	213
J104-1	4779264	1915	2356
J107-1 (F)	3877736	2028	2025
AVG	**4328500**	**2028**	**2190**
STD	637477	80	234

2wk-OV	Whole Midbelly	Avg cell size (μm²)	# (midbelly/cell avg)
C57stk	2580354	2330	1108
F70-2	1977533	1654	1196
AVG	**2278943.5**	**1992**	**1152**
STD	426259	478	62
J95-1	3211185	2372	1354
J95-2	3161743	1855	1705
AVG	**3186464**	**2113**	**1529**
STD	34961	366	248

6wk-OV	Whole Midbelly (μm²)	Avg cell size (μm²)	# (midbelly/cell avg)
E55-1	3750789	2504	1498
B122-1	2591831	2548	1017
AVG	**3171310**	**2526**	**1258**
STD	819507	32	340
J85-1	3019782	2499	1208
J85-3	3632605	2460	1476
AVG	**3326193.5**	**2480**	**1342**
STD	433331	28	190

C) Cross-sectional Area Tables

	I	I/IIA	IIA	IIA/IIX	IIX	IIX/IIB	IIB
C57stk avg	1032.658		1013.991	1089.932	1653.362	2461.128	2472.82
STD			262.1776	287.3973	352.1136	173.2435	417.0976
tot count	1	0	85	54	58	7	137
Proportion	0.277778	0	25.38463	15.30909	16.97673	2.035522	40.01625

	I	I/IIA	IIA	IIA/IIX	IIX	IIX/IIB	IIB
F67-5 avg	705.6319	984.6865	908.4262	1118.913	1864.694	2477.065	2387.985
STD	62.33077	256.1688	204.6837	313.8714	440.6998	424.4641	505.1186
tot count	12	7	75	83	90	21	72

Proportion	2.729277	2.651515	20.67918	23.72571	24.9303	6.163934	19.12009

	I	I/IIA	IIA	IIA/IIX	IIX	IIX/IIB	IIB
G54-5 avg			650.6865	841.0505	1188.497	1549.289	2120.062
STD			126.9817	155.2522	257.9973	228.2416	434.1008
tot count	0	0	28	15	38	18	98
Proportion	0	0	13.87429	8.06982	19.52496	9.124347	49.40658

	I	I/IIA	IIA	IIA/IIX	IIX	IIX/IIB	IIB
Mstn+/+	869.145	984.6865	857.7012	1016.632	1568.851	2162.494	2326.956
STD	62.33077	256.1688	197.9476	252.1736	350.2702	275.3164	452.1057
SE	35.98774	147.9035	114.2885	145.5968	202.2346	158.9587	261.031
tot count	13	7	188	152	186	46	307
proportions	1.002352	0.883838	19.97936	15.70154	20.47733	5.774601	36.18097
prop STD	1.501996	1.530853	5.78699	7.835319	4.061412	3.560414	15.50322
prop SE	0.867204	0.883864	3.341218	4.523856	2.344926	2.055666	8.951054

	I	I/IIA	IIA	IIA/IIX	IIX	IIX/IIB	IIB
J91-4 avg			857.8112	756.4217	1531.941	2804.212	2680.399
STD			56.12335	206.3799	459.1561	571.788	544.3885
tot count	0	0	2	76	70	10	170
Proportion	0	0	0.564972	21.85293	21.21517	2.830763	53.53617

	I	I/IIA	IIA	IIA/IIX	IIX	IIX/IIB	IIB
J92-1 avg			941.0764	1054.084	1573.833	2252.221	2678.834
STD			173.4316	228.0514	494.1454	276.1031	535.0594
tot count	0	0	3	60	53	10	166
Proportion	0	0	0.950617	20.3565	18.65127	3.352814	56.68879

	I	I/IIA	IIA	IIA/IIX	IIX	IIX/IIB	IIB
J90-2 avg			1170.375	1328.396	2103.974	2903.344	2588.63
STD			279.4339	374.9638	510.8226	984.2706	492.1801
tot count	0	0	46	21	62	9	138
Proportion	0	0	17.09714	8.196313	21.90038	3.138355	49.66781

	I	I/IIA	IIA	IIA/IIX	IIX	IIX/IIB	IIB
Mstn-/-	N/A	N/A	989.7542	1046.301	1736.583	2653.259	2649.288
STD	N/A	N/A	169.6629	269.7983	488.0414	610.7206	523.876
SE	N/A	N/A	97.95781	155.7727	281.7791	352.61	302.4688

tot count	0	0	51	157	185	29	474
proportions	0	0	6.204243	16.80191	20.58894	3.107311	53.29759
prop STD	0	0	9.435496	7.490134	1.712686	0.262407	3.516567
prop SE	0	0	5.447746	4.324558	0.988849	0.151505	2.03035

	I	I/IIA	IIA	IIA/IIX	IIX	IIX/IIB	IIB
E65-1 AVG	860.2907		1010.039	1247.419	1650.833	1896.019	2058.606
avg STD	422.701		355.7286	464.8197	485.994	692.2469	711.3196
tot Count	13	0	50	29	42	9	86
Proportions	5.608411	0	21.96415	12.69898	18.29543	4.049068	37.38396

	I	I/IIA	IIA	IIA/IIX	IIX	IIX/IIB	IIB
F74-1 AVG		972.1299	811.4489	1003.5	1596.135	2359.61	2647.27
avg STD			312.8189	439.9762	586.8981	1072.345	925.6269
tot Count	0	1	66	21	46	10	69
Proportions	0	0.510204	31.13844	9.418717	21.7272	4.908322	32.29712

	I	I/IIA	IIA	IIA/IIX	IIX	IIX/IIB	IIB
Mstn+/+	860.2907	972.1299	910.7441	1125.459	1623.484	2127.814	2352.938
avg STD	422.701	#DIV/0!	334.2737	452.3979	536.4461	882.2961	818.4733
tot Count	13	1	116	50	88	19	155
Proportions	2.804205	0.255102	26.55129	11.05885	20.01131	4.478695	34.84054
Prop STD	3.965745	0.360769	6.487203	2.319499	2.426629	0.607584	3.59694
Prop SE	2.804629	0.255141	4.587838	1.640381	1.716145	0.429692	2.543805

	I	I/IIA	IIA	IIA/IIX	IIX	IIX/IIB	IIB
J104-1 AVG			1056.845	1289.447	1621.419	2378.848	2575.143
avg STD			453.5549	483.976	645.5184	837.8236	876.4732
tot Count	0	0	12	27	50	19	108
Proportions	0	0	5.789955	13.17287	23.70575	8.766632	48.56479

	I	I/IIA	IIA	IIA/IIX	IIX	IIX/IIB	IIB
J107-1 AVG			1076.792	1346.13	2053.751	2415.956	2387.552
avg STD			359.6519	477.6955	764.5228	1248.897	807.3472
tot Count	0	0	33	43	31	5	108
Proportions	0	0	15.16171	19.80786	14.00208	2.409836	48.61851

	I	I/IIA	IIA	IIA/IIX	IIX	IIX/IIB	IIB
Mstn-/-	#DIV/0!	#DIV/0!	1066.818	1317.788	1837.585	2397.402	2481.347
avg STD	#DIV/0!	#DIV/0!	406.6034	480.8357	705.0206	1043.36	841.9102
tot Count	0	0	45	70	81	24	216
Proportions	0	0	10.47583	16.49037	18.85392	5.588234	48.59165
Prop STD	0	0	6.626833	4.691649	6.861528	4.494934	0.03798
Prop SE	0	0	4.686586	3.317998	4.852566	3.178878	0.02686

	I	I/IIA	IIA	IIA/IIX	IIX	IIX/IIB	IIB
c57 2wk AVG			1858.311	1951.112	2210.293	2800.153	3076.823
avg STD			697.2627	678.6943	932.2079	998.1036	1027.682
tot Count	0	0	34	13	31	16	23
Proportions	0	0	27.88595	11.3286	25.92403	14.06367	20.79775

	I	I/IIA	IIA	IIA/IIX	IIX	IIX/IIB	IIB
F70-2 AVG	1347.904	1076.178	1291.664	1656.298	2154.118	2181.174	2091.549
avg STD	605.0757	531.2672	554.1779	656.2436	730.644	707.9747	1005.613
tot Count	8	15	66	20	43	11	27
Proportions	4.007243	7.430032	33.82825	10.38272	23.22856	5.91886	15.20433

	I	I/IIA	IIA	IIA/IIX	IIX	IIX/IIB	IIB
Mstn+/+	1347.904	1076.178	1574.987	1803.705	2182.205	2490.663	2584.186
avg STD	605.0757	531.2672	625.7203	667.4689	831.4259	853.0392	1016.648
tot Count	8	15	100	33	74	27	50
Proportions	2.003621	3.715016	30.8571	10.85566	24.57629	9.991267	18.00104
Prop STD	2.833549	5.253826	4.20184	0.668833	1.905985	5.759254	3.955144
Prop SE	2.003924	3.715577	2.971599	0.473008	1.347938	4.073022	2.797131

	I	I/IIA	IIA	IIA/IIX	IIX	IIX/IIB	IIB
J95-1 AVG			1113.263	1600.061	1910.088	2730.934	2838.135
avg STD			443.0009	556.656	730.5794	901.2256	968.1791
tot Count	0	0	13	25	34	24	81
Proportions	0	0	7.301742	13.80076	19.69544	13.52825	45.67381

	I	I/IIA	IIA	IIA/IIX	IIX	IIX/IIB	IIB
J95-2 AVG			973.2195	1366.342	1487.327	2223.759	2311.542
avg STD			551.792	617.7496	553.767	964.1823	830.4141
tot Count			21	18	19	23	76

Proportions			13.335	11.09574	12.20367	14.3996	48.33706

	I	I/IIA	IIA	IIA/IIX	IIX	IIX/IIB	IIB
Mstn-/-	#DIV/0!	#DIV/0!	1043.241	1483.201	1698.708	2477.347	2574.838
avg STD	#DIV/0!	#DIV/0!	497.3965	587.2028	642.1732	932.704	899.2966
tot Count	0	0	34	43	53	47	157
Proportions	0	0	10.31837	12.44825	15.94955	13.96392	47.00544
Prop STD	#DIV/0!	#DIV/0!	4.266159	1.912735	5.297484	0.616135	1.883204
Prop SE	0	0	3.017085	1.352713	3.746452	0.435739	1.331828

	I	I/IIA	IIA	IIA/IIX	IIX	IIX/IIB	IIB
B122-1 AVG	1471.781	1656.937	1770.921	2328.831	2920.012	3551.029	4010.377
avg STD	694.8431	977.4109	725.7374	912.6857	1056.674	2091.4	1546.105
tot Count	16	3	25	12	37	6	16
Proportions	12.94347	2.358674	21.19518	10.6384	33.20541	5.291179	14.36769

	I	I/IIA	IIA	IIA/IIX	IIX	IIX/IIB	IIB
E55-1 AVG	1706.104	1851.792	1987.267	2394.988	2905.957	2838.368	3368.681
avg STD	627.4839	767.85	880.0732	944.8316	990.0099	1398.745	984.6017
tot Count	16	10	49	10	26	12	36
Proportions	10.19843	5.643879	31.83454	6.319321	18.02672	6.194296	21.78281

	I	I/IIA	IIA	IIA/IIX	IIX	IIX/IIB	IIB
Mstn+/+	1588.943	1754.365	1879.094	2361.909	2912.985	3194.698	3689.529
avg STD	661.1635	872.6304	802.9053	928.7587	1023.342	1745.072	1265.353
tot Count	32	13	74	22	63	18	52
Proportions	11.57095	4.001277	26.51486	8.478861	25.61606	5.742738	18.07525
Prop STD	1.941034	2.322991	7.523168	3.054051	10.73296	0.6386	5.243283
Prop SE	1.372725	1.64285	5.320487	2.159867	7.590493	0.451626	3.708121

	I	I/IIA	IIA	IIA/IIX	IIX	IIX/IIB	IIB
J85-1 AVG	#DIV/0!	#DIV/0!	1319.167	1552.109	2086.074	2664.036	2950.479
avg STD	#DIV/0!	#DIV/0!	358.5177	343.3715	598.8195	463.7639	433.8026
tot Count	0	0	23	34	46	32	89
Proportions	0	0	12.12759	15.65579	20.42107	14.74144	37.05411

	I	I/IIA	IIA	IIA/IIX	IIX	IIX/IIB	IIB
J85-3 AVG	#DIV/0!	#DIV/0!	1360.233	1568.985	2278.279	2879.827	3118.376
avg STD	#DIV/0!	#DIV/0!	348.8753	325.111	527.7478	746.7788	546.2249
tot Count	0	0	25	20	34	25	63
Proportions	0	0	14.44134	12.04268	20.5176	15.49085	37.50753

	I	I/IIA	IIA	IIA/IIX	IIX	IIX/IIB	IIB
Mstn-/-	#DIV/0!	#DIV/0!	1339.7	1560.547	2182.176	2771.932	3034.427
avg STD	#DIV/0!	#DIV/0!	353.6965	334.2412	563.2836	605.2713	490.0138
tot Count	0	0	48	54	80	57	152
Proportions	0	0	13.28447	13.84924	20.46933	15.11614	37.28082
Prop STD	0	0	1.636071	2.554856	0.068255	0.529912	0.320618
Prop SE	0	0	1.157052	1.806829	0.048271	0.374761	0.226745

APPENDIX III

PCR Intensity Quantification

Samples	28S	Atrogin-1	Atrgn:28S
C57STK	238	120	50.42017
E62-2	229	115	50.21834
J92-1	264	132	50
J97-1	253	147	58.10277
F74-1	292	110	37.67123
E65-1	248	108	43.54839
J104-1	292	79	27.05479
J107-1	248	125	50.40323
C57STK	254	60	23.62205
F70-2	285	79	27.7193
J95-1	257	48	18.67704
J95-2	260	64	24.61538
E55-1	257	72	28.01556
B122-1	268	82	30.59701
J85-1	260	76	29.23077
J85-3	257	106	41.24514

Samples	non-OV	3d-OV	2wk-OV	6wk-OV
Mstn+/+	50.31925	40.60981	25.67067	29.30629
STD	0.142714	4.155776	2.897194	1.825361
SE	0.100929	2.939021	2.048935	1.29092
Mstn-/-	54.05138	38.72901	21.64621	35.23795
STD	5.729521	16.50983	4.199042	8.49544
SE	4.051995	11.67598	2.969619	6.008091

Samples	28S	Calcineurin A	Cn A:28S
C57STK	238	235	98.7395
E62-2	229	248	108.2969
J92-1	264	289	109.4697
J97-1	253	271	107.1146
F74-1	292	364	124.6575
E65-1	248	333	134.2742
J104-1	292	294	100.6849
J107-1	248	267	107.6613
C57STK	254	206	81.10236
F70-2	285	187	65.61404
J95-1	257	183	71.20623
J95-2	260	171	65.76923
E55-1	257	156	60.70039
B122-1	268	161	60.07463
J85-1	260	196	75.38462

J85-3	257	214	83.26848

Samples	non-OV	3d-OV	2wk-OV	6wk-OV
Mstn+/+	103.5182	129.4659	73.3582	60.38751
STD	6.758136	6.800005	10.9519	0.442481
SE	4.779445	4.809056	7.745333	0.312928
Mstn-/-	108.2922	104.1731	68.48773	79.32655
STD	1.665288	4.933031	3.844536	5.574736
SE	1.177714	3.488706	2.718908	3.942529

Samples	28S	Follistatin	Foll:28S
C57STK	238	27	11.34454
E62-2	229	46	20.08734
J92-1	264	32	12.12121
J97-1	253	45	17.78656
F74-1	292	240	82.19178
E65-1	248	243	97.98387
J104-1	292	62	21.23288
J107-1	248	74	29.83871
C57STK	254	121	47.6378
F70-2	285	106	37.19298
J95-1	257	50	19.45525
J95-2	260	35	13.46154
E55-1	257	125	48.63813
B122-1	268	78	29.10448
J85-1	260	96	36.92308
J85-3	257	0	0

Samples	non-OV	3d-OV	2wk-OV	6wk-OV
Mstn+/+	15.71594	90.08783	42.41539	38.8713
STD	6.182092	11.16669	7.385598	13.81238
SE	4.372059	7.897238	5.223195	9.768302
Mstn-/-	14.95389	25.53579	16.4584	18.46154
STD	4.006007	6.085243	4.238196	26.10856
SE	2.833102	4.303566	2.99731	18.46433

Samples	28S	Myogenin	Mgn:28S
C57STK	238	28	11.76471
E62-2	229	32	13.9738
J92-1	264	47	17.80303
J97-1	253	38	15.01976
F74-1	292	84	28.76712
E65-1	248	76	30.64516
J104-1	292	132	45.20548

J107-1	248	141	56.85484
C57STK	254	163	64.17323
F70-2	285	164	57.54386
J95-1	257	248	96.49805
J95-2	260	258	99.23077
E55-1	257	69	26.84825
B122-1	268	69	25.74627
J85-1	260	94	36.15385
J85-3	257	101	39.29961

Samples	non-OV	3d-OV	2wk-OV	6wk-OV
Mstn+/+	12.86925	29.70614	60.85854	26.29726
STD	1.562065	1.327973	4.687672	0.779218
SE	1.104713	0.939161	3.315185	0.551073
Mstn-/-	16.4114	51.03016	97.86441	37.72673
STD	1.968067	8.237341	1.932321	2.224392
SE	1.391844	5.825559	1.366564	1.57312

Samples	28S	BDNF	BDNF:28S
C57STK	238	245	102.9411765
E62-2	229	265	115.720524
J92-1	264	558	211.3636364
J97-1	253	531	209.8814229
F74-1	292	111	38.01369863
E65-1	248	115	46.37096774
J104-1	292	55	18.83561644
J107-1	248	72	29.03225806
C57STK	254	91	35.82677165
F70-2	285	88	30.87719298
J95-1	257	87	33.85214008
J95-2	260	71	27.30769231
E55-1	257	176	68.48249027
B122-1	268	156	58.20895522
J85-1	260	106	40.76923077
J85-3	257	94	36.57587549

Samples	non-OV	3d-OV	2wk-OV	6wk-OV
Mstn+/+	109.3309	42.19233	33.35198	63.34572
STD	9.036363	5.909482	3.499881	7.264486
SE	6.390639	4.179266	2.475163	5.137543
Mstn-/-	210.6225	23.93394	30.57992	38.67255
STD	1.048083	7.210114	4.627623	2.96515
SE	0.741219	5.099091	3.272718	2.096994

Samples	Myostatin: 28S
C57STK	741
E62-2	786
J92-1	
J97-1	
F74-1	41
E65-1	39
J104-1	
J107-1	
C57STK	67
F70-2	58
J95-1	
J95-2	
E55-1	74
B122-1	71
J85-1	
J85-3	

	non-OV	3d-OV	2wk-OV	6wk-OV
Mstn+/+	764	40	63	73
SE WT	23	1	5	2
Mstn+/+	1	0.05239	0.08186	0.094957
SE WT	0.029474	0.00131	0.005895	0.001965

Samples	28S	MSTN	Ratio (x100)	Ratio
C69-1	177	216	122.0338983	1.220339
C70-2	217	189	87.09677419	0.870968
D84-1	218	300	137.6146789	1.376147
C68-1	221	237	107.239819	1.072398
C69-3	244	232	95.08196721	0.95082
C71-2	265	252	95.09433962	0.950943
D101-2	245	163	66.53061224	0.665306
D101-5	271	126	46.49446494	0.464945
D101-6	236	108	45.76271186	0.457627

Strain	CD1 wt	TnIs-PVHA	TnIs-CamBP
AVG	115.5817838	99.13870861	52.92926302
STD	25.86961558	7.015770125	11.78479492
SE	14.93626765	4.050675592	6.804154109

Strain	CD1	TnIs-PVHA	TnIs-CamBP
AVG	1.155817838	0.991387086	0.52929263
STD	0.258696156	0.070157701	0.117847949
SE	0.149362677	0.040506756	0.068041541

Adjusted	CD1 wt	TnIs-PVHA	TnIs-CamBP
	1	0.857736447	0.457937759

	MSTN		28S			Ratio (mstn/28S)	
	Blab/c 2	N95-2	Balb/c 2	N95-2		Balb/c 2	N95-2
1	535	1785	475	500		1.15	3.44
2		1614	454	488			
AVG	535	1700	465	494	Adjusted	**1**	**2.991304**

	MSTN		28S			Ratio (mstn/28S)	
	Balb/c 1	N95-3	Balb/c 1	N95-3		Balb/c 1	N95-3
1	73793	250078	46574	56985		1.42	3.96
2	61514	205797	48466	58041			
AVG	**67653.5**	**227937.5**	**47520**	**57513**	Adjusted	**1**	**2.788732**

	MSTN		28S			Ratio (mstn/28S)	
	Balb/c 3	NN20-1	Balb/c 3	NN20-1		Balb/c 3	NN20-1
1	146343	620050	20135	53118		3.59	11.11
2		612472	21738	57802			
AVG	**146343**	**616261**	**20936.5**	**55460**	Adjusted	**1**	**3.094708**

	WT	NFATc2 -/-
avg	1.19	2.958248
STD	0.212838	0.155643
SE	0.122886	0.089863

APPENDIX IV

Western Blots Quantification

	α-tubulin	myogenin	Mgn:Tubulin
E60-2 wt	3587	79040	22.0351268
c57 wt	3475	84053	24.1879137
J97-2 ko	3233	230919	71.4256109
J97-3 ko	3226	209396	64.9088655

Mstn+/+	23.11152
STD	1.52225
SE	1.076556
Mstn-/-	68.16724
STD	4.608035
SE	3.258865

Relative Expression

Mstn+/+	1
STD	0.065865
SE	0.046581
Mstn-/-	2.949492
STD	0.199383
SE	0.141006

	Pax7 G	Pax7 R	Pax7 avg	STD	SE
wt non-Ov	526	356	441	120.2082	85.01284
ko non-Ov	426	443	434.5	12.02082	8.501284
wt 3d-Ov	1105	1067	1086	26.87006	19.00287
ko 3d-Ov	758	467	612.5	205.7681	145.522
wt 2wk-Ov	708	737	722.5	20.5061	14.50219
ko 2wk-Ov	505	995	750	346.4823	245.037
wt 6wk-Ov	367	912	639.5	385.3732	272.5412
ko 6wk-Ov	326	738	532	291.328	206.0311

Absoulte Calculations

	non-OV	3day-OV	2wk-OV	6wk-OV
Mstn+/+	441	1086	722.5	639.5
SE	85.01284	19.00287	14.50219	272.5412
Mstn-/-	434.5	612.5	750	532
SE	8.501284	145.522	245.037	206.0311

Relative
Calculations

	non-OV	3day-OV	2wk-OV	6wk-OV
Mstn+/+	0.600916	1.690981	1.180335	0.962352
SE	0.01934	0.039252	0.106907	0.221618
Mstn-/-	0.681884	1.098022	1.192264	0.810194
SE	0.012001	0.101537	0.234829	0.212116

Statistical Outputs

Midbelly Mean Area

	non-OV	3d OV	2wk OV	6wk OV
wt averages	1599491	2187748	2278944	3171310
STD	132945	516628	426259	819507
SE	76758	365366	301456	579567
KO averages	2715284	4328500	3186464	3326194
STD	197776	637477	34961	433331
SE	114190	450832	24725	306458

	non-OV	3d OV	2wk OV	6wk OV
Mstn+/+	1.60	2.19	2.28	3.17
STD	0.13	0.52	0.43	0.82
SE	0.08	0.37	0.30	0.58
Mstn-/-	2.72	4.33	3.19	3.33
STD	0.20	0.64	0.03	0.43
SE	0.11	0.45	0.02	0.31

t-Test: Two-Sample Assuming Unequal Variances

	WT Non-OV	*KO Non-OV*
Mean	1599490.833	2715283.5
Variance	17674488203	39115489250
Observations	3	3
Hypothesized Mean Difference	0	
df	4	
t Stat	-8.10976523	
P(T<=t) one-tail	0.000628492	
t Critical one-tail	2.131846782	
P(T<=t) two-tail	0.001256983	
t Critical two-tail	2.776445105	

t-Test: Two-Sample Assuming Unequal Variances

	WT Non-OV	*WT 3d-OV*
Mean	1599490.833	2187748
Variance	17674488203	2.66904E+11
Observations	3	2
Hypothesized Mean Difference	0	
df	1	
t Stat	-1.57588194	

P(T<=t) one-tail	0.179987747
t Critical one-tail	6.313751514
P(T<=t) two-tail	0.359975494
t Critical two-tail	12.70620473

t-Test: Two-Sample Assuming Unequal Variances

	WT Non-OV	*WT 2wk-OV*
Mean	1599490.833	2278943.5
Variance	17674488203	1.81697E+11
Observations	3	2
Hypothesized Mean Difference	0	
df	1	
t Stat	-2.18452313	
P(T<=t) one-tail	0.136648263	
t Critical one-tail	6.313751514	
P(T<=t) two-tail	0.273296525	
t Critical two-tail	12.70620473	

t-Test: Two-Sample Assuming Unequal Variances

	WT Non-OV	*WT 6wk-OV*
Mean	1599490.833	3171310
Variance	17674488203	6.71592E+11
Observations	3	2
Hypothesized Mean Difference	0	
df	1	
t Stat	-2.68898323	
P(T<=t) one-tail	0.113330848	
t Critical one-tail	6.313751514	
P(T<=t) two-tail	0.226661696	
t Critical two-tail	12.70620473	

t-Test: Two-Sample Assuming Unequal Variances

	WT Non-OV	*KO 3d-OV*
Mean	1599490.833	4328500
Variance	17674488203	4.06376E+11
Observations	3	2
Hypothesized Mean Difference	0	
df	1	

t Stat	-5.96827851
P(T<=t) one-tail	0.052842767
t Critical one-tail	6.313751514
P(T<=t) two-tail	0.105685533
t Critical two-tail	12.70620473

t-Test: Two-Sample Assuming Unequal Variances

	WT 3d-OV	*KO 3d-OV*
Mean	2187748	4328500
Variance	2.66904E+11	4.06376E+11
Observations	2	2
Hypothesized Mean Difference	0	
df	2	
t Stat	-3.6896341	
P(T<=t) one-tail	0.03312076	
t Critical one-tail	2.91998558	
P(T<=t) two-tail	0.066241519	
t Critical two-tail	4.30265273	

Overall Myofibre Mean CSA

	non-OV	3d OV	2wk OV	6wk OV
Mstn+/+	1629	1668	1992	2526
STD	100	124	478	32
SE	58	87	338	22
Mstn-/-	2083	1972	2113	2480
STD	111	80	366	28
SE	64	57	259	19

	non-OV	3d OV	2wk OV	6wk OV
Mstn+/+	1.63	1.67	1.99	2.53
STD	0.10	0.12	0.48	0.03
SE	0.06	0.09	0.34	0.02
Mstn-/-	2.08	1.97	2.11	2.48
STD	0.11	0.08	0.37	0.03
SE	0.06	0.06	0.26	0.02

t-Test: Two-Sample Assuming Unequal Variances

	WT Non-OV	*KO Non-OV*
Mean	1629.333023	2083.338084
Variance	9954.356829	12332.8809
Observations	3	3
Hypothesized Mean Difference	0	
df	4	
	-	
t Stat	5.267362396	
P(T<=t) one-tail	0.00311164	
t Critical one-tail	2.131846782	
P(T<=t) two-tail	0.00622328	
t Critical two-tail	2.776445105	

t-Test: Two-Sample Assuming Unequal Variances

	WT 3d-OV	*KO 3d-OV*
Mean	1667.641938	1971.78383
Variance	15278.70997	6414.370962
Observations	2	2
Hypothesized Mean Difference	0	
df	2	
	-	
t Stat	2.920321209	
P(T<=t) one-tail	0.049990174	
t Critical one-tail	2.91998558	
P(T<=t) two-tail	0.099980348	
t Critical two-tail	4.30265273	

Mean Myofibre Number

	non-OV	3d OV	2wk OV	6wk OV
Mstn+/+	983	1304	1143	1258
STD	77.75871	213.1431	270.5704	340.1817
SE	44.89533	150.7377	191.3511	240.5811
Mstn-/-	1307	2190	1529	1342
STD	137.3657	234.3274	248.085	189.6311
SE	79.31044	165.7195	175.4491	134.1097

	non-OV	3d OV	2wk OV	6wk OV
Mstn+/+	0.98	1.30	1.14	1.26
STD	0.08	0.21	0.27	0.34
SE	0.04	0.15	0.19	0.24

Mstn-/-	1.31	2.19	1.53	1.34
STD	0.14	0.23	0.25	0.19
SE	0.08	0.17	0.18	0.13

t-Test: Two-Sample Assuming Unequal Variances

	WT Non-OV	*KO Non-OV*
Mean	982.5541107	1307.240807
Variance	6046.417411	18869.33056
Observations	3	3
Hypothesized Mean Difference	0	
df	3	
	-	
t Stat	3.562773033	
P(T<=t) one-tail	0.018872785	
t Critical one-tail	2.353363435	
P(T<=t) two-tail	0.03774557	
t Critical two-tail	3.182446305	

t-Test: Two-Sample Assuming Unequal Variances

	WT 3d-OV	*KO 3d-OV*
Mean	1303.98196	2190.461409
Variance	45429.9804	54909.33935
Observations	2	2
Hypothesized Mean Difference	0	
df	2	
	-	
t Stat	3.957747596	
P(T<=t) one-tail	0.029156644	
t Critical one-tail	2.91998558	
P(T<=t) two-tail	0.058313289	
t Critical two-tail	4.30265273	

MyHC I Expressing Myofibres

	control avg	std	SE
Mstn+/+	869.145	231.2423729	133.51176
Mstn-/-	#DIV/0!	#DIV/0!	#DIV/0!

	3day avg	std	SE
Mstn+/+	860.2907	#DIV/0!	#DIV/0!
Mstn-/-	#DIV/0!	#DIV/0!	#DIV/0!

	2wk avg	std	SE
Mstn+/+	1347.904	#DIV/0!	#DIV/0!
Mstn-/-	#DIV/0!	#DIV/0!	#DIV/0!

	2wk avg	std	SE
Mstn+/+	1588.943	165.6919681	117.17961
Mstn-/-	#DIV/0!	#DIV/0!	#DIV/0!

	Mstn+/+	Mstn-/-	WT SE	KO SE
Non-OV	869.145	#DIV/0!	133.51176	#DIV/0!
3day-OV	860.2907	#DIV/0!		#DIV/0!
2wk-OV	1347.904	#DIV/0!		#DIV/0!
6wk-OV	1588.943	#DIV/0!	117.17961	#DIV/0!

MyHC I-IIA Expressing Myofibres

	control avg	std	SE
Mstn+/+	984.6865	#DIV/0!	#DIV/0!
Mstn-/-	#DIV/0!	#DIV/0!	#DIV/0!

	3day avg	std	SE
Mstn+/+	972.1299	#DIV/0!	#DIV/0!
Mstn-/-	#DIV/0!	#DIV/0!	#DIV/0!

	2wk avg	std	SE
Mstn+/+	1076.178	#DIV/0!	#DIV/0!
Mstn-/-	#DIV/0!	#DIV/0!	#DIV/0!

	2wk avg	std	SE
Mstn+/+	1754.365	137.7837927	97.4426
Mstn-/-	#DIV/0!	#DIV/0!	#DIV/0!

	Mstn+/+	Mstn-/-	WT SE	KO SE
Non-OV	984.6865	#DIV/0!		#DIV/0!
3day-OV	972.1299	#DIV/0!		#DIV/0!

2wk-OV	1076.178	#DIV/0!		#DIV/0!
6wk-OV	1754.365	#DIV/0!	97.4426	#DIV/0!

MyHC IIA Expressing Myofibres

	control avg	std	SE
Mstn+/+	857.701224	186.8884636	107.9032699
Mstn-/-	989.754232	161.8678158	93.4571685

	3day avg	std	SE
Mstn+/+	910.744148	140.4246873	99.45091168
Mstn-/-	1066.81848	14.10400384	9.974543026

	2wk avg	std	SE
Mstn+/+	1574.9872	400.6797524	283.3661616
Mstn-/-	1043.24144	99.02594585	70.03249353

	2wk avg	std	SE
Mstn+/+	1879.09393	152.9801176	108.1896164
Mstn-/-	1339.69981	29.03790984	20.53600413

	Mstn+/+	Mstn-/-	WT SE	KO SE
Non-OV	857.701224	989.7542316	107.9032699	93.45717
3day-OV	910.744148	1066.818478	99.45091168	9.974543
2wk-OV	1574.9872	1043.241436	283.3661616	70.03249
6wk-OV	1879.09393	1339.699809	108.1896164	20.536

t-Test: Two-Sample Assuming Unequal Variances

	WT IIA Non-OV	*KO IIA Non-OV*
Mean	857.7012239	989.7542316
Variance	34927.29781	26201.18981
Observations	3	3
Hypothesized Mean Difference	0	
df	4	
t Stat	-0.925096631	
P(T<=t) one-tail	0.203637131	
t Critical one-tail	2.131846782	
P(T<=t) two-tail	0.407274263	
t Critical two-tail	2.776445105	

t-Test: Two-Sample Assuming Unequal Variances

	WT IIA 3day-OV	*KO IIA 3day-OV*
Mean	910.7441484	1066.818478
Variance	19719.0928	198.9229243
Observations	2	2
Hypothesized Mean Difference	0	
df	1	
t Stat	-1.563952078	
P(T<=t) one-tail	0.181083797	
t Critical one-tail	6.313751514	
P(T<=t) two-tail	0.362167594	
t Critical two-tail	12.70620473	

t-Test: Two-Sample Assuming Unequal Variances

	WT IIA 2wk-OV	*KO IIA 2wk-OV*
Mean	1574.987202	1043.241436
Variance	160544.264	9806.137952
Observations	2	2
Hypothesized Mean Difference	0	
df	1	
t Stat	1.821996157	
P(T<=t) one-tail	0.159778439	
t Critical one-tail	6.313751514	
P(T<=t) two-tail	0.319556879	
t Critical two-tail	12.70620473	

t-Test: Two-Sample Assuming Unequal Variances

	WT IIA 6wk-OV	*KO IIA 6wk-OV*
Mean	1879.093926	1339.699809
Variance	23402.91639	843.2002076
Observations	2	2
Hypothesized Mean Difference	0	
df	1	
t Stat	4.898917305	
P(T<=t) one-tail	0.064095009	
t Critical one-tail	6.313751514	
P(T<=t) two-tail	0.128190017	
t Critical two-tail	12.70620473	

MyHC IIA-IIX Expressing Myofibres

	control avg	std	SE
Mstn+/+	1016.632	152.746937	88.19107216
Mstn-/-	1046.301	286.0665858	165.1654652

	3day avg	std	SE
Mstn+/+	1125.459	172.4762868	122.1503448
Mstn-/-	1317.788	40.08101587	28.34583866

	2wk avg	std	SE
Mstn+/+	1803.705	208.4649972	147.4292766
Mstn-/-	1483.201	165.2644518	116.8772643

	2wk avg	std	SE
Mstn+/+	2361.909	46.77992022	33.08339478
Mstn-/-	1560.547	11.93281632	8.439049728

	Mstn+/+	Mstn-/-	WT SE	KO SE
Non-OV	1016.632	1046.300753	88.19107216	165.1655
3day-OV	1125.459	1317.788449	122.1503448	28.34584
2wk-OV	1803.705	1483.201376	147.4292766	116.8773
6wk-OV	2361.909	1560.547191	33.08339478	8.43905

t-Test: Two-Sample Assuming Unequal Variances

	WT IIA/X Non-OV	*KO IIA/X Non-OV*
Mean	1016.631965	1046.300753
Variance	23331.62676	81834.0915
Observations	3	3
Hypothesized Mean Difference	0	
df	3	
t Stat	-0.158461345	
P(T<=t) one-tail	0.442079688	
t Critical one-tail	2.353363435	
P(T<=t) two-tail	0.884159375	
t Critical two-tail	3.182446305	

t-Test: Two-Sample Assuming Unequal Variances

	WT IIA/X 3day-OV	*KO IIA/X 3day-OV*
Mean	1125.459353	1317.788449
Variance	29748.06952	1606.487833
Observations	2	2
Hypothesized Mean Difference	0	
df	1	
t Stat	-1.536065202	
P(T<=t) one-tail	0.183692733	
t Critical one-tail	6.313751514	
P(T<=t) two-tail	0.367385467	
t Critical two-tail	12.70620473	

t-Test: Two-Sample Assuming Unequal Variances

	WT IIA/X 2wk-OV	KO IIA/X 2wk-OV
Mean	1803.70547	1483.201376
Variance	43457.65505	27312.33902
Observations	2	2
Hypothesized Mean Difference	0	
df	2	
t Stat	1.703821131	
P(T<=t) one-tail	0.115264047	
t Critical one-tail	2.91998558	
P(T<=t) two-tail	0.230528094	
t Critical two-tail	4.30265273	

t-Test: Two-Sample Assuming Unequal Variances

	WT IIA/X 6wk-OV	KO IIA/X 6wk-OV
Mean	2361.909315	1560.547191
Variance	2188.360936	142.3921052
Observations	2	2
Hypothesized Mean Difference	0	
df	1	
t Stat	23.47446376	
P(T<=t) one-tail	0.013551643	
t Critical one-tail	6.313751514	
P(T<=t) two-tail	0.027103286	
t Critical two-tail	12.70620473	

MyHC IIX Expressing Myofibres

	control avg	Std	SE
Mstn+/+	1568.851	345.9296734	199.7284488
Mstn-/-	1736.583	318.8588204	184.0986261

	3day avg	Std	SE
Mstn+/+	1623.484	38.6768235	27.39151806
Mstn-/-	1837.585	305.7046471	216.1984774

	2wk avg	Std	SE
Mstn+/+	2182.205	39.72142014	28.09152768
Mstn-/-	1698.708	298.9371099	211.4123833

	2wk avg	Std	SE
Mstn+/+	2912.985	9.938127952	7.028379033
Mstn-/-	2182.176	135.9098665	96.11730305

	Mstn+/+	Mstn-/-	WT SE	KO SE
Non-OV	1568.851	1736.582511	199.7284488	184.0986
3day-OV	1623.484	1837.585101	27.39151806	216.1985
2wk-OV	2182.205	1698.707558	28.09152768	211.4124
6wk-OV	2912.985	2182.176429	7.028379033	96.1173

t-Test: Two-Sample Assuming Unequal Variances

	WT IIX Non-OV	*KO IIX Non-OV*
Mean	1568.851117	1736.582511
Variance	119667.3389	101670.9474
Observations	3	3
Hypothesized Mean Difference	0	
df	4	
t Stat	-0.617513865	
P(T<=t) one-tail	0.285157841	
t Critical one-tail	2.131846782	
P(T<=t) two-tail	0.570315682	
t Critical two-tail	2.776445105	

t-Test: Two-Sample Assuming Unequal Variances

	WT IIX 3day-OV	*KO IIX 3day-OV*
Mean	1623.483913	1837.585101
Variance	1495.896676	93455.33123
Observations	2	2
Hypothesized Mean Difference	0	
df	1	
t Stat	-0.982615886	
P(T<=t) one-tail	0.252790956	
t Critical one-tail	6.313751514	
P(T<=t) two-tail	0.505581912	
t Critical two-tail	12.70620473	

t-Test: Two-Sample Assuming Unequal Variances

	WT IIX 2wk-OV	KO IIX 2wk-OV
Mean	2182.205457	1698.707558
Variance	1577.791218	89363.39569
Observations	2	2
Hypothesized Mean Difference	0	
df	1	
t Stat	2.267405941	
P(T<=t) one-tail	0.132216913	
t Critical one-tail	6.313751514	
P(T<=t) two-tail	0.264433826	
t Critical two-tail	12.70620473	

t-Test: Two-Sample Assuming Unequal Variances

	WT IIX 6wk-OV	KO IIX 6wk-OV
Mean	2912.984661	2182.176429
Variance	98.7663872	18471.49181
Observations	2	2
Hypothesized Mean Difference	0	
df	1	
t Stat	7.584194424	
P(T<=t) one-tail	0.04172945	
t Critical one-tail	6.313751514	
P(T<=t) two-tail	0.083458899	
t Critical two-tail	12.70620473	

MyHC IIX-IIB Expressing Myofibres

	control avg	std	SE
Mstn+/+	2162.494	531.1107786	306.6459461
Mstn-/-	2653.259	350.8280756	202.5566256

	3day avg	std	SE
Mstn+/+	2127.814	327.8081041	232.1587139
Mstn-/-	2397.402	26.23911556	18.55665881

	2wk avg	std	SE
Mstn+/+	2490.663	437.684337	309.5363062
Mstn-/-	2477.347	358.6270818	253.6259418

	2wk avg	std	SE
Mstn+/+	3194.698	503.9273521	356.384266
Mstn-/-	2771.932	152.5870688	107.911647

	Mstn+/+	Mstn-/-	WT SE	KO SE
Non-OV	2162.494	2653.258621	306.6459461	202.5566
3day-OV	2127.814	2397.402143	232.1587139	18.55666
2wk-OV	2490.663	2477.346702	309.5363062	253.6259
6wk-OV	3194.698	2771.931518	356.384266	107.9116

	WT IIX/B Non-OV	*KO IIX/B Non-OV*
Mean	2162.494073	2653.258621
Variance	282078.6592	123080.3386
Observations	3	3
Hypothesized Mean Difference	0	
df	3	
t Stat	-1.335429808	
P(T<=t) one-tail	0.137009045	
t Critical one-tail	2.353363435	
P(T<=t) two-tail	0.274018091	
t Critical two-tail	3.182446305	

t-Test: Two-Sample Assuming Unequal Variances

	WT IIX/B 3day-	*KO IIX/B 3day-*

	OV	*OV*
Mean	2127.814222	2397.402143
Variance	107458.1531	688.4911856
Observations	2	2
Hypothesized Mean Difference	0	
df	1	
t Stat	-1.159334884	
P(T<=t) one-tail	0.226554762	
t Critical one-tail	6.313751514	
P(T<=t) two-tail	0.453109524	
t Critical two-tail	12.70620473	

t-Test: Two-Sample Assuming Unequal Variances

	WT IIX/B 2wk-OV	KO IIX/B 2wk-OV
Mean	2490.663096	2477.346702
Variance	191567.5788	128613.3838
Observations	2	2
Hypothesized Mean Difference	0	
df	2	
t Stat	0.033281575	
P(T<=t) one-tail	0.488236443	
t Critical one-tail	2.91998558	
P(T<=t) two-tail	0.976472887	
t Critical two-tail	4.30265273	

t-Test: Two-Sample Assuming Unequal Variances

	WT IIX/B 6wk-OV	KO IIX/B 6wk-OV
Mean	3194.698135	2771.931518
Variance	253942.7762	23282.81357
Observations	2	2
Hypothesized Mean Difference	0	
df	1	
t Stat	1.135531083	
P(T<=t) one-tail	0.229825578	
t Critical one-tail	6.313751514	
P(T<=t) two-tail	0.459651156	
t Critical two-tail	12.70620473	

MyHC IIB Expressing Myofibres

	control avg	std	SE
Mstn+/+	2326.956	184.1277506	106.3093248
Mstn-/-	2649.288	52.53707233	30.33318264

	3day avg	std	SE
Mstn+/+	2352.938	416.2489113	294.7938465
Mstn-/-	2481.347	132.6465391	93.8094336

	2wk avg	std	SE
Mstn+/+	2584.186	696.693323	492.7109781
Mstn-/-	2574.838	372.3573566	263.3361786

	2wk avg	std	SE
Mstn+/+	3689.529	453.7480049	320.8967502
Mstn-/-	3034.427	118.7209002	83.96103268

	Mstn+/+	Mstn-/-	WT SE	KO SE
Non-OV	2326.956	2649.287692	106.3093248	30.33318
3day-OV	2352.938	2481.347422	294.7938465	93.80943
2wk-OV	2584.186	2574.838267	492.7109781	263.3362
6wk-OV	3689.529	3034.427274	320.8967502	83.96103

t-Test: Two-Sample Assuming Unequal Variances

	WT IIB Non-OV	*KO IIB Non-OV*
Mean	2326.95577	2649.287692
Variance	33903.02855	2760.143969
Observations	3	3
Hypothesized Mean Difference	0	
df	2	
t Stat	-2.915740864	
P(T<=t) one-tail	0.050124509	
t Critical one-tail	2.91998558	
P(T<=t) two-tail	0.100249018	
t Critical two-tail	4.30265273	

t-Test: Two-Sample Assuming Unequal Variances

	WT IIB 3day-OV	*KO IIB 3day-OV*
Mean	2352.938057	2481.347422
Variance	173263.1561	17595.10434
Observations	2	2
Hypothesized Mean Difference	0	
df	1	
t Stat	-0.41567721	
P(T<=t) one-tail	0.374602541	
t Critical one-tail	6.313751514	
P(T<=t) two-tail	0.749205082	
t Critical two-tail	12.70620473	

t-Test: Two-Sample Assuming Unequal Variances

	WT IIB 2wk-OV	KO IIB 2wk-OV
Mean	2584.18594	2574.838267
Variance	485381.5863	138650.001
Observations	2	2
Hypothesized Mean Difference	0	
df	2	
t Stat	0.016734595	
P(T<=t) one-tail	0.494083842	
t Critical one-tail	2.91998558	
P(T<=t) two-tail	0.988167683	
t Critical two-tail	4.30265273	

t-Test: Two-Sample Assuming Unequal Variances

	WT IIB 6wk-OV	KO IIB 6wk-OV
Mean	3689.528971	3034.427274
Variance	205887.2519	14094.65214
Observations	2	2
Hypothesized Mean Difference	0	
df	1	
t Stat	1.975287172	
P(T<=t) one-tail	0.149172579	
t Critical one-tail	6.313751514	
P(T<=t) two-tail	0.298345158	
t Critical two-tail	12.70620473	

ANOVA: Calcineurin A Expression Response to Overloading Mstn+/+ and Mstn-/-

Notes

	Output Created	25-Nov-2009 11:24:23
	Comments	
Input	Data	C:\Users\Moe AK\Documents\Stats for thesis\MOD Midbelly Area Fibre CSA and Fibre Number Raw data.sav
	Active Dataset	DataSet1
	Filter	<none>
	Weight	<none>
	Split File	<none>
	N of Rows in Working Data File	24
Missing Value Handling	Definition of Missing	User-defined missing values are treated as missing.
	Cases Used	Statistics are based on all cases with valid data for all variables in the model.

	Syntax	UNIANOVA CnA BY Group /METHOD=SSTYPE(3) /INTERCEPT=INCLUDE /POSTHOC=Group(TUKEY SCHEFFE LSD) /EMMEANS=TABLES(Group) /PRINT=ETASQ HOMOGENEITY DESCRIPTIVE /CRITERIA=ALPHA(.05) /DESIGN=Group.
Resources	Processor Time	0:00:00.125
	Elapsed Time	0:00:00.186

Between-Subjects Factors

		Value Label	N
Group	1.00	mstn+/+ non-ov	2
	2.00	mstn-/- non-ov	2
	3.00	mstn+/+ 3d-ov	2
	4.00	mstn-/- 3d-ov	2
	5.00	mstn+/+ 2wk-ov	2
	6.00	mstn-/- 2wk-ov	2

7.00	mstn+/+ 6wk-ov	2
8.00	mstn-/- 6wk-ov	2

Descriptive Statistics

Dependent Variable:Relative CnA Expression

Group	Mean	Std. Deviation	N
mstn+/+ non-ov	241.50	9.192	2
mstn-/- non-ov	280.00	12.728	2
mstn+/+ 3d-ov	348.50	21.920	2
mstn-/- 3d-ov	280.50	19.092	2
mstn+/+ 2wk-ov	196.50	13.435	2
mstn-/- 2wk-ov	177.00	8.485	2
mstn+/+ 6wk-ov	158.50	3.536	2
mstn-/- 6wk-ov	205.00	12.728	2
Total	235.94	62.578	16

Tests of Between-Subjects Effects

Dependent Variable:Relative CnA Expression

Source	Type III Sum of Squares	df	Mean Square	F	Sig.	Partial Eta Squared

Corrected Model	57222.437[a]	7	8174.634	43.067	.000	.974
Intercept	890664.063	1	890664.063	4692.336	.000	.998
Group	57222.437	7	8174.634	43.067	.000	.974
Error	1518.500	8	189.813			
Total	949405.000	16				
Corrected Total	58740.937	15				

a. R Squared = .974 (Adjusted R Squared = .952)

Estimated Marginal Means

Group

Dependent Variable:Relative CnA Expression

Group			95% Confidence Interval	
	Mean	Std. Error	Lower Bound	Upper Bound
mstn+/+ non-ov	241.500	9.742	219.035	263.965
mstn-/- non-ov	280.000	9.742	257.535	302.465
mstn+/+ 3d-ov	348.500	9.742	326.035	370.965
mstn-/- 3d-ov	280.500	9.742	258.035	302.965
mstn+/+ 2wk-ov	196.500	9.742	174.035	218.965
mstn-/- 2wk-ov	177.000	9.742	154.535	199.465

mstn+/+ 6wk-ov	158.500	9.742	136.035	180.965
mstn-/- 6wk-ov	205.000	9.742	182.535	227.465

Post Hoc Tests

Group

Multiple Comparisons

Dependent Variable:Relative CnA Expression

					95% Confidence Interval	
(I) Group	(J) Group	Mean Difference (I-J)	Std. Error	Sig.	Lower Bound	Upper Bound
Tukey HSD mstn+/+ non-ov	mstn-/- non-ov	-38.50	13.777	.219	-93.02	16.02
	mstn+/+ 3d-ov	-107.00*	13.777	.001	-161.52	-52.48
	mstn-/- 3d-ov	-39.00	13.777	.209	-93.52	15.52
	mstn+/+ 2wk-ov	45.00	13.777	.121	-9.52	99.52
	mstn-/- 2wk-ov	64.50*	13.777	.020	9.98	119.02
	mstn+/+ 6wk-ov	83.00*	13.777	.004	28.48	137.52
	mstn-/- 6wk-ov	36.50	13.777	.261	-18.02	91.02

mstn-/- non-ov	mstn+/+ non-ov	38.50	13.777	.219	-16.02	93.02
	mstn+/+ 3d-ov	-68.50*	13.777	.014	-123.02	-13.98
	mstn-/- 3d-ov	-.50	13.777	1.000	-55.02	54.02
	mstn+/+ 2wk-ov	83.50*	13.777	.004	28.98	138.02
	mstn-/- 2wk-ov	103.00*	13.777	.001	48.48	157.52
	mstn+/+ 6wk-ov	121.50*	13.777	.000	66.98	176.02
	mstn-/- 6wk-ov	75.00*	13.777	.008	20.48	129.52
mstn+/+ 3d-ov	mstn+/+ non-ov	107.00*	13.777	.001	52.48	161.52
	mstn-/- non-ov	68.50*	13.777	.014	13.98	123.02
	mstn-/- 3d-ov	68.00*	13.777	.015	13.48	122.52
	mstn+/+ 2wk-ov	152.00*	13.777	.000	97.48	206.52
	mstn-/- 2wk-ov	171.50*	13.777	.000	116.98	226.02
	mstn+/+ 6wk-ov	190.00*	13.777	.000	135.48	244.52
	mstn-/- 6wk-ov	143.50*	13.777	.000	88.98	198.02
mstn-/- 3d-ov	mstn+/+ non-ov	39.00	13.777	.209	-15.52	93.52
	mstn-/- non-ov	.50	13.777	1.000	-54.02	55.02
	mstn+/+ 3d-ov	-68.00*	13.777	.015	-122.52	-13.48
	mstn+/+ 2wk-ov	84.00*	13.777	.004	29.48	138.52
	mstn-/- 2wk-ov	103.50*	13.777	.001	48.98	158.02
	mstn+/+ 6wk-ov	122.00*	13.777	.000	67.48	176.52

	mstn-/- 6wk-ov	75.50*	13.777	.008	20.98	130.02
mstn+/+ 2wk-ov	mstn+/+ non-ov	-45.00	13.777	.121	-99.52	9.52
	mstn-/- non-ov	-83.50*	13.777	.004	-138.02	-28.98
	mstn+/+ 3d-ov	-152.00*	13.777	.000	-206.52	-97.48
	mstn-/- 3d-ov	-84.00*	13.777	.004	-138.52	-29.48
	mstn-/- 2wk-ov	19.50	13.777	.829	-35.02	74.02
	mstn+/+ 6wk-ov	38.00	13.777	.229	-16.52	92.52
	mstn-/- 6wk-ov	-8.50	13.777	.997	-63.02	46.02
mstn-/- 2wk-ov	mstn+/+ non-ov	-64.50*	13.777	.020	-119.02	-9.98
	mstn-/- non-ov	-103.00*	13.777	.001	-157.52	-48.48
	mstn+/+ 3d-ov	-171.50*	13.777	.000	-226.02	-116.98
	mstn-/- 3d-ov	-103.50*	13.777	.001	-158.02	-48.98
	mstn+/+ 2wk-ov	-19.50	13.777	.829	-74.02	35.02
	mstn+/+ 6wk-ov	18.50	13.777	.860	-36.02	73.02
	mstn-/- 6wk-ov	-28.00	13.777	.516	-82.52	26.52
mstn+/+ 6wk-ov	mstn+/+ non-ov	-83.00*	13.777	.004	-137.52	-28.48
	mstn-/- non-ov	-121.50*	13.777	.000	-176.02	-66.98
	mstn+/+ 3d-ov	-190.00*	13.777	.000	-244.52	-135.48
	mstn-/- 3d-ov	-122.00*	13.777	.000	-176.52	-67.48
	mstn+/+ 2wk-ov	-38.00	13.777	.229	-92.52	16.52

		mstn-/- 2wk-ov	-18.50	13.777	.860	-73.02	36.02
		mstn-/- 6wk-ov	-46.50	13.777	.105	-101.02	8.02
	mstn-/- 6wk-ov	mstn+/+ non-ov	-36.50	13.777	.261	-91.02	18.02
		mstn-/- non-ov	-75.00*	13.777	.008	-129.52	-20.48
		mstn+/+ 3d-ov	-143.50*	13.777	.000	-198.02	-88.98
		mstn-/- 3d-ov	-75.50*	13.777	.008	-130.02	-20.98
		mstn+/+ 2wk-ov	8.50	13.777	.997	-46.02	63.02
		mstn-/- 2wk-ov	28.00	13.777	.516	-26.52	82.52
		mstn+/+ 6wk-ov	46.50	13.777	.105	-8.02	101.02
Scheffe	mstn+/+ non-ov	mstn-/- non-ov	-38.50	13.777	.436	-106.70	29.70
		mstn+/+ 3d-ov	-107.00*	13.777	.003	-175.20	-38.80
		mstn-/- 3d-ov	-39.00	13.777	.423	-107.20	29.20
		mstn+/+ 2wk-ov	45.00	13.777	.283	-23.20	113.20
		mstn-/- 2wk-ov	64.50	13.777	.066	-3.70	132.70
		mstn+/+ 6wk-ov	83.00*	13.777	.017	14.80	151.20
		mstn-/- 6wk-ov	36.50	13.777	.492	-31.70	104.70
	mstn-/- non-ov	mstn+/+ non-ov	38.50	13.777	.436	-29.70	106.70
		mstn+/+ 3d-ov	-68.50*	13.777	.049	-136.70	-.30
		mstn-/- 3d-ov	-.50	13.777	1.000	-68.70	67.70
		mstn+/+ 2wk-ov	83.50*	13.777	.016	15.30	151.70
		mstn-/- 2wk-ov	103.00*	13.777	.004	34.80	171.20

	mstn+/+ 6wk-ov	121.50*	13.777	.001	53.30	189.70
	mstn-/- 6wk-ov	75.00*	13.777	.030	6.80	143.20
mstn+/+ 3d-ov	mstn+/+ non-ov	107.00*	13.777	.003	38.80	175.20
	mstn-/- non-ov	68.50*	13.777	.049	.30	136.70
	mstn-/- 3d-ov	68.00	13.777	.051	-.20	136.20
	mstn+/+ 2wk-ov	152.00*	13.777	.000	83.80	220.20
	mstn-/- 2wk-ov	171.50*	13.777	.000	103.30	239.70
	mstn+/+ 6wk-ov	190.00*	13.777	.000	121.80	258.20
	mstn-/- 6wk-ov	143.50*	13.777	.000	75.30	211.70
mstn-/- 3d-ov	mstn+/+ non-ov	39.00	13.777	.423	-29.20	107.20
	mstn-/- non-ov	.50	13.777	1.000	-67.70	68.70
	mstn+/+ 3d-ov	-68.00	13.777	.051	-136.20	.20
	mstn+/+ 2wk-ov	84.00*	13.777	.016	15.80	152.20
	mstn-/- 2wk-ov	103.50*	13.777	.004	35.30	171.70
	mstn+/+ 6wk-ov	122.00*	13.777	.001	53.80	190.20
	mstn-/- 6wk-ov	75.50*	13.777	.029	7.30	143.70
mstn+/+ 2wk-ov	mstn+/+ non-ov	-45.00	13.777	.283	-113.20	23.20
	mstn-/- non-ov	-83.50*	13.777	.016	-151.70	-15.30
	mstn+/+ 3d-ov	-152.00*	13.777	.000	-220.20	-83.80
	mstn-/- 3d-ov	-84.00*	13.777	.016	-152.20	-15.80
	mstn-/- 2wk-ov	19.50	13.777	.942	-48.70	87.70

	mstn+/+ 6wk-ov	38.00	13.777	.450	-30.20	106.20
	mstn-/- 6wk-ov	-8.50	13.777	1.000	-76.70	59.70
mstn-/- 2wk-ov	mstn+/+ non-ov	-64.50	13.777	.066	-132.70	3.70
	mstn-/- non-ov	-103.00*	13.777	.004	-171.20	-34.80
	mstn+/+ 3d-ov	-171.50*	13.777	.000	-239.70	-103.30
	mstn-/- 3d-ov	-103.50*	13.777	.004	-171.70	-35.30
	mstn+/+ 2wk-ov	-19.50	13.777	.942	-87.70	48.70
	mstn+/+ 6wk-ov	18.50	13.777	.955	-49.70	86.70
	mstn-/- 6wk-ov	-28.00	13.777	.749	-96.20	40.20
mstn+/+ 6wk-ov	mstn+/+ non-ov	-83.00*	13.777	.017	-151.20	-14.80
	mstn-/- non-ov	-121.50*	13.777	.001	-189.70	-53.30
	mstn+/+ 3d-ov	-190.00*	13.777	.000	-258.20	-121.80
	mstn-/- 3d-ov	-122.00*	13.777	.001	-190.20	-53.80
	mstn+/+ 2wk-ov	-38.00	13.777	.450	-106.20	30.20
	mstn-/- 2wk-ov	-18.50	13.777	.955	-86.70	49.70
	mstn-/- 6wk-ov	-46.50	13.777	.254	-114.70	21.70
mstn-/- 6wk-ov	mstn+/+ non-ov	-36.50	13.777	.492	-104.70	31.70
	mstn-/- non-ov	-75.00*	13.777	.030	-143.20	-6.80
	mstn+/+ 3d-ov	-143.50*	13.777	.000	-211.70	-75.30
	mstn-/- 3d-ov	-75.50*	13.777	.029	-143.70	-7.30
	mstn+/+ 2wk-ov	8.50	13.777	1.000	-59.70	76.70

		mstn-/- 2wk-ov	28.00	13.777	.749	-40.20	96.20
		mstn+/+ 6wk-ov	46.50	13.777	.254	-21.70	114.70
LSD	mstn+/+ non-ov	mstn-/- non-ov	-38.50*	13.777	.023	-70.27	-6.73
		mstn+/+ 3d-ov	-107.00*	13.777	.000	-138.77	-75.23
		mstn-/- 3d-ov	-39.00*	13.777	.022	-70.77	-7.23
		mstn+/+ 2wk-ov	45.00*	13.777	.011	13.23	76.77
		mstn-/- 2wk-ov	64.50*	13.777	.002	32.73	96.27
		mstn+/+ 6wk-ov	83.00*	13.777	.000	51.23	114.77
		mstn-/- 6wk-ov	36.50*	13.777	.029	4.73	68.27
	mstn-/- non-ov	mstn+/+ non-ov	38.50*	13.777	.023	6.73	70.27
		mstn+/+ 3d-ov	-68.50*	13.777	.001	-100.27	-36.73
		mstn-/- 3d-ov	-.50	13.777	.972	-32.27	31.27
		mstn+/+ 2wk-ov	83.50*	13.777	.000	51.73	115.27
		mstn-/- 2wk-ov	103.00*	13.777	.000	71.23	134.77
		mstn+/+ 6wk-ov	121.50*	13.777	.000	89.73	153.27
		mstn-/- 6wk-ov	75.00*	13.777	.001	43.23	106.77
	mstn+/+ 3d-ov	mstn+/+ non-ov	107.00*	13.777	.000	75.23	138.77
		mstn-/- non-ov	68.50*	13.777	.001	36.73	100.27
		mstn-/- 3d-ov	68.00*	13.777	.001	36.23	99.77
		mstn+/+ 2wk-ov	152.00*	13.777	.000	120.23	183.77
		mstn-/- 2wk-ov	171.50*	13.777	.000	139.73	203.27

	mstn+/+ 6wk-ov	190.00*	13.777	.000	158.23	221.77
	mstn-/- 6wk-ov	143.50*	13.777	.000	111.73	175.27
mstn-/- 3d-ov	mstn+/+ non-ov	39.00*	13.777	.022	7.23	70.77
	mstn-/- non-ov	.50	13.777	.972	-31.27	32.27
	mstn+/+ 3d-ov	-68.00*	13.777	.001	-99.77	-36.23
	mstn+/+ 2wk-ov	84.00*	13.777	.000	52.23	115.77
	mstn-/- 2wk-ov	103.50*	13.777	.000	71.73	135.27
	mstn+/+ 6wk-ov	122.00*	13.777	.000	90.23	153.77
	mstn-/- 6wk-ov	75.50*	13.777	.001	43.73	107.27
mstn+/+ 2wk-ov	mstn+/+ non-ov	-45.00*	13.777	.011	-76.77	-13.23
	mstn-/- non-ov	-83.50*	13.777	.000	-115.27	-51.73
	mstn+/+ 3d-ov	-152.00*	13.777	.000	-183.77	-120.23
	mstn-/- 3d-ov	-84.00*	13.777	.000	-115.77	-52.23
	mstn-/- 2wk-ov	19.50	13.777	.195	-12.27	51.27
	mstn+/+ 6wk-ov	38.00*	13.777	.025	6.23	69.77
	mstn-/- 6wk-ov	-8.50	13.777	.554	-40.27	23.27
mstn-/- 2wk-ov	mstn+/+ non-ov	-64.50*	13.777	.002	-96.27	-32.73
	mstn-/- non-ov	-103.00*	13.777	.000	-134.77	-71.23
	mstn+/+ 3d-ov	-171.50*	13.777	.000	-203.27	-139.73
	mstn-/- 3d-ov	-103.50*	13.777	.000	-135.27	-71.73
	mstn+/+ 2wk-ov	-19.50	13.777	.195	-51.27	12.27

	mstn+/+ 6wk-ov	18.50	13.777	.216	-13.27	50.27
	mstn-/- 6wk-ov	-28.00	13.777	.077	-59.77	3.77
mstn+/+ 6wk-ov	mstn+/+ non-ov	-83.00*	13.777	.000	-114.77	-51.23
	mstn-/- non-ov	-121.50*	13.777	.000	-153.27	-89.73
	mstn+/+ 3d-ov	-190.00*	13.777	.000	-221.77	-158.23
	mstn-/- 3d-ov	-122.00*	13.777	.000	-153.77	-90.23
	mstn+/+ 2wk-ov	-38.00*	13.777	.025	-69.77	-6.23
	mstn-/- 2wk-ov	-18.50	13.777	.216	-50.27	13.27
	mstn-/- 6wk-ov	-46.50*	13.777	.010	-78.27	-14.73
mstn-/- 6wk-ov	mstn+/+ non-ov	-36.50*	13.777	.029	-68.27	-4.73
	mstn-/- non-ov	-75.00*	13.777	.001	-106.77	-43.23
	mstn+/+ 3d-ov	-143.50*	13.777	.000	-175.27	-111.73
	mstn-/- 3d-ov	-75.50*	13.777	.001	-107.27	-43.73
	mstn+/+ 2wk-ov	8.50	13.777	.554	-23.27	40.27
	mstn-/- 2wk-ov	28.00	13.777	.077	-3.77	59.77
	mstn+/+ 6wk-ov	46.50*	13.777	.010	14.73	78.27

Based on observed means.

The error term is Mean Square(Error) = 189.813.

*. The mean difference is significant at the .05 level.

Homogeneous Subsets

Relative CnA Expression

	Group	N	Subset 1	2	3	4
Tukey HSD[a,,b]	mstn+/+ 6wk-ov	2	158.50			
	mstn-/- 2wk-ov	2	177.00			
	mstn+/+ 2wk-ov	2	196.50	196.50		
	mstn-/- 6wk-ov	2	205.00	205.00		
	mstn+/+ non-ov	2		241.50	241.50	
	mstn-/- non-ov	2			280.00	
	mstn-/- 3d-ov	2			280.50	
	mstn+/+ 3d-ov	2				348.50
	Sig.		.105	.121	.209	1.000
Scheffe[a,,b]	mstn+/+ 6wk-ov	2	158.50			
	mstn-/- 2wk-ov	2	177.00	177.00		
	mstn+/+ 2wk-ov	2	196.50	196.50		
	mstn-/- 6wk-ov	2	205.00	205.00		
	mstn+/+ non-ov	2		241.50	241.50	
	mstn-/- non-ov	2			280.00	
	mstn-/- 3d-ov	2			280.50	280.50

	mstn+/+ 3d-ov	2				348.50
	Sig.		.254	.066	.423	.051

Means for groups in homogeneous subsets are displayed.

Based on observed means.

The error term is Mean Square(Error) = 189.813.

a. Uses Harmonic Mean Sample Size = 2.000.

b. Alpha = .05.

ANOVA: Atrogin-1 Expression Response to Overloading Mstn+/+ and Mstn-/-

Notes

	Output Created	25-Nov-2009 11:27:30
	Comments	
Input	Data	C:\Users\Moe AK\Documents\Stats for thesis\MOD Midbelly Area Fibre CSA and Fibre Number Raw data.sav
	Active Dataset	DataSet1
	Filter	<none>
	Weight	<none>
	Split File	<none>
	N of Rows in Working Data File	24

Missing Value Handling	Definition of Missing	User-defined missing values are treated as missing.
	Cases Used	Statistics are based on all cases with valid data for all variables in the model.
	Syntax	UNIANOVA Atrogin BY Group /METHOD=SSTYPE(3) /INTERCEPT=INCLUDE /POSTHOC=Group(TUKEY SCHEFFE LSD) /EMMEANS=TABLES(Group) /PRINT=ETASQ HOMOGENEITY DESCRIPTIVE /CRITERIA=ALPHA(.05) /DESIGN=Group.
Resources	Processor Time	0:00:00.125
	Elapsed Time	0:00:00.135

Between-Subjects Factors

		Value Label	N
Group	1.00	mstn+/+ non-ov	2
	2.00	mstn-/- non-ov	2
	3.00	mstn+/+ 3d-ov	2

4.00	mstn-/- 3d-ov	2
5.00	mstn+/+ 2wk-ov	2
6.00	mstn-/- 2wk-ov	2
7.00	mstn+/+ 6wk-ov	2
8.00	mstn-/- 6wk-ov	2

Descriptive Statistics

Dependent Variable:Relative Atrogin Expression

Group	Mean	Std. Deviation	N
mstn+/+ non-ov	117.50	3.536	2
mstn-/- non-ov	139.50	10.607	2
mstn+/+ 3d-ov	109.00	1.414	2
mstn-/- 3d-ov	102.00	32.527	2
mstn+/+ 2wk-ov	69.50	13.435	2
mstn-/- 2wk-ov	56.00	11.314	2
mstn+/+ 6wk-ov	77.00	7.071	2
mstn-/- 6wk-ov	91.00	21.213	2
Total	95.19	28.843	16

Tests of Between-Subjects Effects

Dependent Variable:Relative Atrogin Expression

Source	Type III Sum of Squares	df	Mean Square	F	Sig.	Partial Eta Squared
Corrected Model	10484.938[a]	7	1497.848	6.011	.011	.840
Intercept	144970.563	1	144970.563	581.773	.000	.986
Group	10484.938	7	1497.848	6.011	.011	.840
Error	1993.500	8	249.188			
Total	157449.000	16				
Corrected Total	12478.438	15				

a. R Squared = .840 (Adjusted R Squared = .700)

Estimated Marginal Means

Group

Dependent Variable:Relative Atrogin Expression

Group			95% Confidence Interval	
	Mean	Std. Error	Lower Bound	Upper Bound
mstn+/+ non-ov	117.500	11.162	91.760	143.240
mstn-/- non-ov	139.500	11.162	113.760	165.240

mstn+/+ 3d-ov	109.000	11.162	83.260	134.740
mstn-/- 3d-ov	102.000	11.162	76.260	127.740
mstn+/+ 2wk-ov	69.500	11.162	43.760	95.240
mstn-/- 2wk-ov	56.000	11.162	30.260	81.740
mstn+/+ 6wk-ov	77.000	11.162	51.260	102.740
mstn-/- 6wk-ov	91.000	11.162	65.260	116.740

Post Hoc Tests

Group

Multiple Comparisons

Dependent Variable:Relative Atrogin Expression

						95% Confidence Interval	
	(I) Group	(J) Group	Mean Difference (I-J)	Std. Error	Sig.	Lower Bound	Upper Bound
Tukey HSD	mstn+/+ non-ov	mstn-/- non-ov	-22.00	15.786	.838	-84.47	40.47
		mstn+/+ 3d-ov	8.50	15.786	.999	-53.97	70.97
		mstn-/- 3d-ov	15.50	15.786	.965	-46.97	77.97

	mstn+/+ 2wk-ov	48.00	15.786	.161	-14.47	110.47
	mstn-/- 2wk-ov	61.50	15.786	.054	-.97	123.97
	mstn+/+ 6wk-ov	40.50	15.786	.289	-21.97	102.97
	mstn-/- 6wk-ov	26.50	15.786	.700	-35.97	88.97
mstn-/- non-ov	mstn+/+ non-ov	22.00	15.786	.838	-40.47	84.47
	mstn+/+ 3d-ov	30.50	15.786	.567	-31.97	92.97
	mstn-/- 3d-ov	37.50	15.786	.359	-24.97	99.97
	mstn+/+ 2wk-ov	70.00*	15.786	.028	7.53	132.47
	mstn-/- 2wk-ov	83.50*	15.786	.010	21.03	145.97
	mstn+/+ 6wk-ov	62.50*	15.786	.050	.03	124.97
	mstn-/- 6wk-ov	48.50	15.786	.155	-13.97	110.97
mstn+/+ 3d-ov	mstn+/+ non-ov	-8.50	15.786	.999	-70.97	53.97
	mstn-/- non-ov	-30.50	15.786	.567	-92.97	31.97
	mstn-/- 3d-ov	7.00	15.786	1.000	-55.47	69.47
	mstn+/+ 2wk-ov	39.50	15.786	.311	-22.97	101.97
	mstn-/- 2wk-ov	53.00	15.786	.108	-9.47	115.47
	mstn+/+ 6wk-ov	32.00	15.786	.519	-30.47	94.47
	mstn-/- 6wk-ov	18.00	15.786	.929	-44.47	80.47
mstn-/- 3d-ov	mstn+/+ non-ov	-15.50	15.786	.965	-77.97	46.97
	mstn-/- non-ov	-37.50	15.786	.359	-99.97	24.97

	mstn+/+ 3d-ov	-7.00	15.786	1.000	-69.47	55.47
	mstn+/+ 2wk-ov	32.50	15.786	.503	-29.97	94.97
	mstn-/- 2wk-ov	46.00	15.786	.189	-16.47	108.47
	mstn+/+ 6wk-ov	25.00	15.786	.749	-37.47	87.47
	mstn-/- 6wk-ov	11.00	15.786	.995	-51.47	73.47
mstn+/+ 2wk-ov	mstn+/+ non-ov	-48.00	15.786	.161	-110.47	14.47
	mstn-/- non-ov	-70.00*	15.786	.028	-132.47	-7.53
	mstn+/+ 3d-ov	-39.50	15.786	.311	-101.97	22.97
	mstn-/- 3d-ov	-32.50	15.786	.503	-94.97	29.97
	mstn-/- 2wk-ov	13.50	15.786	.983	-48.97	75.97
	mstn+/+ 6wk-ov	-7.50	15.786	.999	-69.97	54.97
	mstn-/- 6wk-ov	-21.50	15.786	.852	-83.97	40.97
mstn-/- 2wk-ov	mstn+/+ non-ov	-61.50	15.786	.054	-123.97	.97
	mstn-/- non-ov	-83.50*	15.786	.010	-145.97	-21.03
	mstn+/+ 3d-ov	-53.00	15.786	.108	-115.47	9.47
	mstn-/- 3d-ov	-46.00	15.786	.189	-108.47	16.47
	mstn+/+ 2wk-ov	-13.50	15.786	.983	-75.97	48.97
	mstn+/+ 6wk-ov	-21.00	15.786	.865	-83.47	41.47
	mstn-/- 6wk-ov	-35.00	15.786	.427	-97.47	27.47
mstn+/+ 6wk-ov	mstn+/+ non-ov	-40.50	15.786	.289	-102.97	21.97

		mstn-/- non-ov	-62.50	15.786	.050	-124.97	-.03
		mstn+/+ 3d-ov	-32.00	15.786	.519	-94.47	30.47
		mstn-/- 3d-ov	-25.00	15.786	.749	-87.47	37.47
		mstn+/+ 2wk-ov	7.50	15.786	.999	-54.97	69.97
		mstn-/- 2wk-ov	21.00	15.786	.865	-41.47	83.47
		mstn-/- 6wk-ov	-14.00	15.786	.979	-76.47	48.47
	mstn-/- 6wk-ov	mstn+/+ non-ov	-26.50	15.786	.700	-88.97	35.97
		mstn-/- non-ov	-48.50	15.786	.155	-110.97	13.97
		mstn+/+ 3d-ov	-18.00	15.786	.929	-80.47	44.47
		mstn-/- 3d-ov	-11.00	15.786	.995	-73.47	51.47
		mstn+/+ 2wk-ov	21.50	15.786	.852	-40.97	83.97
		mstn-/- 2wk-ov	35.00	15.786	.427	-27.47	97.47
		mstn+/+ 6wk-ov	14.00	15.786	.979	-48.47	76.47
Scheffe	mstn+/+ non-ov	mstn-/- non-ov	-22.00	15.786	.946	-100.14	56.14
		mstn+/+ 3d-ov	8.50	15.786	1.000	-69.64	86.64
		mstn-/- 3d-ov	15.50	15.786	.992	-62.64	93.64
		mstn+/+ 2wk-ov	48.00	15.786	.350	-30.14	126.14
		mstn-/- 2wk-ov	61.50	15.786	.150	-16.64	139.64
		mstn+/+ 6wk-ov	40.50	15.786	.526	-37.64	118.64
		mstn-/- 6wk-ov	26.50	15.786	.876	-51.64	104.64
	mstn-/- non-ov	mstn+/+ non-ov	22.00	15.786	.946	-56.14	100.14

	mstn+/+ 3d-ov	30.50	15.786	.789	-47.64	108.64
	mstn-/- 3d-ov	37.50	15.786	.605	-40.64	115.64
	mstn+/+ 2wk-ov	70.00	15.786	.086	-8.14	148.14
	mstn-/- 2wk-ov	83.50	15.786	.035	5.36	161.64
	mstn+/+ 6wk-ov	62.50	15.786	.141	-15.64	140.64
	mstn-/- 6wk-ov	48.50	15.786	.340	-29.64	126.64
mstn+/+ 3d-ov	mstn+/+ non-ov	-8.50	15.786	1.000	-86.64	69.64
	mstn-/- non-ov	-30.50	15.786	.789	-108.64	47.64
	mstn-/- 3d-ov	7.00	15.786	1.000	-71.14	85.14
	mstn+/+ 2wk-ov	39.50	15.786	.552	-38.64	117.64
	mstn-/- 2wk-ov	53.00	15.786	.259	-25.14	131.14
	mstn+/+ 6wk-ov	32.00	15.786	.752	-46.14	110.14
	mstn-/- 6wk-ov	18.00	15.786	.981	-60.14	96.14
mstn-/- 3d-ov	mstn+/+ non-ov	-15.50	15.786	.992	-93.64	62.64
	mstn-/- non-ov	-37.50	15.786	.605	-115.64	40.64
	mstn+/+ 3d-ov	-7.00	15.786	1.000	-85.14	71.14
	mstn+/+ 2wk-ov	32.50	15.786	.739	-45.64	110.64
	mstn-/- 2wk-ov	46.00	15.786	.393	-32.14	124.14
	mstn+/+ 6wk-ov	25.00	15.786	.903	-53.14	103.14
	mstn-/- 6wk-ov	11.00	15.786	.999	-67.14	89.14
mstn+/+ 2wk-ov	mstn+/+ non-ov	-48.00	15.786	.350	-126.14	30.14

	mstn-/- non-ov	-70.00	15.786	.086	-148.14	8.14
	mstn+/+ 3d-ov	-39.50	15.786	.552	-117.64	38.64
	mstn-/- 3d-ov	-32.50	15.786	.739	-110.64	45.64
	mstn-/- 2wk-ov	13.50	15.786	.996	-64.64	91.64
	mstn+/+ 6wk-ov	-7.50	15.786	1.000	-85.64	70.64
	mstn-/- 6wk-ov	-21.50	15.786	.952	-99.64	56.64
mstn-/- 2wk-ov	mstn+/+ non-ov	-61.50	15.786	.150	-139.64	16.64
	mstn-/- non-ov	-83.50*	15.786	.035	-161.64	-5.36
	mstn+/+ 3d-ov	-53.00	15.786	.259	-131.14	25.14
	mstn-/- 3d-ov	-46.00	15.786	.393	-124.14	32.14
	mstn+/+ 2wk-ov	-13.50	15.786	.996	-91.64	64.64
	mstn+/+ 6wk-ov	-21.00	15.786	.957	-99.14	57.14
	mstn-/- 6wk-ov	-35.00	15.786	.673	-113.14	43.14
mstn+/+ 6wk-ov	mstn+/+ non-ov	-40.50	15.786	.526	-118.64	37.64
	mstn-/- non-ov	-62.50	15.786	.141	-140.64	15.64
	mstn+/+ 3d-ov	-32.00	15.786	.752	-110.14	46.14
	mstn-/- 3d-ov	-25.00	15.786	.903	-103.14	53.14
	mstn+/+ 2wk-ov	7.50	15.786	1.000	-70.64	85.64
	mstn-/- 2wk-ov	21.00	15.786	.957	-57.14	99.14
	mstn-/- 6wk-ov	-14.00	15.786	.995	-92.14	64.14
mstn-/- 6wk-ov	mstn+/+ non-ov	-26.50	15.786	.876	-104.64	51.64

		mstn-/- non-ov	-48.50	15.786	.340	-126.64	29.64
		mstn+/+ 3d-ov	-18.00	15.786	.981	-96.14	60.14
		mstn-/- 3d-ov	-11.00	15.786	.999	-89.14	67.14
		mstn+/+ 2wk-ov	21.50	15.786	.952	-56.64	99.64
		mstn-/- 2wk-ov	35.00	15.786	.673	-43.14	113.14
		mstn+/+ 6wk-ov	14.00	15.786	.995	-64.14	92.14
LSD	mstn+/+ non-ov	mstn-/- non-ov	-22.00	15.786	.201	-58.40	14.40
		mstn+/+ 3d-ov	8.50	15.786	.605	-27.90	44.90
		mstn-/- 3d-ov	15.50	15.786	.355	-20.90	51.90
		mstn+/+ 2wk-ov	48.00*	15.786	.016	11.60	84.40
		mstn-/- 2wk-ov	61.50*	15.786	.005	25.10	97.90
		mstn+/+ 6wk-ov	40.50*	15.786	.033	4.10	76.90
		mstn-/- 6wk-ov	26.50	15.786	.132	-9.90	62.90
	mstn-/- non-ov	mstn+/+ non-ov	22.00	15.786	.201	-14.40	58.40
		mstn+/+ 3d-ov	30.50	15.786	.089	-5.90	66.90
		mstn-/- 3d-ov	37.50*	15.786	.045	1.10	73.90
		mstn+/+ 2wk-ov	70.00*	15.786	.002	33.60	106.40
		mstn-/- 2wk-ov	83.50*	15.786	.001	47.10	119.90
		mstn+/+ 6wk-ov	62.50*	15.786	.004	26.10	98.90
		mstn-/- 6wk-ov	48.50*	15.786	.015	12.10	84.90
	mstn+/+ 3d-ov	mstn+/+ non-ov	-8.50	15.786	.605	-44.90	27.90

	mstn-/- non-ov	-30.50	15.786	.089	-66.90	5.90
	mstn-/- 3d-ov	7.00	15.786	.669	-29.40	43.40
	mstn+/+ 2wk-ov	39.50*	15.786	.037	3.10	75.90
	mstn-/- 2wk-ov	53.00*	15.786	.010	16.60	89.40
	mstn+/+ 6wk-ov	32.00	15.786	.077	-4.40	68.40
	mstn-/- 6wk-ov	18.00	15.786	.287	-18.40	54.40
mstn-/- 3d-ov	mstn+/+ non-ov	-15.50	15.786	.355	-51.90	20.90
	mstn-/- non-ov	-37.50*	15.786	.045	-73.90	-1.10
	mstn+/+ 3d-ov	-7.00	15.786	.669	-43.40	29.40
	mstn+/+ 2wk-ov	32.50	15.786	.073	-3.90	68.90
	mstn-/- 2wk-ov	46.00*	15.786	.019	9.60	82.40
	mstn+/+ 6wk-ov	25.00	15.786	.152	-11.40	61.40
	mstn-/- 6wk-ov	11.00	15.786	.506	-25.40	47.40
mstn+/+ 2wk-ov	mstn+/+ non-ov	-48.00*	15.786	.016	-84.40	-11.60
	mstn-/- non-ov	-70.00*	15.786	.002	-106.40	-33.60
	mstn+/+ 3d-ov	-39.50*	15.786	.037	-75.90	-3.10
	mstn-/- 3d-ov	-32.50	15.786	.073	-68.90	3.90
	mstn-/- 2wk-ov	13.50	15.786	.417	-22.90	49.90
	mstn+/+ 6wk-ov	-7.50	15.786	.647	-43.90	28.90
	mstn-/- 6wk-ov	-21.50	15.786	.210	-57.90	14.90
mstn-/- 2wk-ov	mstn+/+ non-ov	-61.50*	15.786	.005	-97.90	-25.10

	mstn-/- non-ov	-83.50*	15.786	.001	-119.90	-47.10
	mstn+/+ 3d-ov	-53.00*	15.786	.010	-89.40	-16.60
	mstn-/- 3d-ov	-46.00*	15.786	.019	-82.40	-9.60
	mstn+/+ 2wk-ov	-13.50	15.786	.417	-49.90	22.90
	mstn+/+ 6wk-ov	-21.00	15.786	.220	-57.40	15.40
	mstn-/- 6wk-ov	-35.00	15.786	.057	-71.40	1.40
mstn+/+ 6wk-ov	mstn+/+ non-ov	-40.50*	15.786	.033	-76.90	-4.10
	mstn-/- non-ov	-62.50*	15.786	.004	-98.90	-26.10
	mstn+/+ 3d-ov	-32.00	15.786	.077	-68.40	4.40
	mstn-/- 3d-ov	-25.00	15.786	.152	-61.40	11.40
	mstn+/+ 2wk-ov	7.50	15.786	.647	-28.90	43.90
	mstn-/- 2wk-ov	21.00	15.786	.220	-15.40	57.40
	mstn-/- 6wk-ov	-14.00	15.786	.401	-50.40	22.40
mstn-/- 6wk-ov	mstn+/+ non-ov	-26.50	15.786	.132	-62.90	9.90
	mstn-/- non-ov	-48.50*	15.786	.015	-84.90	-12.10
	mstn+/+ 3d-ov	-18.00	15.786	.287	-54.40	18.40
	mstn-/- 3d-ov	-11.00	15.786	.506	-47.40	25.40
	mstn+/+ 2wk-ov	21.50	15.786	.210	-14.90	57.90
	mstn-/- 2wk-ov	35.00	15.786	.057	-1.40	71.40
	mstn+/+ 6wk-ov	14.00	15.786	.401	-22.40	50.40

Based on observed means.

The error term is Mean Square(Error) = 249.188.

*. The mean difference is significant at the .05 level.

Homogeneous Subsets

Relative Atrogin Expression

	Group	N	Subset 1	Subset 2
Tukey HSD[a,,b]	mstn-/- 2wk-ov	2	56.00	
	mstn+/+ 2wk-ov	2	69.50	
	mstn+/+ 6wk-ov	2	77.00	
	mstn-/- 6wk-ov	2	91.00	91.00
	mstn-/- 3d-ov	2	102.00	102.00
	mstn+/+ 3d-ov	2	109.00	109.00
	mstn+/+ non-ov	2	117.50	117.50
	mstn-/- non-ov	2		139.50
	Sig.		.054	.155
Scheffe[a,,b]	mstn-/- 2wk-ov	2	56.00	

	mstn+/+ 2wk-ov	2	69.50	69.50
	mstn+/+ 6wk-ov	2	77.00	77.00
	mstn-/- 6wk-ov	2	91.00	91.00
	mstn-/- 3d-ov	2	102.00	102.00
	mstn+/+ 3d-ov	2	109.00	109.00
	mstn+/+ non-ov	2	117.50	117.50
	mstn-/- non-ov	2		139.50
	Sig.		.150	.086

Means for groups in homogeneous subsets are displayed.

Based on observed means.

The error term is Mean Square(Error) = 249.188.

a. Uses Harmonic Mean Sample Size = 2.000.

b. Alpha = .05.

ANOVA: Follistatin Expression Response to Overloading Mstn+/+ and Mstn-/-

Notes

Output Created	25-Nov-2009 11:29:24
Comments	

Input	Data	C:\Users\Moe AK\Documents\Stats for thesis\MOD Midbelly Area Fibre CSA and Fibre Number Raw data.sav
	Active Dataset	DataSet1
	Filter	<none>
	Weight	<none>
	Split File	<none>
	N of Rows in Working Data File	24
Missing Value Handling	Definition of Missing	User-defined missing values are treated as missing.
	Cases Used	Statistics are based on all cases with valid data for all variables in the model.
	Syntax	UNIANOVA Follistatin BY Group /METHOD=SSTYPE(3) /INTERCEPT=INCLUDE /POSTHOC=Group(TUKEY SCHEFFE LSD) /EMMEANS=TABLES(Group) /PRINT=ETASQ HOMOGENEITY DESCRIPTIVE /CRITERIA=ALPHA(.05) /DESIGN=Group.
Resources	Processor Time	0:00:00.062
	Elapsed Time	0:00:00.166

Between-Subjects Factors

		Value Label	N
Group	1.00	mstn+/+ non-ov	2
	2.00	mstn-/- non-ov	2
	3.00	mstn+/+ 3d-ov	2
	4.00	mstn-/- 3d-ov	2
	5.00	mstn+/+ 2wk-ov	2
	6.00	mstn-/- 2wk-ov	2
	7.00	mstn+/+ 6wk-ov	2
	8.00	mstn-/- 6wk-ov	2

Descriptive Statistics

Dependent Variable:Relative Follistatin Expression

Group	Mean	Std. Deviation	N
mstn+/+ non-ov	36.50	13.435	2
mstn-/- non-ov	38.50	9.192	2
mstn+/+ 3d-ov	241.50	2.121	2
mstn-/- 3d-ov	68.00	8.485	2

mstn+/+ 2wk-ov	113.50	10.607	2
mstn-/- 2wk-ov	42.50	10.607	2
mstn+/+ 6wk-ov	101.50	33.234	2
mstn-/- 6wk-ov	48.00	67.882	2
Total	86.25	69.936	16

Tests of Between-Subjects Effects

Dependent Variable:Relative Follistatin Expression

Source	Type III Sum of Squares	df	Mean Square	F	Sig.	Partial Eta Squared
Corrected Model	67086.000[a]	7	9583.714	12.210	.001	.914
Intercept	119025.000	1	119025.000	151.648	.000	.950
Group	67086.000	7	9583.714	12.210	.001	.914
Error	6279.000	8	784.875			
Total	192390.000	16				
Corrected Total	73365.000	15				

a. R Squared = .914 (Adjusted R Squared = .840)

Estimated Marginal Means

Group

Dependent Variable:Relative Follistatin Expression

Group			95% Confidence Interval	
	Mean	Std. Error	Lower Bound	Upper Bound
mstn+/+ non-ov	36.500	19.810	-9.182	82.182
mstn-/- non-ov	38.500	19.810	-7.182	84.182
mstn+/+ 3d-ov	241.500	19.810	195.818	287.182
mstn-/- 3d-ov	68.000	19.810	22.318	113.682
mstn+/+ 2wk-ov	113.500	19.810	67.818	159.182
mstn-/- 2wk-ov	42.500	19.810	-3.182	88.182
mstn+/+ 6wk-ov	101.500	19.810	55.818	147.182
mstn-/- 6wk-ov	48.000	19.810	2.318	93.682

Post Hoc Tests

Group

Multiple Comparisons

Dependent Variable:Relative Follistatin Expression

	(I) Group	(J) Group	Mean Difference (I-J)	Std. Error	Sig.	95% Confidence Interval Lower Bound	95% Confidence Interval Upper Bound
Tukey HSD	mstn+/+ non-ov	mstn-/- non-ov	-2.00	28.016	1.000	-112.86	108.86
		mstn+/+ 3d-ov	-205.00*	28.016	.001	-315.86	-94.14
		mstn-/- 3d-ov	-31.50	28.016	.933	-142.36	79.36
		mstn+/+ 2wk-ov	-77.00	28.016	.232	-187.86	33.86
		mstn-/- 2wk-ov	-6.00	28.016	1.000	-116.86	104.86
		mstn+/+ 6wk-ov	-65.00	28.016	.382	-175.86	45.86
		mstn-/- 6wk-ov	-11.50	28.016	1.000	-122.36	99.36
	mstn-/- non-ov	mstn+/+ non-ov	2.00	28.016	1.000	-108.86	112.86
		mstn+/+ 3d-ov	-203.00*	28.016	.001	-313.86	-92.14
		mstn-/- 3d-ov	-29.50	28.016	.951	-140.36	81.36
		mstn+/+ 2wk-ov	-75.00	28.016	.253	-185.86	35.86
		mstn-/- 2wk-ov	-4.00	28.016	1.000	-114.86	106.86
		mstn+/+ 6wk-ov	-63.00	28.016	.413	-173.86	47.86
		mstn-/- 6wk-ov	-9.50	28.016	1.000	-120.36	101.36
	mstn+/+ 3d-ov	mstn+/+ non-ov	205.00*	28.016	.001	94.14	315.86
		mstn-/- non-ov	203.00*	28.016	.001	92.14	313.86
		mstn-/- 3d-ov	173.50*	28.016	.004	62.64	284.36

	mstn+/+ 2wk-ov	128.00*	28.016	.023	17.14	238.86
	mstn-/- 2wk-ov	199.00*	28.016	.001	88.14	309.86
	mstn+/+ 6wk-ov	140.00*	28.016	.014	29.14	250.86
	mstn-/- 6wk-ov	193.50*	28.016	.002	82.64	304.36
mstn-/- 3d-ov	mstn+/+ non-ov	31.50	28.016	.933	-79.36	142.36
	mstn-/- non-ov	29.50	28.016	.951	-81.36	140.36
	mstn+/+ 3d-ov	-173.50*	28.016	.004	-284.36	-62.64
	mstn+/+ 2wk-ov	-45.50	28.016	.729	-156.36	65.36
	mstn-/- 2wk-ov	25.50	28.016	.976	-85.36	136.36
	mstn+/+ 6wk-ov	-33.50	28.016	.913	-144.36	77.36
	mstn-/- 6wk-ov	20.00	28.016	.994	-90.86	130.86
mstn+/+ 2wk-ov	mstn+/+ non-ov	77.00	28.016	.232	-33.86	187.86
	mstn-/- non-ov	75.00	28.016	.253	-35.86	185.86
	mstn+/+ 3d-ov	-128.00*	28.016	.023	-238.86	-17.14
	mstn-/- 3d-ov	45.50	28.016	.729	-65.36	156.36
	mstn-/- 2wk-ov	71.00	28.016	.299	-39.86	181.86
	mstn+/+ 6wk-ov	12.00	28.016	1.000	-98.86	122.86
	mstn-/- 6wk-ov	65.50	28.016	.375	-45.36	176.36
mstn-/- 2wk-ov	mstn+/+ non-ov	6.00	28.016	1.000	-104.86	116.86
	mstn-/- non-ov	4.00	28.016	1.000	-106.86	114.86

		mstn+/+ 3d-ov	-199.00*	28.016	.001	-309.86	-88.14
		mstn-/- 3d-ov	-25.50	28.016	.976	-136.36	85.36
		mstn+/+ 2wk-ov	-71.00	28.016	.299	-181.86	39.86
		mstn+/+ 6wk-ov	-59.00	28.016	.480	-169.86	51.86
		mstn-/- 6wk-ov	-5.50	28.016	1.000	-116.36	105.36
	mstn+/+ 6wk-ov	mstn+/+ non-ov	65.00	28.016	.382	-45.86	175.86
		mstn-/- non-ov	63.00	28.016	.413	-47.86	173.86
		mstn+/+ 3d-ov	-140.00*	28.016	.014	-250.86	-29.14
		mstn-/- 3d-ov	33.50	28.016	.913	-77.36	144.36
		mstn+/+ 2wk-ov	-12.00	28.016	1.000	-122.86	98.86
		mstn-/- 2wk-ov	59.00	28.016	.480	-51.86	169.86
		mstn-/- 6wk-ov	53.50	28.016	.579	-57.36	164.36
	mstn-/- 6wk-ov	mstn+/+ non-ov	11.50	28.016	1.000	-99.36	122.36
		mstn-/- non-ov	9.50	28.016	1.000	-101.36	120.36
		mstn+/+ 3d-ov	-193.50*	28.016	.002	-304.36	-82.64
		mstn-/- 3d-ov	-20.00	28.016	.994	-130.86	90.86
		mstn+/+ 2wk-ov	-65.50	28.016	.375	-176.36	45.36
		mstn-/- 2wk-ov	5.50	28.016	1.000	-105.36	116.36
		mstn+/+ 6wk-ov	-53.50	28.016	.579	-164.36	57.36
Scheffe	mstn+/+ non-ov	mstn-/- non-ov	-2.00	28.016	1.000	-140.68	136.68

	mstn+/+ 3d-ov	-205.00*	28.016	.005	-343.68	-66.32
	mstn-/- 3d-ov	-31.50	28.016	.982	-170.18	107.18
	mstn+/+ 2wk-ov	-77.00	28.016	.453	-215.68	61.68
	mstn-/- 2wk-ov	-6.00	28.016	1.000	-144.68	132.68
	mstn+/+ 6wk-ov	-65.00	28.016	.629	-203.68	73.68
	mstn-/- 6wk-ov	-11.50	28.016	1.000	-150.18	127.18
mstn-/- non-ov	mstn+/+ non-ov	2.00	28.016	1.000	-136.68	140.68
	mstn+/+ 3d-ov	-203.00*	28.016	.005	-341.68	-64.32
	mstn-/- 3d-ov	-29.50	28.016	.987	-168.18	109.18
	mstn+/+ 2wk-ov	-75.00	28.016	.481	-213.68	63.68
	mstn-/- 2wk-ov	-4.00	28.016	1.000	-142.68	134.68
	mstn+/+ 6wk-ov	-63.00	28.016	.659	-201.68	75.68
	mstn-/- 6wk-ov	-9.50	28.016	1.000	-148.18	129.18
mstn+/+ 3d-ov	mstn+/+ non-ov	205.00*	28.016	.005	66.32	343.68
	mstn-/- non-ov	203.00*	28.016	.005	64.32	341.68
	mstn-/- 3d-ov	173.50*	28.016	.014	34.82	312.18
	mstn+/+ 2wk-ov	128.00	28.016	.074	-10.68	266.68
	mstn-/- 2wk-ov	199.00*	28.016	.006	60.32	337.68
	mstn+/+ 6wk-ov	140.00*	28.016	.048	1.32	278.68
	mstn-/- 6wk-ov	193.50*	28.016	.007	54.82	332.18
mstn-/- 3d-ov	mstn+/+ non-ov	31.50	28.016	.982	-107.18	170.18

	mstn-/- non-ov	29.50	28.016	.987	-109.18	168.18
	mstn+/+ 3d-ov	-173.50*	28.016	.014	-312.18	-34.82
	mstn+/+ 2wk-ov	-45.50	28.016	.892	-184.18	93.18
	mstn-/- 2wk-ov	25.50	28.016	.995	-113.18	164.18
	mstn+/+ 6wk-ov	-33.50	28.016	.975	-172.18	105.18
	mstn-/- 6wk-ov	20.00	28.016	.999	-118.68	158.68
mstn+/+ 2wk-ov	mstn+/+ non-ov	77.00	28.016	.453	-61.68	215.68
	mstn-/- non-ov	75.00	28.016	.481	-63.68	213.68
	mstn+/+ 3d-ov	-128.00	28.016	.074	-266.68	10.68
	mstn-/- 3d-ov	45.50	28.016	.892	-93.18	184.18
	mstn-/- 2wk-ov	71.00	28.016	.539	-67.68	209.68
	mstn+/+ 6wk-ov	12.00	28.016	1.000	-126.68	150.68
	mstn-/- 6wk-ov	65.50	28.016	.621	-73.18	204.18
mstn-/- 2wk-ov	mstn+/+ non-ov	6.00	28.016	1.000	-132.68	144.68
	mstn-/- non-ov	4.00	28.016	1.000	-134.68	142.68
	mstn+/+ 3d-ov	-199.00*	28.016	.006	-337.68	-60.32
	mstn-/- 3d-ov	-25.50	28.016	.995	-164.18	113.18
	mstn+/+ 2wk-ov	-71.00	28.016	.539	-209.68	67.68
	mstn+/+ 6wk-ov	-59.00	28.016	.719	-197.68	79.68
	mstn-/- 6wk-ov	-5.50	28.016	1.000	-144.18	133.18
mstn+/+ 6wk-ov	mstn+/+ non-ov	65.00	28.016	.629	-73.68	203.68

		mstn-/- non-ov	63.00	28.016	.659	-75.68	201.68
		mstn+/+ 3d-ov	-140.00*	28.016	.048	-278.68	-1.32
		mstn-/- 3d-ov	33.50	28.016	.975	-105.18	172.18
		mstn+/+ 2wk-ov	-12.00	28.016	1.000	-150.68	126.68
		mstn-/- 2wk-ov	59.00	28.016	.719	-79.68	197.68
		mstn-/- 6wk-ov	53.50	28.016	.797	-85.18	192.18
	mstn-/- 6wk-ov	mstn+/+ non-ov	11.50	28.016	1.000	-127.18	150.18
		mstn-/- non-ov	9.50	28.016	1.000	-129.18	148.18
		mstn+/+ 3d-ov	-193.50*	28.016	.007	-332.18	-54.82
		mstn-/- 3d-ov	-20.00	28.016	.999	-158.68	118.68
		mstn+/+ 2wk-ov	-65.50	28.016	.621	-204.18	73.18
		mstn-/- 2wk-ov	5.50	28.016	1.000	-133.18	144.18
		mstn+/+ 6wk-ov	-53.50	28.016	.797	-192.18	85.18
LSD	mstn+/+ non-ov	mstn-/- non-ov	-2.00	28.016	.945	-66.60	62.60
		mstn+/+ 3d-ov	-205.00*	28.016	.000	-269.60	-140.40
		mstn-/- 3d-ov	-31.50	28.016	.293	-96.10	33.10
		mstn+/+ 2wk-ov	-77.00*	28.016	.025	-141.60	-12.40
		mstn-/- 2wk-ov	-6.00	28.016	.836	-70.60	58.60
		mstn+/+ 6wk-ov	-65.00*	28.016	.049	-129.60	-.40
		mstn-/- 6wk-ov	-11.50	28.016	.692	-76.10	53.10
	mstn-/- non-ov	mstn+/+ non-ov	2.00	28.016	.945	-62.60	66.60

	mstn+/+ 3d-ov	-203.00*	28.016	.000	-267.60	-138.40
	mstn-/- 3d-ov	-29.50	28.016	.323	-94.10	35.10
	mstn+/+ 2wk-ov	-75.00*	28.016	.028	-139.60	-10.40
	mstn-/- 2wk-ov	-4.00	28.016	.890	-68.60	60.60
	mstn+/+ 6wk-ov	-63.00	28.016	.055	-127.60	1.60
	mstn-/- 6wk-ov	-9.50	28.016	.743	-74.10	55.10
mstn+/+ 3d-ov	mstn+/+ non-ov	205.00*	28.016	.000	140.40	269.60
	mstn-/- non-ov	203.00*	28.016	.000	138.40	267.60
	mstn-/- 3d-ov	173.50*	28.016	.000	108.90	238.10
	mstn+/+ 2wk-ov	128.00*	28.016	.002	63.40	192.60
	mstn-/- 2wk-ov	199.00*	28.016	.000	134.40	263.60
	mstn+/+ 6wk-ov	140.00*	28.016	.001	75.40	204.60
	mstn-/- 6wk-ov	193.50*	28.016	.000	128.90	258.10
mstn-/- 3d-ov	mstn+/+ non-ov	31.50	28.016	.293	-33.10	96.10
	mstn-/- non-ov	29.50	28.016	.323	-35.10	94.10
	mstn+/+ 3d-ov	-173.50*	28.016	.000	-238.10	-108.90
	mstn+/+ 2wk-ov	-45.50	28.016	.143	-110.10	19.10
	mstn-/- 2wk-ov	25.50	28.016	.389	-39.10	90.10
	mstn+/+ 6wk-ov	-33.50	28.016	.266	-98.10	31.10
	mstn-/- 6wk-ov	20.00	28.016	.496	-44.60	84.60
mstn+/+ 2wk-ov	mstn+/+ non-ov	77.00*	28.016	.025	12.40	141.60

	mstn-/- non-ov	75.00*	28.016	.028	10.40	139.60
	mstn+/+ 3d-ov	-128.00*	28.016	.002	-192.60	-63.40
	mstn-/- 3d-ov	45.50	28.016	.143	-19.10	110.10
	mstn-/- 2wk-ov	71.00*	28.016	.035	6.40	135.60
	mstn+/+ 6wk-ov	12.00	28.016	.680	-52.60	76.60
	mstn-/- 6wk-ov	65.50*	28.016	.048	.90	130.10
mstn-/- 2wk-ov	mstn+/+ non-ov	6.00	28.016	.836	-58.60	70.60
	mstn-/- non-ov	4.00	28.016	.890	-60.60	68.60
	mstn+/+ 3d-ov	-199.00*	28.016	.000	-263.60	-134.40
	mstn-/- 3d-ov	-25.50	28.016	.389	-90.10	39.10
	mstn+/+ 2wk-ov	-71.00*	28.016	.035	-135.60	-6.40
	mstn+/+ 6wk-ov	-59.00	28.016	.068	-123.60	5.60
	mstn-/- 6wk-ov	-5.50	28.016	.849	-70.10	59.10
mstn+/+ 6wk-ov	mstn+/+ non-ov	65.00*	28.016	.049	.40	129.60
	mstn-/- non-ov	63.00	28.016	.055	-1.60	127.60
	mstn+/+ 3d-ov	-140.00*	28.016	.001	-204.60	-75.40
	mstn-/- 3d-ov	33.50	28.016	.266	-31.10	98.10
	mstn+/+ 2wk-ov	-12.00	28.016	.680	-76.60	52.60
	mstn-/- 2wk-ov	59.00	28.016	.068	-5.60	123.60
	mstn-/- 6wk-ov	53.50	28.016	.093	-11.10	118.10
mstn-/- 6wk-ov	mstn+/+ non-ov	11.50	28.016	.692	-53.10	76.10

	mstn-/- non-ov	9.50	28.016	.743	-55.10	74.10
	mstn+/+ 3d-ov	-193.50*	28.016	.000	-258.10	-128.90
	mstn-/- 3d-ov	-20.00	28.016	.496	-84.60	44.60
	mstn+/+ 2wk-ov	-65.50*	28.016	.048	-130.10	-.90
	mstn-/- 2wk-ov	5.50	28.016	.849	-59.10	70.10
	mstn+/+ 6wk-ov	-53.50	28.016	.093	-118.10	11.10

Based on observed means.

The error term is Mean Square(Error) = 784.875.

*. The mean difference is significant at the .05 level.

Homogeneous Subsets

Relative Follistatin Expression

	Group	N	Subset 1	Subset 2
Tukey HSD[a,,b]	mstn+/+ non-ov	2	36.50	
	mstn-/- non-ov	2	38.50	
	mstn-/- 2wk-ov	2	42.50	
	mstn-/- 6wk-ov	2	48.00	

	mstn-/- 3d-ov	2	68.00	
	mstn+/+ 6wk-ov	2	101.50	
	mstn+/+ 2wk-ov	2	113.50	
	mstn+/+ 3d-ov	2		241.50
	Sig.		.232	1.000
Scheffe[a,,b]	mstn+/+ non-ov	2	36.50	
	mstn-/- non-ov	2	38.50	
	mstn-/- 2wk-ov	2	42.50	
	mstn-/- 6wk-ov	2	48.00	
	mstn-/- 3d-ov	2	68.00	
	mstn+/+ 6wk-ov	2	101.50	
	mstn+/+ 2wk-ov	2	113.50	113.50
	mstn+/+ 3d-ov	2		241.50
	Sig.		.453	.074

Means for groups in homogeneous subsets are displayed.

Based on observed means.

The error term is Mean Square(Error) = 784.875.

a. Uses Harmonic Mean Sample Size = 2.000.

b. Alpha = .05.

ANOVA: Myogenin Expression Response to Overloading Mstn+/+ and Mstn-/-

Notes

	Output Created	25-Nov-2009 11:31:14
	Comments	
Input	Data	C:\Users\Moe AK\Documents\Stats for thesis\MOD Midbelly Area Fibre CSA and Fibre Number Raw data.sav
	Active Dataset	DataSet1
	Filter	<none>
	Weight	<none>
	Split File	<none>
	N of Rows in Working Data File	24
Missing Value Handling	Definition of Missing	User-defined missing values are treated as missing.
	Cases Used	Statistics are based on all cases with valid data for all variables in the model.

	Syntax	UNIANOVA Myogenin BY Group /METHOD=SSTYPE(3) /INTERCEPT=INCLUDE /POSTHOC=Group(TUKEY SCHEFFE LSD) /EMMEANS=TABLES(Group) /PRINT=ETASQ HOMOGENEITY DESCRIPTIVE /CRITERIA=ALPHA(.05) /DESIGN=Group.
Resources	Processor Time	0:00:00.125
	Elapsed Time	0:00:00.149

Between-Subjects Factors

		Value Label	N
Group	1.00	mstn+/+ non-ov	2
	2.00	mstn-/- non-ov	2
	3.00	mstn+/+ 3d-ov	2
	4.00	mstn-/- 3d-ov	2
	5.00	mstn+/+ 2wk-ov	2
	6.00	mstn-/- 2wk-ov	2

7.00	mstn+/+ 6wk-ov	2
8.00	mstn-/- 6wk-ov	2

Descriptive Statistics

Dependent Variable:Relative Myogenin Expression

Group	Mean	Std. Deviation	N
mstn+/+ non-ov	30.00	2.828	2
mstn-/- non-ov	42.50	6.364	2
mstn+/+ 3d-ov	80.00	5.657	2
mstn-/- 3d-ov	136.50	6.364	2
mstn+/+ 2wk-ov	163.50	.707	2
mstn-/- 2wk-ov	253.00	7.071	2
mstn+/+ 6wk-ov	69.00	.000	2
mstn-/- 6wk-ov	97.50	4.950	2
Total	109.00	70.990	16

Tests of Between-Subjects Effects

Dependent Variable:Relative Myogenin Expression

Source	Type III Sum of Squares	df	Mean Square	F	Sig.	Partial Eta Squared

Corrected Model	75398.000[a]	7	10771.143	439.638	.000	.997
Intercept	190096.000	1	190096.000	7759.020	.000	.999
Group	75398.000	7	10771.143	439.638	.000	.997
Error	196.000	8	24.500			
Total	265690.000	16				
Corrected Total	75594.000	15				

a. R Squared = .997 (Adjusted R Squared = .995)

Estimated Marginal Means

Group

Dependent Variable:Relative Myogenin Expression

Group			95% Confidence Interval	
	Mean	Std. Error	Lower Bound	Upper Bound
mstn+/+ non-ov	30.000	3.500	21.929	38.071
mstn-/- non-ov	42.500	3.500	34.429	50.571
mstn+/+ 3d-ov	80.000	3.500	71.929	88.071
mstn-/- 3d-ov	136.500	3.500	128.429	144.571
mstn+/+ 2wk-ov	163.500	3.500	155.429	171.571
mstn-/- 2wk-ov	253.000	3.500	244.929	261.071

mstn+/+ 6wk-ov	69.000	3.500	60.929	77.071
mstn-/- 6wk-ov	97.500	3.500	89.429	105.571

Post Hoc Tests

Group

Multiple Comparisons

Dependent Variable:Relative Myogenin Expression

					95% Confidence Interval	
(I) Group	(J) Group	Mean Difference (I-J)	Std. Error	Sig.	Lower Bound	Upper Bound
Tukey HSD mstn+/+ non-ov	mstn-/- non-ov	-12.50	4.950	.303	-32.09	7.09
	mstn+/+ 3d-ov	-50.00*	4.950	.000	-69.59	-30.41
	mstn-/- 3d-ov	-106.50*	4.950	.000	-126.09	-86.91
	mstn+/+ 2wk-ov	-133.50*	4.950	.000	-153.09	-113.91
	mstn-/- 2wk-ov	-223.00*	4.950	.000	-242.59	-203.41
	mstn+/+ 6wk-ov	-39.00*	4.950	.001	-58.59	-19.41
	mstn-/- 6wk-ov	-67.50*	4.950	.000	-87.09	-47.91

	mstn-/- non-ov	mstn+/+ non-ov	12.50	4.950	.303	-7.09	32.09
		mstn+/+ 3d-ov	-37.50*	4.950	.001	-57.09	-17.91
		mstn-/- 3d-ov	-94.00*	4.950	.000	-113.59	-74.41
		mstn+/+ 2wk-ov	-121.00*	4.950	.000	-140.59	-101.41
		mstn-/- 2wk-ov	-210.50*	4.950	.000	-230.09	-190.91
		mstn+/+ 6wk-ov	-26.50*	4.950	.009	-46.09	-6.91
		mstn-/- 6wk-ov	-55.00*	4.950	.000	-74.59	-35.41
	mstn+/+ 3d-ov	mstn+/+ non-ov	50.00*	4.950	.000	30.41	69.59
		mstn-/- non-ov	37.50*	4.950	.001	17.91	57.09
		mstn-/- 3d-ov	-56.50*	4.950	.000	-76.09	-36.91
		mstn+/+ 2wk-ov	-83.50*	4.950	.000	-103.09	-63.91
		mstn-/- 2wk-ov	-173.00*	4.950	.000	-192.59	-153.41
		mstn+/+ 6wk-ov	11.00	4.950	.425	-8.59	30.59
		mstn-/- 6wk-ov	-17.50	4.950	.086	-37.09	2.09
	mstn-/- 3d-ov	mstn+/+ non-ov	106.50*	4.950	.000	86.91	126.09
		mstn-/- non-ov	94.00*	4.950	.000	74.41	113.59
		mstn+/+ 3d-ov	56.50*	4.950	.000	36.91	76.09
		mstn+/+ 2wk-ov	-27.00*	4.950	.008	-46.59	-7.41
		mstn-/- 2wk-ov	-116.50*	4.950	.000	-136.09	-96.91
		mstn+/+ 6wk-ov	67.50*	4.950	.000	47.91	87.09

	mstn-/- 6wk-ov	39.00*	4.950	.001	19.41	58.59
mstn+/+ 2wk-ov	mstn+/+ non-ov	133.50*	4.950	.000	113.91	153.09
	mstn-/- non-ov	121.00*	4.950	.000	101.41	140.59
	mstn+/+ 3d-ov	83.50*	4.950	.000	63.91	103.09
	mstn-/- 3d-ov	27.00*	4.950	.008	7.41	46.59
	mstn-/- 2wk-ov	-89.50*	4.950	.000	-109.09	-69.91
	mstn+/+ 6wk-ov	94.50*	4.950	.000	74.91	114.09
	mstn-/- 6wk-ov	66.00*	4.950	.000	46.41	85.59
mstn-/- 2wk-ov	mstn+/+ non-ov	223.00*	4.950	.000	203.41	242.59
	mstn-/- non-ov	210.50*	4.950	.000	190.91	230.09
	mstn+/+ 3d-ov	173.00*	4.950	.000	153.41	192.59
	mstn-/- 3d-ov	116.50*	4.950	.000	96.91	136.09
	mstn+/+ 2wk-ov	89.50*	4.950	.000	69.91	109.09
	mstn+/+ 6wk-ov	184.00*	4.950	.000	164.41	203.59
	mstn-/- 6wk-ov	155.50*	4.950	.000	135.91	175.09
mstn+/+ 6wk-ov	mstn+/+ non-ov	39.00*	4.950	.001	19.41	58.59
	mstn-/- non-ov	26.50*	4.950	.009	6.91	46.09
	mstn+/+ 3d-ov	-11.00	4.950	.425	-30.59	8.59
	mstn-/- 3d-ov	-67.50*	4.950	.000	-87.09	-47.91
	mstn+/+ 2wk-ov	-94.50*	4.950	.000	-114.09	-74.91

		mstn-/- 2wk-ov	-184.00*	4.950	.000	-203.59	-164.41
		mstn-/- 6wk-ov	-28.50*	4.950	.006	-48.09	-8.91
	mstn-/- 6wk-ov	mstn+/+ non-ov	67.50*	4.950	.000	47.91	87.09
		mstn-/- non-ov	55.00*	4.950	.000	35.41	74.59
		mstn+/+ 3d-ov	17.50	4.950	.086	-2.09	37.09
		mstn-/- 3d-ov	-39.00*	4.950	.001	-58.59	-19.41
		mstn+/+ 2wk-ov	-66.00*	4.950	.000	-85.59	-46.41
		mstn-/- 2wk-ov	-155.50*	4.950	.000	-175.09	-135.91
		mstn+/+ 6wk-ov	28.50*	4.950	.006	8.91	48.09
Scheffe	mstn+/+ non-ov	mstn-/- non-ov	-12.50	4.950	.542	-37.00	12.00
		mstn+/+ 3d-ov	-50.00*	4.950	.001	-74.50	-25.50
		mstn-/- 3d-ov	-106.50*	4.950	.000	-131.00	-82.00
		mstn+/+ 2wk-ov	-133.50*	4.950	.000	-158.00	-109.00
		mstn-/- 2wk-ov	-223.00*	4.950	.000	-247.50	-198.50
		mstn+/+ 6wk-ov	-39.00*	4.950	.003	-63.50	-14.50
		mstn-/- 6wk-ov	-67.50*	4.950	.000	-92.00	-43.00
	mstn-/- non-ov	mstn+/+ non-ov	12.50	4.950	.542	-12.00	37.00
		mstn+/+ 3d-ov	-37.50*	4.950	.004	-62.00	-13.00
		mstn-/- 3d-ov	-94.00*	4.950	.000	-118.50	-69.50
		mstn+/+ 2wk-ov	-121.00*	4.950	.000	-145.50	-96.50
		mstn-/- 2wk-ov	-210.50*	4.950	.000	-235.00	-186.00

	mstn+/+ 6wk-ov	-26.50*	4.950	.033	-51.00	-2.00
	mstn-/- 6wk-ov	-55.00*	4.950	.000	-79.50	-30.50
mstn+/+ 3d-ov	mstn+/+ non-ov	50.00*	4.950	.001	25.50	74.50
	mstn-/- non-ov	37.50*	4.950	.004	13.00	62.00
	mstn-/- 3d-ov	-56.50*	4.950	.000	-81.00	-32.00
	mstn+/+ 2wk-ov	-83.50*	4.950	.000	-108.00	-59.00
	mstn-/- 2wk-ov	-173.00*	4.950	.000	-197.50	-148.50
	mstn+/+ 6wk-ov	11.00	4.950	.671	-13.50	35.50
	mstn-/- 6wk-ov	-17.50	4.950	.217	-42.00	7.00
mstn-/- 3d-ov	mstn+/+ non-ov	106.50*	4.950	.000	82.00	131.00
	mstn-/- non-ov	94.00*	4.950	.000	69.50	118.50
	mstn+/+ 3d-ov	56.50*	4.950	.000	32.00	81.00
	mstn+/+ 2wk-ov	-27.00*	4.950	.030	-51.50	-2.50
	mstn-/- 2wk-ov	-116.50*	4.950	.000	-141.00	-92.00
	mstn+/+ 6wk-ov	67.50*	4.950	.000	43.00	92.00
	mstn-/- 6wk-ov	39.00*	4.950	.003	14.50	63.50
mstn+/+ 2wk-ov	mstn+/+ non-ov	133.50*	4.950	.000	109.00	158.00
	mstn-/- non-ov	121.00*	4.950	.000	96.50	145.50
	mstn+/+ 3d-ov	83.50*	4.950	.000	59.00	108.00
	mstn-/- 3d-ov	27.00*	4.950	.030	2.50	51.50
	mstn-/- 2wk-ov	-89.50*	4.950	.000	-114.00	-65.00

	mstn+/+ 6wk-ov	94.50*	4.950	.000	70.00	119.00
	mstn-/- 6wk-ov	66.00*	4.950	.000	41.50	90.50
mstn-/- 2wk-ov	mstn+/+ non-ov	223.00*	4.950	.000	198.50	247.50
	mstn-/- non-ov	210.50*	4.950	.000	186.00	235.00
	mstn+/+ 3d-ov	173.00*	4.950	.000	148.50	197.50
	mstn-/- 3d-ov	116.50*	4.950	.000	92.00	141.00
	mstn+/+ 2wk-ov	89.50*	4.950	.000	65.00	114.00
	mstn+/+ 6wk-ov	184.00*	4.950	.000	159.50	208.50
	mstn-/- 6wk-ov	155.50*	4.950	.000	131.00	180.00
mstn+/+ 6wk-ov	mstn+/+ non-ov	39.00*	4.950	.003	14.50	63.50
	mstn-/- non-ov	26.50*	4.950	.033	2.00	51.00
	mstn+/+ 3d-ov	-11.00	4.950	.671	-35.50	13.50
	mstn-/- 3d-ov	-67.50*	4.950	.000	-92.00	-43.00
	mstn+/+ 2wk-ov	-94.50*	4.950	.000	-119.00	-70.00
	mstn-/- 2wk-ov	-184.00*	4.950	.000	-208.50	-159.50
	mstn-/- 6wk-ov	-28.50*	4.950	.022	-53.00	-4.00
mstn-/- 6wk-ov	mstn+/+ non-ov	67.50*	4.950	.000	43.00	92.00
	mstn-/- non-ov	55.00*	4.950	.000	30.50	79.50
	mstn+/+ 3d-ov	17.50	4.950	.217	-7.00	42.00
	mstn-/- 3d-ov	-39.00*	4.950	.003	-63.50	-14.50
	mstn+/+ 2wk-ov	-66.00*	4.950	.000	-90.50	-41.50

		mstn-/- 2wk-ov	-155.50*	4.950	.000	-180.00	-131.00
		mstn+/+ 6wk-ov	28.50*	4.950	.022	4.00	53.00
LSD	mstn+/+ non-ov	mstn-/- non-ov	-12.50*	4.950	.036	-23.91	-1.09
		mstn+/+ 3d-ov	-50.00*	4.950	.000	-61.41	-38.59
		mstn-/- 3d-ov	-106.50*	4.950	.000	-117.91	-95.09
		mstn+/+ 2wk-ov	-133.50*	4.950	.000	-144.91	-122.09
		mstn-/- 2wk-ov	-223.00*	4.950	.000	-234.41	-211.59
		mstn+/+ 6wk-ov	-39.00*	4.950	.000	-50.41	-27.59
		mstn-/- 6wk-ov	-67.50*	4.950	.000	-78.91	-56.09
	mstn-/- non-ov	mstn+/+ non-ov	12.50*	4.950	.036	1.09	23.91
		mstn+/+ 3d-ov	-37.50*	4.950	.000	-48.91	-26.09
		mstn-/- 3d-ov	-94.00*	4.950	.000	-105.41	-82.59
		mstn+/+ 2wk-ov	-121.00*	4.950	.000	-132.41	-109.59
		mstn-/- 2wk-ov	-210.50*	4.950	.000	-221.91	-199.09
		mstn+/+ 6wk-ov	-26.50*	4.950	.001	-37.91	-15.09
		mstn-/- 6wk-ov	-55.00*	4.950	.000	-66.41	-43.59
	mstn+/+ 3d-ov	mstn+/+ non-ov	50.00*	4.950	.000	38.59	61.41
		mstn-/- non-ov	37.50*	4.950	.000	26.09	48.91
		mstn-/- 3d-ov	-56.50*	4.950	.000	-67.91	-45.09
		mstn+/+ 2wk-ov	-83.50*	4.950	.000	-94.91	-72.09
		mstn-/- 2wk-ov	-173.00*	4.950	.000	-184.41	-161.59

	mstn+/+ 6wk-ov	11.00	4.950	.057	-.41	22.41
	mstn-/- 6wk-ov	-17.50*	4.950	.008	-28.91	-6.09
mstn-/- 3d-ov	mstn+/+ non-ov	106.50*	4.950	.000	95.09	117.91
	mstn-/- non-ov	94.00*	4.950	.000	82.59	105.41
	mstn+/+ 3d-ov	56.50*	4.950	.000	45.09	67.91
	mstn+/+ 2wk-ov	-27.00*	4.950	.001	-38.41	-15.59
	mstn-/- 2wk-ov	-116.50*	4.950	.000	-127.91	-105.09
	mstn+/+ 6wk-ov	67.50*	4.950	.000	56.09	78.91
	mstn-/- 6wk-ov	39.00*	4.950	.000	27.59	50.41
mstn+/+ 2wk-ov	mstn+/+ non-ov	133.50*	4.950	.000	122.09	144.91
	mstn-/- non-ov	121.00*	4.950	.000	109.59	132.41
	mstn+/+ 3d-ov	83.50*	4.950	.000	72.09	94.91
	mstn-/- 3d-ov	27.00*	4.950	.001	15.59	38.41
	mstn-/- 2wk-ov	-89.50*	4.950	.000	-100.91	-78.09
	mstn+/+ 6wk-ov	94.50*	4.950	.000	83.09	105.91
	mstn-/- 6wk-ov	66.00*	4.950	.000	54.59	77.41
mstn-/- 2wk-ov	mstn+/+ non-ov	223.00*	4.950	.000	211.59	234.41
	mstn-/- non-ov	210.50*	4.950	.000	199.09	221.91
	mstn+/+ 3d-ov	173.00*	4.950	.000	161.59	184.41
	mstn-/- 3d-ov	116.50*	4.950	.000	105.09	127.91
	mstn+/+ 2wk-ov	89.50*	4.950	.000	78.09	100.91

	mstn+/+ 6wk-ov	184.00*	4.950	.000	172.59	195.41
	mstn-/- 6wk-ov	155.50*	4.950	.000	144.09	166.91
mstn+/+ 6wk-ov	mstn+/+ non-ov	39.00*	4.950	.000	27.59	50.41
	mstn-/- non-ov	26.50*	4.950	.001	15.09	37.91
	mstn+/+ 3d-ov	-11.00	4.950	.057	-22.41	.41
	mstn-/- 3d-ov	-67.50*	4.950	.000	-78.91	-56.09
	mstn+/+ 2wk-ov	-94.50*	4.950	.000	-105.91	-83.09
	mstn-/- 2wk-ov	-184.00*	4.950	.000	-195.41	-172.59
	mstn-/- 6wk-ov	-28.50*	4.950	.000	-39.91	-17.09
mstn-/- 6wk-ov	mstn+/+ non-ov	67.50*	4.950	.000	56.09	78.91
	mstn-/- non-ov	55.00*	4.950	.000	43.59	66.41
	mstn+/+ 3d-ov	17.50*	4.950	.008	6.09	28.91
	mstn-/- 3d-ov	-39.00*	4.950	.000	-50.41	-27.59
	mstn+/+ 2wk-ov	-66.00*	4.950	.000	-77.41	-54.59
	mstn-/- 2wk-ov	-155.50*	4.950	.000	-166.91	-144.09
	mstn+/+ 6wk-ov	28.50*	4.950	.000	17.09	39.91

Based on observed means.

The error term is Mean Square(Error) = 24.500.

*. The mean difference is significant at the .05 level.

Homogeneous Subsets

Relative Myogenin Expression

	Group	N	Subset 1	Subset 2	Subset 3	Subset 4
Tukey HSD[a,,b]	mstn+/+ non-ov	2	30.00			
	mstn-/- non-ov	2	42.50			
	mstn+/+ 6wk-ov	2		69.00		
	mstn+/+ 3d-ov	2		80.00	80.00	
	mstn-/- 6wk-ov	2			97.50	
	mstn-/- 3d-ov	2				136.50
	mstn+/+ 2wk-ov	2				
	mstn-/- 2wk-ov	2				
	Sig.		.303	.425	.086	1.000
Scheffe[a,,b]	mstn+/+ non-ov	2	30.00			
	mstn-/- non-ov	2	42.50			
	mstn+/+ 6wk-ov	2		69.00		
	mstn+/+ 3d-ov	2		80.00	80.00	
	mstn-/- 6wk-ov	2			97.50	
	mstn-/- 3d-ov	2				136.50
	mstn+/+ 2wk-ov	2				

	mstn-/- 2wk-ov	2				
	Sig.		.542	.671	.217	1.000

Means for groups in homogeneous subsets are displayed.

Based on observed means.

The error term is Mean Square(Error) = 24.500.

a. Uses Harmonic Mean Sample Size = 2.000.

b. Alpha = .05.

Relative Myogenin Expression

		Subset	
	Group	5	6
Tukey HSD[a,,b]	mstn+/+ 2wk-ov	163.50	
	mstn-/- 2wk-ov		253.00
	Sig.	1.000	1.000
Scheffe[a,,b]	mstn+/+ 2wk-ov	163.50	
	mstn-/- 2wk-ov		253.00
	Sig.	1.000	1.000

Means for groups in homogeneous subsets are displayed.

Based on observed means.

The error term is Mean Square(Error) = 24.500.

a. Uses Harmonic Mean Sample Size = 2.000.

b. Alpha = .05.

ANOVA: BDNF Expression Response to Overloading Mstn+/+ and Mstn-/-

Notes

	Output Created	25-Nov-2009 11:32:46
	Comments	
Input	Data	C:\Users\Moe AK\Documents\Stats for thesis\MOD Midbelly Area Fibre CSA and Fibre Number Raw data.sav
	Active Dataset	DataSet1
	Filter	<none>
	Weight	<none>
	Split File	<none>
	N of Rows in Working Data File	24
Missing Value Handling	Definition of Missing	User-defined missing values are treated as missing.
	Cases Used	Statistics are based on all cases with valid data for all variables in the model.

	Syntax	UNIANOVA BDNF BY Group /METHOD=SSTYPE(3) /INTERCEPT=INCLUDE /POSTHOC=Group(TUKEY SCHEFFE LSD) /EMMEANS=TABLES(Group) /PRINT=ETASQ HOMOGENEITY DESCRIPTIVE /CRITERIA=ALPHA(.05) /DESIGN=Group.
Resources	Processor Time	0:00:00.078
	Elapsed Time	0:00:00.110

Between-Subjects Factors

		Value Label	N
Group	1.00	mstn+/+ non-ov	2
	2.00	mstn-/- non-ov	2
	3.00	mstn+/+ 3d-ov	2
	4.00	mstn-/- 3d-ov	2
	5.00	mstn+/+ 2wk-ov	2
	6.00	mstn-/- 2wk-ov	2

7.00	mstn+/+ 6wk-ov	2
8.00	mstn-/- 6wk-ov	2

Descriptive Statistics

Dependent Variable:Relative BDNF Expression

Group	Mean	Std. Deviation	N
mstn+/+ non-ov	255.00	14.142	2
mstn-/- non-ov	544.50	19.092	2
mstn+/+ 3d-ov	113.00	2.828	2
mstn-/- 3d-ov	63.50	12.021	2
mstn+/+ 2wk-ov	89.50	2.121	2
mstn-/- 2wk-ov	79.00	11.314	2
mstn+/+ 6wk-ov	166.00	14.142	2
mstn-/- 6wk-ov	100.00	8.485	2
Total	176.31	155.772	16

Tests of Between-Subjects Effects

Dependent Variable:Relative BDNF Expression

Source	Type III Sum of Squares	df	Mean Square	F	Sig.	Partial Eta Squared

Corrected Model	362849.938[a]	7	51835.705	369.760	.000	.997
Intercept	497377.563	1	497377.563	3547.945	.000	.998
Group	362849.938	7	51835.705	369.760	.000	.997
Error	1121.500	8	140.188			
Total	861349.000	16				
Corrected Total	363971.438	15				

a. R Squared = .997 (Adjusted R Squared = .994)

Estimated Marginal Means

Group

Dependent Variable:Relative BDNF Expression

Group			95% Confidence Interval	
	Mean	Std. Error	Lower Bound	Upper Bound
mstn+/+ non-ov	255.000	8.372	235.694	274.306
mstn-/- non-ov	544.500	8.372	525.194	563.806
mstn+/+ 3d-ov	113.000	8.372	93.694	132.306
mstn-/- 3d-ov	63.500	8.372	44.194	82.806
mstn+/+ 2wk-ov	89.500	8.372	70.194	108.806
mstn-/- 2wk-ov	79.000	8.372	59.694	98.306

mstn+/+ 6wk-ov	166.000	8.372	146.694	185.306
mstn-/- 6wk-ov	100.000	8.372	80.694	119.306

Post Hoc Tests

Group

Multiple Comparisons

Dependent Variable:Relative BDNF Expression

					95% Confidence Interval	
(I) Group	(J) Group	Mean Difference (I-J)	Std. Error	Sig.	Lower Bound	Upper Bound
Tukey HSD mstn+/+ non-ov	mstn-/- non-ov	-289.50*	11.840	.000	-336.35	-242.65
	mstn+/+ 3d-ov	142.00*	11.840	.000	95.15	188.85
	mstn-/- 3d-ov	191.50*	11.840	.000	144.65	238.35
	mstn+/+ 2wk-ov	165.50*	11.840	.000	118.65	212.35
	mstn-/- 2wk-ov	176.00*	11.840	.000	129.15	222.85
	mstn+/+ 6wk-ov	89.00*	11.840	.001	42.15	135.85
	mstn-/- 6wk-ov	155.00*	11.840	.000	108.15	201.85

	mstn-/- non-ov	mstn+/+ non-ov	289.50*	11.840	.000	242.65	336.35
		mstn+/+ 3d-ov	431.50*	11.840	.000	384.65	478.35
		mstn-/- 3d-ov	481.00*	11.840	.000	434.15	527.85
		mstn+/+ 2wk-ov	455.00*	11.840	.000	408.15	501.85
		mstn-/- 2wk-ov	465.50*	11.840	.000	418.65	512.35
		mstn+/+ 6wk-ov	378.50*	11.840	.000	331.65	425.35
		mstn-/- 6wk-ov	444.50*	11.840	.000	397.65	491.35
	mstn+/+ 3d-ov	mstn+/+ non-ov	-142.00*	11.840	.000	-188.85	-95.15
		mstn-/- non-ov	-431.50*	11.840	.000	-478.35	-384.65
		mstn-/- 3d-ov	49.50*	11.840	.038	2.65	96.35
		mstn+/+ 2wk-ov	23.50	11.840	.540	-23.35	70.35
		mstn-/- 2wk-ov	34.00	11.840	.199	-12.85	80.85
		mstn+/+ 6wk-ov	-53.00*	11.840	.026	-99.85	-6.15
		mstn-/- 6wk-ov	13.00	11.840	.940	-33.85	59.85
	mstn-/- 3d-ov	mstn+/+ non-ov	-191.50*	11.840	.000	-238.35	-144.65
		mstn-/- non-ov	-481.00*	11.840	.000	-527.85	-434.15
		mstn+/+ 3d-ov	-49.50*	11.840	.038	-96.35	-2.65
		mstn+/+ 2wk-ov	-26.00	11.840	.437	-72.85	20.85
		mstn-/- 2wk-ov	-15.50	11.840	.873	-62.35	31.35
		mstn+/+ 6wk-ov	-102.50*	11.840	.000	-149.35	-55.65

	mstn-/- 6wk-ov	-36.50	11.840	.153	-83.35	10.35
mstn+/+ 2wk-ov	mstn+/+ non-ov	-165.50*	11.840	.000	-212.35	-118.65
	mstn-/- non-ov	-455.00*	11.840	.000	-501.85	-408.15
	mstn+/+ 3d-ov	-23.50	11.840	.540	-70.35	23.35
	mstn-/- 3d-ov	26.00	11.840	.437	-20.85	72.85
	mstn-/- 2wk-ov	10.50	11.840	.979	-36.35	57.35
	mstn+/+ 6wk-ov	-76.50*	11.840	.003	-123.35	-29.65
	mstn-/- 6wk-ov	-10.50	11.840	.979	-57.35	36.35
mstn-/- 2wk-ov	mstn+/+ non-ov	-176.00*	11.840	.000	-222.85	-129.15
	mstn-/- non-ov	-465.50*	11.840	.000	-512.35	-418.65
	mstn+/+ 3d-ov	-34.00	11.840	.199	-80.85	12.85
	mstn-/- 3d-ov	15.50	11.840	.873	-31.35	62.35
	mstn+/+ 2wk-ov	-10.50	11.840	.979	-57.35	36.35
	mstn+/+ 6wk-ov	-87.00*	11.840	.001	-133.85	-40.15
	mstn-/- 6wk-ov	-21.00	11.840	.651	-67.85	25.85
mstn+/+ 6wk-ov	mstn+/+ non-ov	-89.00*	11.840	.001	-135.85	-42.15
	mstn-/- non-ov	-378.50*	11.840	.000	-425.35	-331.65
	mstn+/+ 3d-ov	53.00*	11.840	.026	6.15	99.85
	mstn-/- 3d-ov	102.50*	11.840	.000	55.65	149.35
	mstn+/+ 2wk-ov	76.50*	11.840	.003	29.65	123.35

		mstn-/- 2wk-ov	87.00*	11.840	.001	40.15	133.85
		mstn-/- 6wk-ov	66.00*	11.840	.007	19.15	112.85
	mstn-/- 6wk-ov	mstn+/+ non-ov	-155.00*	11.840	.000	-201.85	-108.15
		mstn-/- non-ov	-444.50*	11.840	.000	-491.35	-397.65
		mstn+/+ 3d-ov	-13.00	11.840	.940	-59.85	33.85
		mstn-/- 3d-ov	36.50	11.840	.153	-10.35	83.35
		mstn+/+ 2wk-ov	10.50	11.840	.979	-36.35	57.35
		mstn-/- 2wk-ov	21.00	11.840	.651	-25.85	67.85
		mstn+/+ 6wk-ov	-66.00*	11.840	.007	-112.85	-19.15
Scheffe	mstn+/+ non-ov	mstn-/- non-ov	-289.50*	11.840	.000	-348.11	-230.89
		mstn+/+ 3d-ov	142.00*	11.840	.000	83.39	200.61
		mstn-/- 3d-ov	191.50*	11.840	.000	132.89	250.11
		mstn+/+ 2wk-ov	165.50*	11.840	.000	106.89	224.11
		mstn-/- 2wk-ov	176.00*	11.840	.000	117.39	234.61
		mstn+/+ 6wk-ov	89.00*	11.840	.004	30.39	147.61
		mstn-/- 6wk-ov	155.00*	11.840	.000	96.39	213.61
	mstn-/- non-ov	mstn+/+ non-ov	289.50*	11.840	.000	230.89	348.11
		mstn+/+ 3d-ov	431.50*	11.840	.000	372.89	490.11
		mstn-/- 3d-ov	481.00*	11.840	.000	422.39	539.61
		mstn+/+ 2wk-ov	455.00*	11.840	.000	396.39	513.61
		mstn-/- 2wk-ov	465.50*	11.840	.000	406.89	524.11

	mstn+/+ 6wk-ov	378.50*	11.840	.000	319.89	437.11
	mstn-/- 6wk-ov	444.50*	11.840	.000	385.89	503.11
mstn+/+ 3d-ov	mstn+/+ non-ov	-142.00*	11.840	.000	-200.61	-83.39
	mstn-/- non-ov	-431.50*	11.840	.000	-490.11	-372.89
	mstn-/- 3d-ov	49.50	11.840	.112	-9.11	108.11
	mstn+/+ 2wk-ov	23.50	11.840	.768	-35.11	82.11
	mstn-/- 2wk-ov	34.00	11.840	.408	-24.61	92.61
	mstn+/+ 6wk-ov	-53.00	11.840	.082	-111.61	5.61
	mstn-/- 6wk-ov	13.00	11.840	.984	-45.61	71.61
mstn-/- 3d-ov	mstn+/+ non-ov	-191.50*	11.840	.000	-250.11	-132.89
	mstn-/- non-ov	-481.00*	11.840	.000	-539.61	-422.39
	mstn+/+ 3d-ov	-49.50	11.840	.112	-108.11	9.11
	mstn+/+ 2wk-ov	-26.00	11.840	.682	-84.61	32.61
	mstn-/- 2wk-ov	-15.50	11.840	.960	-74.11	43.11
	mstn+/+ 6wk-ov	-102.50*	11.840	.002	-161.11	-43.89
	mstn-/- 6wk-ov	-36.50	11.840	.337	-95.11	22.11
mstn+/+ 2wk-ov	mstn+/+ non-ov	-165.50*	11.840	.000	-224.11	-106.89
	mstn-/- non-ov	-455.00*	11.840	.000	-513.61	-396.39
	mstn+/+ 3d-ov	-23.50	11.840	.768	-82.11	35.11
	mstn-/- 3d-ov	26.00	11.840	.682	-32.61	84.61
	mstn-/- 2wk-ov	10.50	11.840	.995	-48.11	69.11

	mstn+/+ 6wk-ov	-76.50*	11.840	.011	-135.11	-17.89
	mstn-/- 6wk-ov	-10.50	11.840	.995	-69.11	48.11
mstn-/- 2wk-ov	mstn+/+ non-ov	-176.00*	11.840	.000	-234.61	-117.39
	mstn-/- non-ov	-465.50*	11.840	.000	-524.11	-406.89
	mstn+/+ 3d-ov	-34.00	11.840	.408	-92.61	24.61
	mstn-/- 3d-ov	15.50	11.840	.960	-43.11	74.11
	mstn+/+ 2wk-ov	-10.50	11.840	.995	-69.11	48.11
	mstn+/+ 6wk-ov	-87.00*	11.840	.005	-145.61	-28.39
	mstn-/- 6wk-ov	-21.00	11.840	.846	-79.61	37.61
mstn+/+ 6wk-ov	mstn+/+ non-ov	-89.00*	11.840	.004	-147.61	-30.39
	mstn-/- non-ov	-378.50*	11.840	.000	-437.11	-319.89
	mstn+/+ 3d-ov	53.00	11.840	.082	-5.61	111.61
	mstn-/- 3d-ov	102.50*	11.840	.002	43.89	161.11
	mstn+/+ 2wk-ov	76.50*	11.840	.011	17.89	135.11
	mstn-/- 2wk-ov	87.00*	11.840	.005	28.39	145.61
	mstn-/- 6wk-ov	66.00*	11.840	.026	7.39	124.61
mstn-/- 6wk-ov	mstn+/+ non-ov	-155.00*	11.840	.000	-213.61	-96.39
	mstn-/- non-ov	-444.50*	11.840	.000	-503.11	-385.89
	mstn+/+ 3d-ov	-13.00	11.840	.984	-71.61	45.61
	mstn-/- 3d-ov	36.50	11.840	.337	-22.11	95.11
	mstn+/+ 2wk-ov	10.50	11.840	.995	-48.11	69.11

		mstn-/- 2wk-ov	21.00	11.840	.846	-37.61	79.61
		mstn+/+ 6wk-ov	-66.00*	11.840	.026	-124.61	-7.39
LSD	mstn+/+ non-ov	mstn-/- non-ov	-289.50*	11.840	.000	-316.80	-262.20
		mstn+/+ 3d-ov	142.00*	11.840	.000	114.70	169.30
		mstn-/- 3d-ov	191.50*	11.840	.000	164.20	218.80
		mstn+/+ 2wk-ov	165.50*	11.840	.000	138.20	192.80
		mstn-/- 2wk-ov	176.00*	11.840	.000	148.70	203.30
		mstn+/+ 6wk-ov	89.00*	11.840	.000	61.70	116.30
		mstn-/- 6wk-ov	155.00*	11.840	.000	127.70	182.30
	mstn-/- non-ov	mstn+/+ non-ov	289.50*	11.840	.000	262.20	316.80
		mstn+/+ 3d-ov	431.50*	11.840	.000	404.20	458.80
		mstn-/- 3d-ov	481.00*	11.840	.000	453.70	508.30
		mstn+/+ 2wk-ov	455.00*	11.840	.000	427.70	482.30
		mstn-/- 2wk-ov	465.50*	11.840	.000	438.20	492.80
		mstn+/+ 6wk-ov	378.50*	11.840	.000	351.20	405.80
		mstn-/- 6wk-ov	444.50*	11.840	.000	417.20	471.80
	mstn+/+ 3d-ov	mstn+/+ non-ov	-142.00*	11.840	.000	-169.30	-114.70
		mstn-/- non-ov	-431.50*	11.840	.000	-458.80	-404.20
		mstn-/- 3d-ov	49.50*	11.840	.003	22.20	76.80
		mstn+/+ 2wk-ov	23.50	11.840	.082	-3.80	50.80
		mstn-/- 2wk-ov	34.00*	11.840	.021	6.70	61.30

	mstn+/+ 6wk-ov	-53.00*	11.840	.002	-80.30	-25.70
	mstn-/- 6wk-ov	13.00	11.840	.304	-14.30	40.30
mstn-/- 3d-ov	mstn+/+ non-ov	-191.50*	11.840	.000	-218.80	-164.20
	mstn-/- non-ov	-481.00*	11.840	.000	-508.30	-453.70
	mstn+/+ 3d-ov	-49.50*	11.840	.003	-76.80	-22.20
	mstn+/+ 2wk-ov	-26.00	11.840	.059	-53.30	1.30
	mstn-/- 2wk-ov	-15.50	11.840	.227	-42.80	11.80
	mstn+/+ 6wk-ov	-102.50*	11.840	.000	-129.80	-75.20
	mstn-/- 6wk-ov	-36.50*	11.840	.015	-63.80	-9.20
mstn+/+ 2wk-ov	mstn+/+ non-ov	-165.50*	11.840	.000	-192.80	-138.20
	mstn-/- non-ov	-455.00*	11.840	.000	-482.30	-427.70
	mstn+/+ 3d-ov	-23.50	11.840	.082	-50.80	3.80
	mstn-/- 3d-ov	26.00	11.840	.059	-1.30	53.30
	mstn-/- 2wk-ov	10.50	11.840	.401	-16.80	37.80
	mstn+/+ 6wk-ov	-76.50*	11.840	.000	-103.80	-49.20
	mstn-/- 6wk-ov	-10.50	11.840	.401	-37.80	16.80
mstn-/- 2wk-ov	mstn+/+ non-ov	-176.00*	11.840	.000	-203.30	-148.70
	mstn-/- non-ov	-465.50*	11.840	.000	-492.80	-438.20
	mstn+/+ 3d-ov	-34.00*	11.840	.021	-61.30	-6.70
	mstn-/- 3d-ov	15.50	11.840	.227	-11.80	42.80
	mstn+/+ 2wk-ov	-10.50	11.840	.401	-37.80	16.80

	mstn+/+ 6wk-ov	-87.00*	11.840	.000	-114.30	-59.70
	mstn-/- 6wk-ov	-21.00	11.840	.114	-48.30	6.30
mstn+/+ 6wk-ov	mstn+/+ non-ov	-89.00*	11.840	.000	-116.30	-61.70
	mstn-/- non-ov	-378.50*	11.840	.000	-405.80	-351.20
	mstn+/+ 3d-ov	53.00*	11.840	.002	25.70	80.30
	mstn-/- 3d-ov	102.50*	11.840	.000	75.20	129.80
	mstn+/+ 2wk-ov	76.50*	11.840	.000	49.20	103.80
	mstn-/- 2wk-ov	87.00*	11.840	.000	59.70	114.30
	mstn-/- 6wk-ov	66.00*	11.840	.001	38.70	93.30
mstn-/- 6wk-ov	mstn+/+ non-ov	-155.00*	11.840	.000	-182.30	-127.70
	mstn-/- non-ov	-444.50*	11.840	.000	-471.80	-417.20
	mstn+/+ 3d-ov	-13.00	11.840	.304	-40.30	14.30
	mstn-/- 3d-ov	36.50*	11.840	.015	9.20	63.80
	mstn+/+ 2wk-ov	10.50	11.840	.401	-16.80	37.80
	mstn-/- 2wk-ov	21.00	11.840	.114	-6.30	48.30
	mstn+/+ 6wk-ov	-66.00*	11.840	.001	-93.30	-38.70

Based on observed means.

The error term is Mean Square(Error) = 140.188.

*. The mean difference is significant at the .05 level.

Homogeneous Subsets

Relative BDNF Expression

	Group	N	Subset 1	2	3	4	5
Tukey HSD[a,,b]	mstn-/- 3d-ov	2	63.50				
	mstn-/- 2wk-ov	2	79.00	79.00			
	mstn+/+ 2wk-ov	2	89.50	89.50			
	mstn-/- 6wk-ov	2	100.00	100.00			
	mstn+/+ 3d-ov	2		113.00			
	mstn+/+ 6wk-ov	2			166.00		
	mstn+/+ non-ov	2				255.00	
	mstn-/- non-ov	2					544.50
	Sig.		.153	.199	1.000	1.000	1.000
Scheffe[a,,b]	mstn-/- 3d-ov	2	63.50				
	mstn-/- 2wk-ov	2	79.00				
	mstn+/+ 2wk-ov	2	89.50				
	mstn-/- 6wk-ov	2	100.00				
	mstn+/+ 3d-ov	2	113.00	113.00			
	mstn+/+ 6wk-ov	2		166.00			
	mstn+/+ non-ov	2			255.00		

	mstn-/- non-ov	2				544.50	
	Sig.		.112	.082	1.000	1.000	

Means for groups in homogeneous subsets are displayed.

Based on observed means.

The error term is Mean Square(Error) = 140.188.

a. Uses Harmonic Mean Sample Size = 2.000.

b. Alpha = .05.

ANOVA: Myostatin Expression Response to Overloading Mstn+/+

Notes

	Output Created	25-Nov-2009 11:34:40
	Comments	
Input	Data	C:\Users\Moe AK\Documents\Stats for thesis\MOD Midbelly Area Fibre CSA and Fibre Number Raw data.sav
	Active Dataset	DataSet1
	Filter	<none>
	Weight	<none>
	Split File	<none>
	N of Rows in Working Data File	24

Missing Value Handling	Definition of Missing	User-defined missing values are treated as missing.
	Cases Used	Statistics are based on all cases with valid data for all variables in the model.
	Syntax	UNIANOVA Myostatin BY Group /METHOD=SSTYPE(3) /INTERCEPT=INCLUDE /POSTHOC=Group(TUKEY SCHEFFE LSD) /EMMEANS=TABLES(Group) /PRINT=ETASQ HOMOGENEITY DESCRIPTIVE /CRITERIA=ALPHA(.05) /DESIGN=Group.
Resources	Processor Time	0:00:00.031
	Elapsed Time	0:00:00.104

Between-Subjects Factors

		Value Label	N
Group	1.00	mstn+/+ non-ov	2
	3.00	mstn+/+ 3d-ov	2
	5.00	mstn+/+ 2wk-ov	2

Between-Subjects Factors

		Value Label	N
Group	1.00	mstn+/+ non-ov	2
	3.00	mstn+/+ 3d-ov	2
	5.00	mstn+/+ 2wk-ov	2
	7.00	mstn+/+ 6wk-ov	2

Descriptive Statistics

Dependent Variable:Relative Mstn Expression

Group	Mean	Std. Deviation	N
mstn+/+ non-ov	763.50	31.820	2
mstn+/+ 3d-ov	40.00	1.414	2
mstn+/+ 2wk-ov	62.50	6.364	2
mstn+/+ 6wk-ov	72.50	2.121	2
Total	234.63	326.903	8

Tests of Between-Subjects Effects

Dependent Variable:Relative Mstn Expression

Source	Type III Sum of Squares	df	Mean Square	F	Sig.	Partial Eta Squared
Corrected Model	746998.375[a]	3	248999.458	940.064	.000	.999
Intercept	440391.125	1	440391.125	1662.638	.000	.998
Group	746998.375	3	248999.458	940.064	.000	.999
Error	1059.500	4	264.875			
Total	1188449.000	8				
Corrected Total	748057.875	7				

a. R Squared = .999 (Adjusted R Squared = .998)

Estimated Marginal Means

Group

Dependent Variable:Relative Mstn Expression

Group			95% Confidence Interval	
	Mean	Std. Error	Lower Bound	Upper Bound
mstn+/+ non-ov	763.500	11.508	731.548	795.452
mstn+/+ 3d-ov	40.000	11.508	8.048	71.952
mstn+/+ 2wk-ov	62.500	11.508	30.548	94.452
mstn+/+ 6wk-ov	72.500	11.508	40.548	104.452

Post Hoc Tests

Group

Multiple Comparisons

Dependent Variable:Relative Mstn Expression

	(I) Group	(J) Group	Mean Difference (I-J)	Std. Error	Sig.
Tukey HSD	mstn+/+ non-ov	mstn+/+ 3d-ov	723.50*	16.275	.000
		mstn+/+ 2wk-ov	701.00*	16.275	.000
		mstn+/+ 6wk-ov	691.00*	16.275	.000
	mstn+/+ 3d-ov	mstn+/+ non-ov	-723.50*	16.275	.000
		mstn+/+ 2wk-ov	-22.50	16.275	.568
		mstn+/+ 6wk-ov	-32.50	16.275	.323
	mstn+/+ 2wk-ov	mstn+/+ non-ov	-701.00*	16.275	.000
		mstn+/+ 3d-ov	22.50	16.275	.568
		mstn+/+ 6wk-ov	-10.00	16.275	.922

	mstn+/+ 6wk-ov	mstn+/+ non-ov	-691.00*	16.275	.000
		mstn+/+ 3d-ov	32.50	16.275	.323
		mstn+/+ 2wk-ov	10.00	16.275	.922
Scheffe	mstn+/+ non-ov	mstn+/+ 3d-ov	723.50*	16.275	.000
		mstn+/+ 2wk-ov	701.00*	16.275	.000
		mstn+/+ 6wk-ov	691.00*	16.275	.000
	mstn+/+ 3d-ov	mstn+/+ non-ov	-723.50*	16.275	.000
		mstn+/+ 2wk-ov	-22.50	16.275	.630
		mstn+/+ 6wk-ov	-32.50	16.275	.382
	mstn+/+ 2wk-ov	mstn+/+ non-ov	-701.00*	16.275	.000
		mstn+/+ 3d-ov	22.50	16.275	.630
		mstn+/+ 6wk-ov	-10.00	16.275	.940
	mstn+/+ 6wk-ov	mstn+/+ non-ov	-691.00*	16.275	.000
		mstn+/+ 3d-ov	32.50	16.275	.382
		mstn+/+ 2wk-ov	10.00	16.275	.940
LSD	mstn+/+ non-ov	mstn+/+ 3d-ov	723.50*	16.275	.000
		mstn+/+ 2wk-ov	701.00*	16.275	.000
		mstn+/+ 6wk-ov	691.00*	16.275	.000
	mstn+/+ 3d-ov	mstn+/+ non-ov	-723.50*	16.275	.000
		mstn+/+ 2wk-ov	-22.50	16.275	.239
		mstn+/+ 6wk-ov	-32.50	16.275	.117

	mstn+/+ 2wk-ov	mstn+/+ non-ov	-701.00*	16.275	.000
		mstn+/+ 3d-ov	22.50	16.275	.239
		mstn+/+ 6wk-ov	-10.00	16.275	.572
	mstn+/+ 6wk-ov	mstn+/+ non-ov	-691.00*	16.275	.000
		mstn+/+ 3d-ov	32.50	16.275	.117
		mstn+/+ 2wk-ov	10.00	16.275	.572

Based on observed means.

The error term is Mean Square(Error) = 264.875.

*. The mean difference is significant at the .05 level.

Multiple Comparisons

Dependent Variable:Relative Mstn Expression

			95% Confidence Interval	
	(I) Group	(J) Group	Lower Bound	Upper Bound
Tukey HSD	mstn+/+ non-ov	mstn+/+ 3d-ov	657.25	789.75
		mstn+/+ 2wk-ov	634.75	767.25
		mstn+/+ 6wk-ov	624.75	757.25
	mstn+/+ 3d-ov	mstn+/+ non-ov	-789.75	-657.25
		mstn+/+ 2wk-ov	-88.75	43.75
		mstn+/+ 6wk-ov	-98.75	33.75
	mstn+/+ 2wk-ov	mstn+/+ non-ov	-767.25	-634.75

		mstn+/+ 3d-ov	-43.75	88.75
		mstn+/+ 6wk-ov	-76.25	56.25
	mstn+/+ 6wk-ov	mstn+/+ non-ov	-757.25	-624.75
		mstn+/+ 3d-ov	-33.75	98.75
		mstn+/+ 2wk-ov	-56.25	76.25
Scheffe	mstn+/+ non-ov	mstn+/+ 3d-ov	651.13	795.87
		mstn+/+ 2wk-ov	628.63	773.37
		mstn+/+ 6wk-ov	618.63	763.37
	mstn+/+ 3d-ov	mstn+/+ non-ov	-795.87	-651.13
		mstn+/+ 2wk-ov	-94.87	49.87
		mstn+/+ 6wk-ov	-104.87	39.87
	mstn+/+ 2wk-ov	mstn+/+ non-ov	-773.37	-628.63
		mstn+/+ 3d-ov	-49.87	94.87
		mstn+/+ 6wk-ov	-82.37	62.37
	mstn+/+ 6wk-ov	mstn+/+ non-ov	-763.37	-618.63
		mstn+/+ 3d-ov	-39.87	104.87
		mstn+/+ 2wk-ov	-62.37	82.37
LSD	mstn+/+ non-ov	mstn+/+ 3d-ov	678.31	768.69
		mstn+/+ 2wk-ov	655.81	746.19
		mstn+/+ 6wk-ov	645.81	736.19
	mstn+/+ 3d-ov	mstn+/+ non-ov	-768.69	-678.31

		mstn+/+ 2wk-ov	-67.69	22.69
		mstn+/+ 6wk-ov	-77.69	12.69
	mstn+/+ 2wk-ov	mstn+/+ non-ov	-746.19	-655.81
		mstn+/+ 3d-ov	-22.69	67.69
		mstn+/+ 6wk-ov	-55.19	35.19
	mstn+/+ 6wk-ov	mstn+/+ non-ov	-736.19	-645.81
		mstn+/+ 3d-ov	-12.69	77.69
		mstn+/+ 2wk-ov	-35.19	55.19

Based on observed means.

The error term is Mean Square(Error) = 264.875.

Homogeneous Subsets

Relative Mstn Expression

	Group	N	Subset 1	Subset 2
Tukey HSD[a,,b]	mstn+/+ 3d-ov	2	40.00	
	mstn+/+ 2wk-ov	2	62.50	

	mstn+/+ 6wk-ov	2	72.50	
	mstn+/+ non-ov	2		763.50
	Sig.		.323	1.000
Scheffe[a,,b]	mstn+/+ 3d-ov	2	40.00	
	mstn+/+ 2wk-ov	2	62.50	
	mstn+/+ 6wk-ov	2	72.50	
	mstn+/+ non-ov	2		763.50
	Sig.		.382	1.000

Means for groups in homogeneous subsets are displayed.

Based on observed means.

The error term is Mean Square(Error) = 264.875.

a. Uses Harmonic Mean Sample Size = 2.000.

b. Alpha = .05.